

Kingdom of Saudi Arabia  
Ministry of Education  
Umm Al Qura University  
Faculty of Applied Sciences  
Chemistry Department



# Uses of some Water Soluble Polymers as Inhibitors for the Corrosion of Carbon Steel in Aqueous Solutions

By

**Hanaa Mohammed Ibraheem Hawsawi**

(M.Sc.Chemistry)

**A Thesis**

Submitted in Partial Fulfillment of the Requirement for the degree of  
Doctor of Philosophy in Chemistry (Physical Chemistry)

Supervisors

Prof. Dr. Metwally Abdallah

Prof of physical Chemistry

Prof. Dr. Ahmed Fawzy

Prof of physical Chemistry

Chemistry Department

College of Applied of Science

Umm Al Qura University

(1441-2020)

Kingdom of Saudi Arabia  
Ministry of Education  
Umm Al Qura University  
Faculty of Applied Sciences  
Chemistry Department



# **Uses of some Water Soluble Polymers as Inhibitors for the Corrosion of Carbon Steel in Aqueous Solutions**

By

**Hanaa Mohammed Ibraheem Hawsawi**

(M.Sc.Chemistry)

**A Thesis**

Submitted in Partial Fulfillment of the Requirement for the degree of  
Doctor of Philosophy in Chemistry (Physical Chemistry)

**Supervisors**

**Prof. Dr. . Metwally Abdallah**

Prof of physical Chemistry

**Prof. Dr. Ahmed Fawzy**

Prof of physical Chemistry

Chemistry Department  
College of Applied of Science  
Umm Al Qura University  
(1441-2020)

Kingdom of Saudi Arabia  
Ministry of Education  
Umm Al-Qura University  
Faculty of Applied Sciences  
Chemistry Department



## *Uses of some Water Soluble Polymers as Inhibitors for the Corrosion of Carbon Steel in Aqueous Solutions*

**Name:** Hanaa Hawsawi

**Supervisors**

<b>Name</b>	<b>Position</b>	<b>Signature</b>
<b>Prof Dr.Metwally Abdullah Mohamed</b>	Prof. of Physical Chemistry	
<b>Prof Dr Ahmed Fawzy Saad</b>	Prof. of Physical Chemistry	

**The Examiners**

<b>Name</b>	<b>Position</b>	<b>Signature</b>
<b>Prof Dr.Metwally Abdallah Mohamed</b>	Prof. of Physical Chemistry Chemistry Department Faculty of Applied Science Umm Al-Qura university	
<b>Prof .Dr. Reda Abd El Hameed</b>	Prof. of Physical Chemistry Chemistry Department Faculty of Science Hail University	
<b>Dr. Ameena Mohsen Albonayan</b>	Prof. of Physical Chemistry Chemistry Department Faculty of Applied Science Umm Al-Qura university	

**Head of Chemistry  
Department  
Dr. Motaz H. Morad**

**Vice Dean for Post  
Graduate Studies  
Prof. Dr. Basim Asghar**

**Dean of Faculty  
Dr. Hatem M Altass**

بِسْمِ اللَّهِ الرَّحْمَنِ الرَّحِيمِ

﴿ قَالَ رَبِّ أَوْزِعْنِي أَنْ أَشْكُرَ نِعْمَتَكَ الَّتِي أَنْعَمْتَ عَلَيَّ وَعَلَىٰ وَالِدَيَّ وَأَنْ أَعْمَلَ صَالِحًا تَرْضَاهُ وَأَصْلِحْ لِي فِي ذُرِّيَّتِي إِنِّي تُبْتُ إِلَيْكَ وَإِنِّي مِنَ الْمُسْلِمِينَ ﴾ [سورة الأحقاف: ١٥]

## ACKNOWLEDGMENT

First and most I would like to thank Allah, whom without his grace, the progress and success of this work was impossible.

I am immensely grateful and highly indebted to my revered guide Prof. Dr. Metwally Abdallah, professor of physical Chemistry, Faculty of Science for his excellent guidance, invaluable help and support throughout the past period while preparing my thesis, right from the inception phase till very end and are highly appreciated.

My deep appreciation and gratitude to Dr. Ahmad Fawzy Professor of physical Chemistry, for generous help and continuous advice in this work.

Special thanks go to Dr. Moatiz Morad, Head of Chemistry Department, Dr. Ismail Althagafi, previous Head of Chemistry Department, Prof. Dr. Basim Asghar, Vice Dean for Graduate Studies and Dr. Hatem Altass, Dean of the College of Applied Sciences.

I am grateful to the Chemistry Department - College of Applied Sciences - Umm Al-Qura University for their valuable suggestions, encouragement, and guidance throughout my study.

My deep thank the Deanship of Scientific Research at Umm Al-Qura University for their valuable suggestions, and encouragement throughout my study.

My deep thanks and gratitude for my parents, my husband, my daughter and my brothers for their great interest and motivation and for giving so much and asking for little in return.

Lastly, I offer my regards and blessings to all of those who supported me in any respect during the completion of this study.

The 2<sup>nd</sup> International Conference of Egyptian committee for Pure and Applied  
Chemistry (NCPAC19)  
CHEMISTRY FOR SUSTAINABLE FUTURE



## Certificate

This is to certify that: **Dr. Hanaa Hawsawi**

Has participated and delivered an accepted research paper entitled:

Title: **Use of some water-soluble polymers as inhibitors for the corrosion of carbon steel in aqueous solutions**

As (Poster) Presentation in the activities of the:

2<sup>nd</sup> international Conference of Egyptian committee for Pure and Applied  
Chemistry "CHEMISTRY FOR SUSTAINABLE FUTURE (NCPAC19) "

Held on 20-22 October, 2019 – Hurghada, Egypt

اللجنة الوطنية للكيمياء البحتة والتطبيقية  
National Committee for Pure and Applied Chemistry

Conference Chairman  
*Kamal Z. Aly*  
Prof. Dr. Kamal H. Aly

**PUBLISHED PAPER**

## **Maltodextrin and Chitosan Polymers as Inhibitors for the Corrosion of Carbon Steel in 1.0 M Hydrochloric Acid**

*M. Abdallah*<sup>1,2,\*</sup>, *A. Fawzy*<sup>1,3</sup>, *H. Hawsawi*<sup>1</sup>

<sup>1</sup> Chemistry Department, Faculty of Applied Science, Umm Al-Qura University, Makkah, Saudi Arabia

<sup>2</sup> Chemistry Department, Faculty of Science, Benha University, Benha, Egypt

<sup>3</sup> Chemistry Department, Faculty of Science, Assiut University, Assiut, Egypt

\*E-mail: [metwally555@yahoo.com](mailto:metwally555@yahoo.com)

*Received:* 20 February 2020 / *Accepted:* 13 April 2020 / *Published:* 10 May 2020

---

The inhibition impacts of two water-soluble polymers viz., maltodextrin and chitosan on the dissolution of carbon steel in 1.0 M HCl solution were investigated by three dissimilar techniques. The investigation results indicated that the inhibition efficiencies of the examined polymers increased with their concentrations and reduced by raising temperature. The results obtained from polarization measurements proved that the investigated polymers act as mixed type inhibitors. The acquired high inhibition efficiencies of the studied polymers may be owing to powerful adsorption of the polymer molecules on the C-steel surface resulting in the construction of protective layers. Adsorption of the tested polymers on the steel surface was set to accord with Freundlich adsorption isotherm. The inhibition efficiency of chitosan was set to be higher than maltodextrin because of its high molecular mass that increases the surface area of steel covered by the polymer. The acquired thermodynamic parameters for adsorption indicated that the adsorption process is spontaneous and endothermic, and the type of adsorption is physical. The acquired outcomes from the dissimilar measurements were in a good agreement.

---

**Keyword:** Carbon steel; Polymers; Corrosion Inhibitors; Kinetic parameters; Adsorption

### **1. INTRODUCTION**

Corrosion of carbon steel (C-steel) in hydrochloric acid media and trying to inhibit it using organic compounds is an important topic that has multiple applications in many industries that serve the national economy. Scientists are trying to discover new compounds that are inexpensive, nontoxic, environment friendly and have high effectiveness in inhibiting corrosion [1]. In recent years, scientists have intensified their efforts to reduce the risk of carbon steel corrosion by using many synthetic organic compounds [2-8], surface active agent (ionic, nonionic, cationic, Gemini) molecules [8-14], natural plant extracts [15-20] and pharmaceutical drug [21-24]. The inhibition capacity of these compounds ascribed



to their adsorption characteristics. There are several factors that affect the efficiency of these compounds as corrosion inhibitors, including the type of inhibitor, whether it is an organic or inorganic compound or a mixture, the type of solution used, the temperature, the hydrogen ion concentration, the presence of electro donating or repelling groups, the presence of the active centers and other factors [25].

Some scientists have used some polymers as inhibitors because their functional groups form complexes with metal ions. These complexes coverage a large surface area and isolate the metals from the aggressive attack solutions [26-28]. The main objective of this study was to investigate the inhibiting affinity of two significant naturally-occurring water-soluble polymers, namely, maltodextrin (I) and chitosan (II), on the corrosion of carbon steel in 1.0 M HCl solution using various techniques; weight loss, (WL) galvanostatic polarization (GAP), potentiodynamic anodic polarization (PAP) and electrochemical impedance spectroscopy (EIS) measurements.

## 2. EXPERIMENTAL

### 2.1. Measurements

Carbon steel used in the corrosion measurements for this study is produced by Saudi SABIC. It is in the form of a cylindrical rod used in chemical or electrochemical measurements. Its chemical composition is inserted in Table 1. All chemicals were obtained from Sigma Chemicals. The stock solutions of HCl and the two polymer compounds (maltodextrin and chitosan) were prepared with bidistilled water and the required concentrations were acquired by appropriate dilution.

**Table 1.** Compositions (wt. %) of the investigated carbon steel specimen.

Element	C	Mn	S	P	Si	Al	Fe
Weight (%)	0.110	0.450	0.050	0.040	0.250	0.039	balance

### 2.2. Inhibitors

Two polymer molecules were used as received from Sigma-Aldrich. Their structures are illustrated in Figure 1.

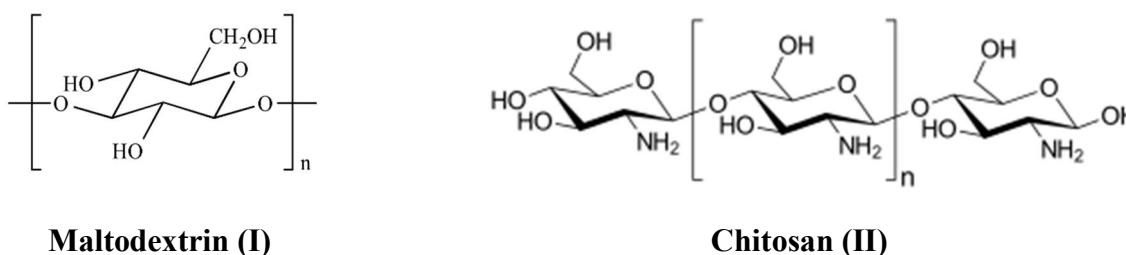


**Figure 1.** Chemical names and structures of the polymers used.

### 2.3. Weight-loss (WL) measurements

WL measurements were carried out in a temperature-controlled system. The cylindrical carbon steel samples with surface areas of about 12.78 cm<sup>2</sup>. Before any measurements, the carbon steel rods were polished with various grades of sanding paper from 200 to 1200, then washed with distilled water and lately washed with acetone. The procedure of the WL method as mentioned previously [29]. The corrosion rate (CR) was computed in mils penetration per year (mpy) using the following equation [30]:

$$CR = \frac{KW}{Atd} \quad (1)$$

where,  $K$  is a constant,  $W$  is the WL in grams,  $A$  is the surface area in cm<sup>2</sup>,  $t$  is time in hour and  $d$  is the density.

The inhibition efficiencies (% IE) and the degrees of surface coverage ( $\theta$ ) of the polymer molecules were calculated as follows [30]:

$$\% \text{ IE} = \theta \times 100 = \left[ 1 - \frac{CR_{inh}}{CR} \right] \times 100 \quad (2)$$

where, CR and CR<sub>inh</sub> are the corrosion rates in the free 1.0 M HCl and with the addition of the polymer compounds, respectively.

### 2.4. Electrochemical measurements

The galvanostatic polarization measurements (GPM) and potentiodynamic polarization measurements (PDP) were done using PGSTAT30 potentiostat / galvanostat in a triple cell with platinum electrode (CE), reference electrode (RE) and working electrode (WE), carbon steel. All measurements were made at a constant temperature in a temperature-controlled system. The values of %IE were calculated for the tested polymers from the following equation [30]:

$$\% \text{ IE} = 1 - \left[ 1 - \frac{I_{corr(inh)}}{I_{corr}} \right] \times 100 \quad (3)$$

where,  $I_{corr}$  and  $I_{corr(inh)}$  are the corrosion current densities in the free 1.0 M HCl and with addition of the polymer compounds, respectively. PDP measurements were carried out at a scan rate of 1.0 mVsec<sup>-1</sup>. The values  $I_{corr}$  was determined by extrapolation of the slopes of cathodic and anodic Tafel lines ( $\beta_c$ ,  $\beta_a$ ), of the polarization curves with the corrosion potentials ( $E_{corr}$ ).

EIS measurements were conveyed out in a frequency range of 100 kHz to 0.1 Hz with an amplitude of 4.0 mV peak-to-peak using AC signals at OCP. The %IE values were computed from the charge transfer resistance ( $R_{ct}$ ) data using the following equation [30]:

$$\% \text{ IE} = \left[ 1 - \frac{R_{ct}}{R_{ct(inh)}} \right] \times 100 \quad (4)$$

where,  $R_{ct}$  and  $R_{ct(inh)}$  in the free 1.0 M HCl and with the addition of the polymer compounds, respectively.

### 3. RESULTS AND DISCUSSION

#### 3.1. WL Measurements

##### 3.1.1. Effect of Polymers Concentrations

Figure 2 presents the relationship between WL and immersion time for C-steel in the free 1.0 M HCl solution and in the presence of some concentrations of chitosan polymer, ranging from 100 to 500 ppm. Like curves are acquired in the presence of maltodextrin, but do not appear here. It is evident that WL decreases with increasing chitosan concentration. This donates that the examined polymer molecules act as inhibitors by reducing the rate of steel corrosion of in the aggressive medium, 1.0 M HCl solution. Examining Figure 2, it can be observe that the plots in this figure were linear, which indicates that there is no insoluble film formation on the iron surface throughout corrosion, and the polymer molecules are absorbed on the iron surface. The process of suppression of corrosion is carried out either by blocking the interactive sites or by modifying both the cathodic and partial process mechanisms.

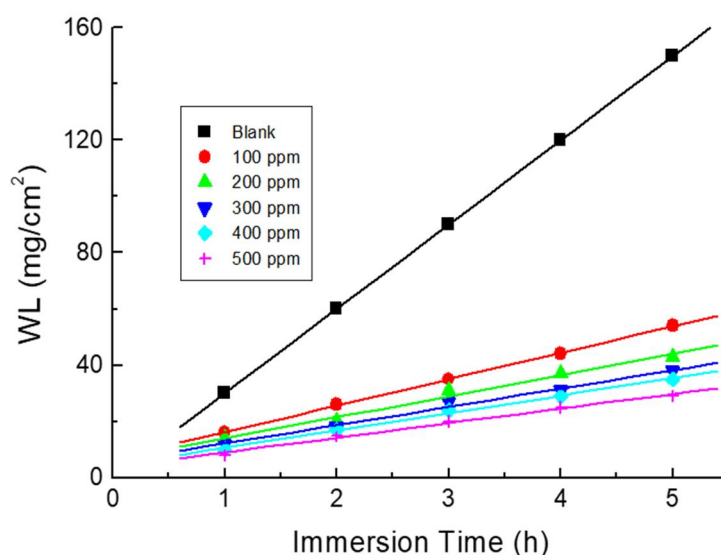


**Figure 2.** Weight loss (WL) versus immersion time for the corrosion of C-steel in 1.0 M HCl solution (blank) and with various concentrations of chitosan at 298 K.

The computed values of CR, %IE and  $\theta$  are included in Table 2. With an increase in the concentration of maltodextrin and chitosan, CR is reduced and the values of %IE and  $\theta$  increase, which proves the inhibitory impacts of the two examined polymer compounds. Also, the values of %IE of chitosan at all concentrations studied were found to be more than those of maltodextrin. This point will be interpreted later in the mechanism of inhibition.

**Table 2.** Corrosion parameters acquired from the corrosion of C-steel in 1.0 M HCl solution and in the presence of maltodextrin and chitosan at 298 K.

Inhibitors	Inh. Conc. (ppm)	$10^5$ CR $\text{mg cm}^{-2} \text{min}^{-1}$	% IE	$\Theta$
--	0	0.580	-	-
Maltodextrin	100	0.129	77.76	0.777
	200	0.118	79.65	0.796
	300	0.115	80.17	0.802
	400	0.113	80.60	0.806
	500	0.108	81.38	0.814
Chitosan	100	0.121	79.13	0.791
	200	0.078	86.55	0.865
	300	0.075	87.10	0.871
	400	0.071	87.79	0.878
	500	0.066	88.62	0.886

### 3.1.2. Temperature Effect

The influence of temperature rise on WL of C-steel was studied in a free 1.0 M HCl solution and in the presence of a 500 ppm of the polymers by WL measurements at different temperatures from 298 K to 328 K. The values of CR and %IE are inserted in Table 3. From the data listed in Table 3, it is evident that, the CR values increase with increasing temperature and, therefore, the values of %IE increase. This explained by the desorption of the film formed at the surface of C-steel at an elevated temperature. This showed that the adsorption of maltodextrin and chitosan compounds was physical.

**Table 3.** Impact of rising temperature on the corrosion parameters for C-steel in 1.0 M HCl solution and in the presence of a 500 ppm of maltodextrin and chitosan.

Medium	T K	CR $\text{mg cm}^{-2} \text{h}^{-1}$	% IE
1.0 M HCl	298	0.680	--
	308	0.842	--
	318	1.020	--
	328	1.141	--
1.0 M HCl + 500 ppm of Maltodextrin	298	0.108	81.38
	308	0.198	77.24
	318	0.286	71.96
	328	0.374	68.07
1.0 M HCl + 500 ppm of Chitosan	298	0.066	88.62
	308	0.168	80.69
	318	0.242	76.27
	328	0.316	73.15

The activation thermodynamic parameters such as the activation energy ( $E_a^*$ ) enthalpy of activation ( $\Delta H^*$ ) and entropy of activation ( $\Delta S^*$ ) were determined from the Arrhenius and transition state equations [31,32]:

$$\ln CR = \ln A - \frac{E_a^*}{RT} \quad (5)$$

$$\ln\left(\frac{CR}{T}\right) = \left(\ln\frac{R}{Nh} + \frac{\Delta S^*}{R}\right) - \frac{\Delta H^*}{R} \frac{1}{T} \quad (6)$$

where, A, R, T, N and h are Arrhenius constant, universal gas constant, temperature Avogadro's number and Planck's constant, respectively.

From the slopes of the linear relationship between  $\log(R_{\text{corr}})$  with  $(1/T)$  (Fig. 3) we can compute the values of  $E_a^*$  which were found to be 18.19 KJ mol<sup>-1</sup> for free 1.0 M HCl solution and equal to 26.81 and 27.72 KJ mol<sup>-1</sup> in the presence of a 500 ppm of maltodextrin and chitosan, respectively. Evidently, the  $E_a^*$  values increase in the presence of polymer compounds indicating their adsorption on the C-steel surface by creating a barrier for mass and charge transfer.

The enthalpy and entropy of activation for C-steel corrosion in free 1.0 M HCl and in the presence of polymer molecules have been calculated from the slope [ $-\Delta H^*/2.303 R$ ] and the intercept [ $\log(R/Nh - \Delta S^*/2.303R)$ ] of the relationship between of  $(\log R_{\text{corr}}/T)$ , with  $(1/T)$  as shown in Fig. 4. The  $\Delta H^*$  values were found to be 16.14 KJ mol<sup>-1</sup> in free 1.0 M HCl and equal to 24.98 and 28.72 KJ mol<sup>-1</sup> in the presence of a 500 ppm of maltodextrin and chitosan, respectively. The positive signs of  $\Delta H^*$  denote that the adsorption the two polymer compounds onto the C-steel surface is an endothermic process. The calculated values of  $\Delta S^*$  are equal to -163.12 J mol<sup>-1</sup> K<sup>-1</sup> in the free 1.0 M HCl solution and equal to -53.36 and -261.81 J mol<sup>-1</sup> K<sup>-1</sup> in presence of a 500 ppm of maltodextrin and chitosan, respectively. The values of  $\Delta S^*$  are negative suggesting that the construction of the activation complex is the rate-determining step which represents an association rather than dissociation [33].

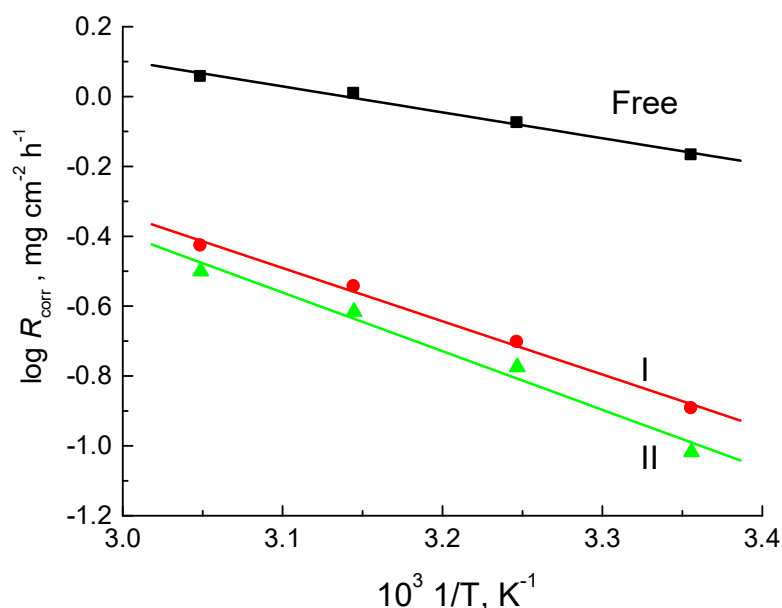


**Figure 3.** Arrhenius plots for the corrosion of C-steel in 1.0 M HCl solution and in the presence of a 500

ppm of: I) maltodextrin, II) chitosan.

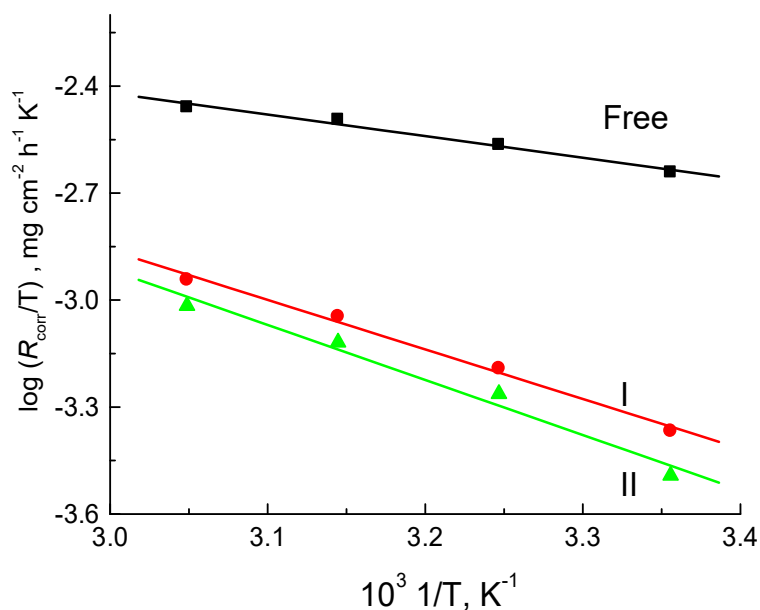


**Figure 4.** Transition state plots for the corrosion of C-steel in 1.0 M HCl solution and in the presence of 500 ppm of: I) maltodextrin, II) chitosan.

### 3.1.3. Galvanostatic Polarization Measurements (GPM)

Figure 5 displays the GPM for C-steel in a free 1.0 M HCl solution and in the presence of some concentrations of chitosan ranging from 100 to 500 ppm. Similar curves were obtained in the presence of maltodextrin but did not inserted here. Some corrosion parameters such as corrosion potential,  $E_{\text{corr}}$ , corrosion current density,  $I_{\text{corr}}$ ,  $\beta_a$ ,  $\beta_c$  and %IE are computed and recorded in Table 4.

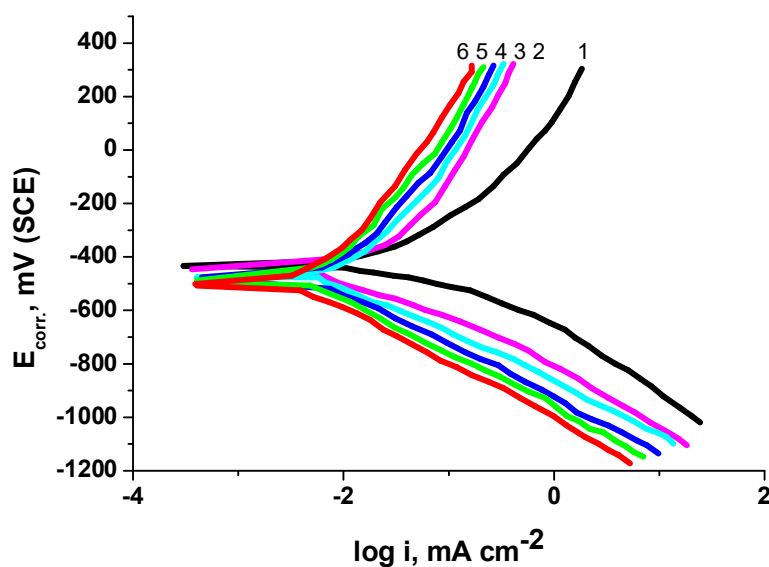


**Figure 5.** GPM for C-steel in 1.0 M HCl solution and in the presence of different concentrations (ppm)

of chitosan: 1) 00.0 2) 100 3) 200 4) 300 5) 400 6) 500.

Examining Table 4, it is evident that, the increased concentration of the two polymers resulted in slightly shifting the values of  $E_{\text{corr}}$  towards negative direction and the  $I_{\text{corr}}$  values were reduced at all studied concentrations, suggesting the inhibitory action of these polymeric compounds. The values of Tafel slopes ( $\beta_a$  &  $\beta_c$ ) were changed slightly in the presence of the polymers, indicating that maltodextrin and chitosan polymers are considered as mixed type inhibitors [34]. That is, these compounds influenced both cathodic hydrogen evolution and anodic steel corrosion reactions. The order of the inhibition efficiency of the studied polymeric compounds is chitosan > maltodextrin.

**Table 4.** Effect of increasing concentrations (ppm) of the examined polymers on the corrosion parameters obtained from GPM of C-steel in 1.0 M HCl solution at 298 K.

Inhibitors	Inh. Conc. (ppm)	$-E_{\text{corr}}$ (mV (SCE))	$\beta_a$ (mV/decade)	$-\beta_c$ (mV/decade)	$I_{\text{corr}}$ ( $\mu\text{A}/\text{cm}^2$ )	%IE
--	0	434	78	113	0.780	--
Maltodextrin	100	440	80	118	0.342	80.78
	200	454	81	120	0.291	83.65
	300	487	88	130	0.258	85.50
	400	492	98	133	0.223	87.47
	500	498	102	134	0.183	89.72
Chitosan	100	492	79	112	0.284	84.04
	200	498	80	119	0.218	87.75
	300	511	87	124	0.180	89.88
	400	537	94	129	0.162	90.89
	500	539	110	133	0.132	92.58

### 3.1.4. Polymer compounds as pitting corrosion inhibitors

The two selected polymer compounds, chitosan and maltodextrin, have been examined as inhibitors for pitting corrosion of C-steel. Figure 6 displays the PDP curves of C-steel in the free 1.0 M HCl solution and in the presence of some concentrations of chitosan (ranging from 100 to 500 ppm) at a scan rate  $1.0 \text{ mVs}^{-1}$ . Similar curves in the presence of maltodextrin are obtained, but not appeared here. Through this figure there are no anodic peaks suggesting a good stable oxide film on the surface of C-steel. As the potential increase, the current remains constant until a certain potential, then the current increase rapidly due to breakdown of the passive film formed on the C-steel surface and the initiation of pitting attack. This potential is defined as pitting corrosion potential ( $E_{\text{pit}}$ ) [35-38]. As the concentration of polymer compounds increases the values of  $E_{\text{pit}}$  is transferred to more positive potentials donating the resistance of pitting attack.

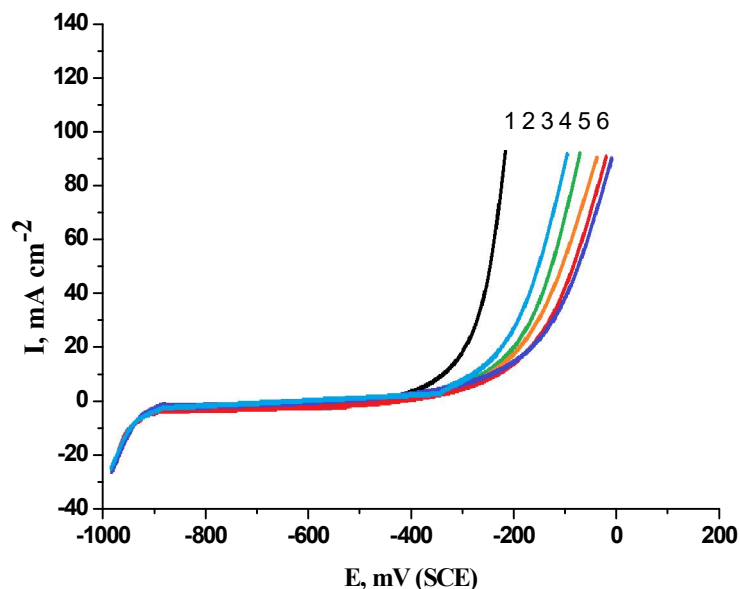


**Figure 6.** PDAP curves for C-steel in 1.0 M HCl + 0.1 M NaCl solution and in the presence of different concentrations (ppm) of chitosan: 1) 00.0 2) 100 3) 200 4) 300 5) 400 6) 500.

Figure 7 displays the relationship between  $E_{pit}$  and the logarithm of the concentrations of polymer compounds. Obviously from this figure the values of  $E_{pit}$  is directed to more positive direction as the concentrations of the two polymer compounds increases satisfying the following equation [37,38]:

$$E_{pit} = A + B \log C_{inh} \tag{7}$$

where, A and B are constants depending on the types of the electrode and inhibitor employed.

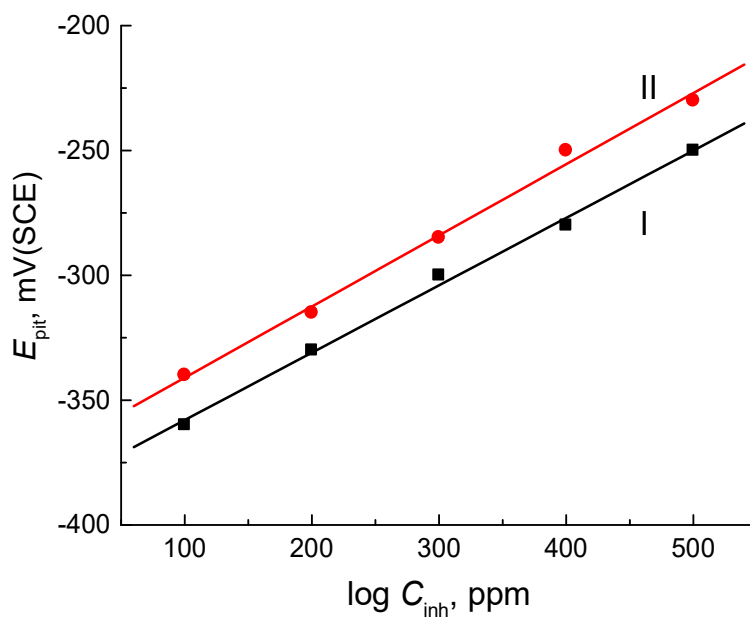


**Figure 7.** The relationship between  $E_{pit}$  and  $\log(\text{conc.})$  of polymer compounds: I) maltodextrin



and II) chitosan for C-steel in 1.0 M HCl + 0.1 M NaCl solution.

3.1.5. EIS Measurements

Nyquist plots of C-steel in 1.0 M HCl solution and in the presence of some concentrations of chitosan compound are shown in Figure 8. Similar curves in the presence of maltodextrin are obtained but not appeared here. It is clear from this figure, that in most of these cases the impedance diagram does not show a complete half-circle. This due to the frequency dispersion [39] as a result of roughness and homogeneity of steel surface. The increase in semicircle diameters with the concentration of two polymer compounds indicates an increase in the protective properties of C-steel surface. The impedance diagrams for two polymer compounds have a semicircular appearance; proving that C-steel corrosion is mainly controlled by a charge transfer process [40].

The equivalent circuit proposed by Randles has been used previously as mentioned above [41]. Two parameters were derived from analysis of Nyquist plots, the first parameter being the charge transfer resistance ( $R_{ct}$ ) obtained from the intercepts of the semicircle with the axis of the real component. The second parameter is the capacity of double layer ( $C_{dl}$ ) computed from the angular frequency ( $\omega = 2\pi f$ ) at the maximum imaginary component and the  $R_{ct}$  according to the following equation:

$$C_{dl} = [1/\omega_{max} R_{ct}] = [1 / 2\pi f_{max} R_{ct}] \tag{8}$$

where,  $f$  is frequency,  $\omega$  is the angular velocity.

The inhibition efficiency, %IE, was determined from the following equation:

$$\%IE = \left( 1 - \frac{(R_{ct})_{free}}{(R_{ct})_{add.}} \right) \times 100 \tag{9}$$

where,  $(R_{ct})_{free}$  and  $(R_{ct})_{add}$  are the charge transfer resistance in the free 1.0 M HCl solution and in the presence of the polymer compounds, respectively. Values of  $R_{ct}$ ,  $C_{dl}$  and %IE are inserted in Table 5.

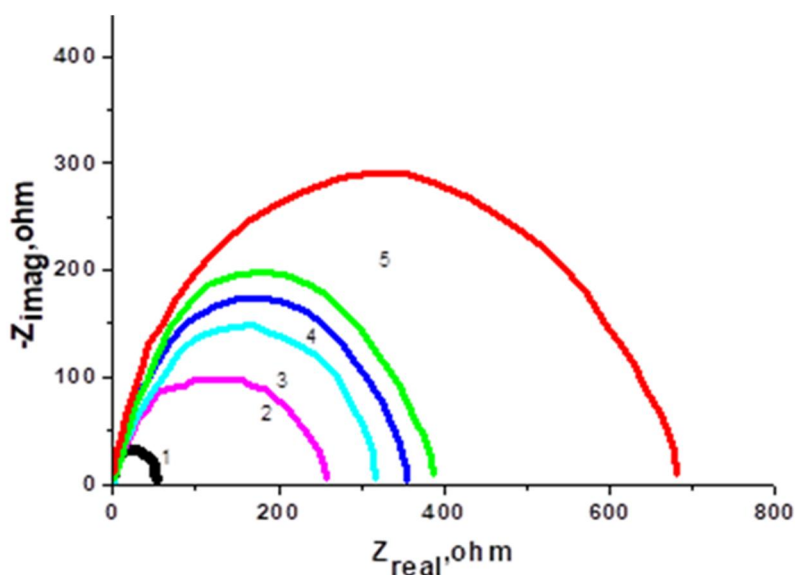


**Figure 8.** Nyquist plot of C-steel in 1.0 M HCl solution and in the presence of different concentrations (ppm) of chitosan: 1) 00.0 2) 100 3) 200 4) 300 5) 400 6) 500.

It was observed from Table 5 that with increasing the concentrations of the two polymer compounds, the  $R_{ct}$  values increase owing to the construction of protective film at the interface between the steel and electrolytic solution. On the other hand, the values of  $C_{dl}$  decreased due to the water molecules at the electrode interface are replaced by polymer compounds of lower dielectric constant through adsorption. Also, values of %IE of chitosan were set to more than those of maltodextrin. These results are in a good agreement with the previous measurements used.

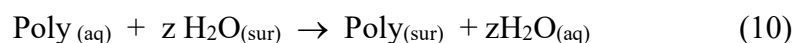
**Table 5.** Electrochemical parameters obtained by the EIS technique for C- steel in 1.0 M HCl solution and containing various concentrations of the examined polymer compounds.

Inhibitors	Inh. Conc. (ppm)	$C_{dl}$ , $\mu\text{F cm}^{-2}$	$R_{ct}$ , $\Omega \text{cm}^{-2}$	%IE
--	0	187	58	--
Maltodextrin	100	151	206	71.84
	200	147	249	76.70
	300	139	271	78.60
	400	132	286	79.72
	500	128	327	82.26
Chitosan	100	166	254	77.16
	200	158	311	81.35
	300	151	345	83.20
	400	148	371	84.36
	500	142	678	91.44

### 3.1.6. Adsorption Isotherm and Inhibition Mechanism

The inhibiting vigor of the two investigated polymeric compounds on the C-steel corrosion in 1.0 M HCl solution based on their adsorption onto the steel surface. The adsorption strength depends on the chemical structure and the molar mass of the studied polymer compounds, the chemical composition of the steel, the type of the aggressive acid, the pH value, the temperature and the electrochemical potential of the steel /electrolyte interface.

In theory, the adsorption process can be considered as replacement process between the polymer compounds in the aqueous phase [ $\text{Poly}_{(aq)}$ ] and water molecules at the carbon steel surface [ $\text{H}_2\text{O}_{(sur)}$ ] to give the polymer compounds adsorbed on the surface of carbon steel [ $\text{Poly}_{(sur)}$ ] and thus increased inhibition efficiency due to subsequent equation:



where,  $z$  is the size ratio and simply equals the number of adsorbed water molecules replaced by a single inhibitor molecule. In order to obtain the best isotherm match the results obtained. It was found that the obtained results obeyed Freundlich isotherm which governed by Eq. (11) [42]:

$$\log \theta = \log K_{\text{ads}} + n \log C_{\text{inh}} \quad (11)$$

where,  $K_{\text{ads}}$  and  $C_{\text{inh}}$  are the equilibrium constant for the adsorption and concentration of the polymer, respectively.

Figure 9 displays the relationship of Freundlich isotherm ( $\log \theta$  vs  $\log C_{\text{inh}}$ ) of C-steel electrode in 1.0 M HCl solution and containing various concentrations of two polymer compounds. Straight lines were obtained. From the intercept, the  $K_{\text{ads}}$  values are calculated which relates to the standard free energy of adsorption,  $\Delta G^{\circ}_{\text{ads}}$ , according to the following equation:

$$K_{\text{ads}} = 1/55.5 \exp(-\Delta G^{\circ}_{\text{ads}}/RT) \quad (12)$$

The computed values of  $\Delta G^{\circ}_{\text{ads}}$  are equal to  $-45.23 \text{ kJ mol}^{-1}$  and  $-52.18 \text{ kJ mol}^{-1}$  for maltodextrin and chitosan, respectively. The negative value of  $\Delta G^{\circ}_{\text{ads}}$  suggests spontaneous adsorption process and strong interaction of the two polymer compounds onto the carbon steel surface.

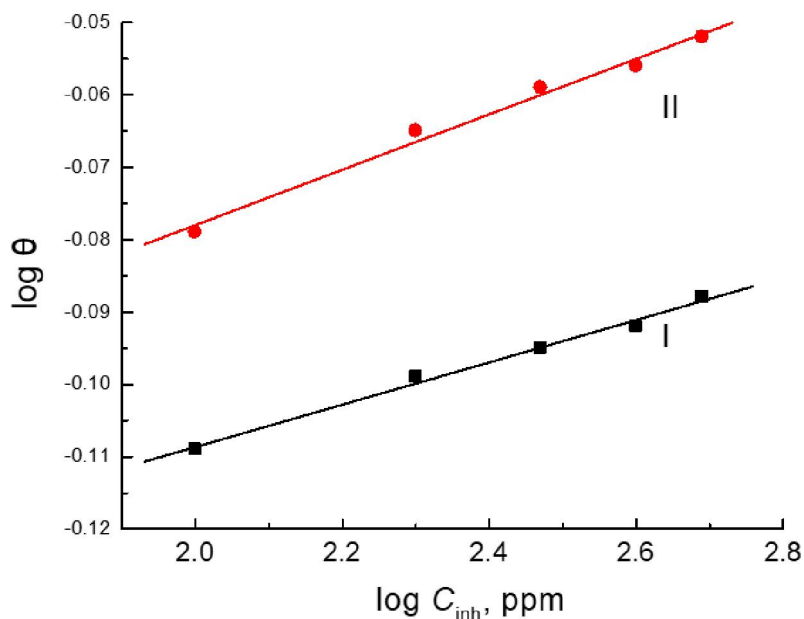


**Figure 9.** Freundlich isotherms for C-steel in 1.0 M HCl solution and in the presence of 500 ppm of: I) maltodextrin, II) chitosan.

The studied polymer compounds act as a good inhibitor for the carbon steel corrosion in 1.0 M HCl solution. The inhibition ability depends on the concentration, temperature, molar mass and chemical structure of the polymer compounds. The existence of some hetero oxygen atoms, OH group and  $\text{NH}_2$  facilitates the adsorption process by forming a coordination bond between the polymer compound and steel by transferring lone pairs of electrons from hetero oxygen atoms to the steel surface. The formed complex is blocked adsorbed onto the steel surface due the formation of more than one active centre. Among all four techniques used the %IE of chitosan is more efficient than maltodextrin. This is due to the possibility of a more complex formation in the chitosan molecule due to the presence of more than

an oxygen hetro atoms and the presence of many OH and NH<sub>2</sub> accelerates the adsorption process. Also, the molar mass of chitosan is higher than maltodextrin, which increases the surface area covered by the

polymer, which increases the inhibition efficiency. On the other hand, the obtained results in the present research work indicated that inhibitive impact of chitosan as a green corrosion inhibitor for carbon steel in the investigated corrosive medium was set to be higher than that obtained in previous work [43,44].

#### 4. CONCLUSIONS

1. The examined polymer compounds, maltodextrin and chitosan, were found to act as effective inhibitors to reduce the corrosion of C-steel 1.0 M HCl solution.
2. The inhibition efficiency increased with rising concentrations of polymer compounds and lowered with rising temperature.
3. The studied polymers were found to behave as mixed type inhibitors.
4. The inhibiting action of the investigated polymer compounds is due to their spontaneous adsorption on the surface of C-steel.
5. The adsorption of the inhibitors followed Freundlich isotherm.
6. The studied polymers acted as pitting corrosion inhibitors.
7. The inhibition efficiency of chitosan was found to higher than that of maltodextrin.

#### References

1. K. S. Jacob and G. Parameswaran, *Corros. Sci.*, 52 (2010) 224.
2. X. Tang, X. Yang, W. Yang, Y. Chen and R. Wan, *Corros. Sci.*, 52 (2010) 242.
3. A. El Defrawy, M. Abdallah and J. Al-Fahemi, *J. Mol. Liq.*, 288 (2019) 110994.
4. S. Deng, X. Li and H. Fu, *Corros. Sci.*, 53 (2011) 3596.
5. S. M. A. Hosseini, M. Salari, E. Jamalizadeh, S. Khezripoor and M. Seifi, *Mater. Chem. Phys.*, 119 (2010) 1008.
6. M. Abdallah, H. M. Al-Tass, A. M. Alharbi, N. F. Hasan, S. S. Al-Juaid and E. M. Mabrouk, *Egy. J. Petr.*, 28 (2019) 393.
7. R. S. Abdel Hameed and M. Abdalla, *Prot. Met. Phys. Chem. Surf.*, 54 (2018) 113.
8. M. Abdallah, H.M. Al-Tass, B.A.AL Jahdaly and A. S. Fouda, *J. Mol. Liq.*, 216 (2016) 590.
9. M. Sobhi, R, El-Sayed and M. Abdallah, *J. Surf. Deterg.*, 16 (2013) 937.
10. A. Fawzy, M. Abdallah, M. Alfakeer and H. M. Ali, *Int. J. Electrochem. Sci.*, 14 (2019) 2063.
11. M. Hegazy, M. Abdallah, M. Alfakeer, H. Ahmed, *Int J Electrochem Sci.*, 13 (2018) 6824.
12. M. Alfakeer, M. Abdallah and R.S. Abdel Hameed, *Prot. Met. Phys. Chem. Surf.*, 54 (2020) 225.
13. M. Hegazy, M. Abdallah and H. Ahmed, *Corros. Sci.*, 52 (2010) 2897.
14. E. F. Heakel and A.E. Elkoly, *J. Mol. Liq.*, 230 (2017) 395.
15. P. B. Raja and M. G. Sethuraman, *Mater. Lett.*, 62 (2008) 113.
16. O. K. Abiola, J.O.E. Otaigbe and O.J. Kio, *Corros. Sci.*, 51 (2009) 1879.
17. M. Abdallah, H. M. Al-Tass, B. A. AL Jahdaly and M. M. Salem, *Green Chem. Lett. Rev.*, 11 (2018) 189.
18. G. Khan, K. Md. S. Newaz, W. J. Basirun, H. B. M. Ali, F. L. Faraj and G. M. Khan, *Int. J. Electrochem. Sci.*, 10 (2015) 6120.

19. C. Verma, E. E. Ebenso, I. Bahadur and M. A. Quraishi, *J. Mol. Liq.*, 266 (2018) 577.
20. S. Marzorati, L. Verotta and S. P. Trasatti, *Molecules*, 24 (3019) 48.
21. M. Alfakeer, M. Abdallah and A. Fawzy, *Int. J. Electrochem. Sci.*, 15 (2020) 3283.
22. M. Abdallah, M. Alfakeer, A. M. Alonazi and S. S. Al-Juaid, *Int. J. Electrochem. Sci.*, 14 (2019) 10227.
23. J. H. Al-Fahemia, M. Abdallah, E. A. M. Gad and B. A. AL Jahdaly, *J. Mol. Liq.* 222 (2016) 1157.
24. C. Verma, D. S. Chauhan and M. A. Quraishi, *J. Mater. Env. Sci.*, 8 (2017) 4040.
25. M. Abdallah and M. M. El-Naggar, *Mater. Chem. Phys.*, 71 (2001) 291.
26. D. E. Arthur, A. Jonathan, P. O. Ameh and C. Anya, *Int. J. Ind. Chem.*, 4 (2013) 2.
27. G. H. Sedahmed, M. N. Soliman and N. S. El-Kholy, *J. Appl. Electrochem.*, 12 (1982) 479.
28. K. S. Khairou and A. El Sayed, *J. Appl. Poly. Sci.*, 88 (2003) 866.
29. A. Fawzy, I. A. Zaaferany, H. M. Ali and M. Abdallah, *Int. Electrochem. Sci.*, 13 (2018) 4575.
30. I. Putilova, S. Balezin, I. N. Barannik and V. P. Bioshop, *Metallic Corrosion Inhibitors*, Pergamon, Oxford, 1960, p. 196.
31. O. L. Riggs and R. M. Hurd, *Corrosion*, 23 (1967) 252.
32. K. J. Laidler, "Chemical Kinetics", Mc Graw Hill Publishing Company Ltd (1965).
33. M. Abdallah, O. A. Hazzazi, A. F. Saad, S. El-Shafei and A. S. Fouda, *Prot. Met. Phys Chem. Surf.*, 50 (2014) 659.
34. X. M. Abdallah and B. A. Al Jahdaly, *Int. J. Electrochem. Sci.*, 10 (2015) 9808.
35. M. Abdallah and A. I. Mead, *Ann. di Chimica*, 83 (1993) 424.
36. M. Abdallah, S. O. Al Karane and A. A. Abdel Fattah, *Chem. Eng. Commun.*, 196 (2009) 1406.
37. M. Abdallah, S. O. Al Karane and A. A. Abdel Fattah, *Chem. Eng. Commun.*, 197 (2010) 1446.
38. M. Abdallah, I. Zaaferany, K. S. Khairou and Y. Emad, *Chem. Tech. Fuels Oils*, 48 (2012) 234.
39. K. Juttner, *Electrochim. Acta*, 35 (1990) 1501.
40. A. Fawzy, M. Abdallah, I. A. Zaaferany, S. A. Ahmed and I. I. Althagafi, *J. Mol. Liq.*, 265 (2018) 276.
41. M. Abdallah, I. Zaaferany, J. H. Al-Fahemi, Y. Abdallah and A.S. Fouda, *Int. J. Electrochem. Sci.*, 7 (2012) 6622.
42. F. M. Al-Nowaiser, M. Abdallah and E. H. El-Mossalamy, *Chem. Tech. Fuels .Oils*, 47 (2012) 453.
43. S.A.Umoren, M.J.Banera, T.Alonso-Garcia, C.A.Gervasi and M.V.Mirifico, *Cellulose*, 20(2013)
44. M. N. El-Haddad, *Int. J. Biological. Macromol.*, 55(2013)142.

# CONTENTS

# CONTENTS

List of Figures.....	I
List of Table.....	V

## Chapter (1):Introduction

1.1 .Definition of corrosion.....	1
1.2. Various forms of corrosion.....	1
1.3.Theories of corrosion.....	4
1.4.Corrosion monitoring techniques.....	14
1.5.corrosion inhibitor.....	14
1.6.Literature survey for corrosion inhibition of carbon steel In aqueous solution.....	19
1.6.1.Organic compound as corrosion inhibitor.....	19
1.6.2.Inorganic as corrosion inhibitor.....	36
1.6.3.Drugs as corrosion inhibitors.....	38
1.6.4.Surfactant as corrosion inhibitors.....	40
1.6.5.Natural compound as corrosion inhibitor.....	42
1.6.6.Polymer as corrosion inhibitor.....	50
Aim of the Present Work.....	54

## Chapter (2): Experimental Techniques

2.1.Chemical composition of carbon steel.....	56
2.2. Chemical additives and solution.....	56
2.3. The chemical structure of polymer and uses.....	57
2.4.Experimental techniques.....	61
2.5.Electrochemical cell.....	63
2.6.Electrodes.....	64

## Chapter (3):Results and Discussion

## Part(A)

Studying the Corrosion Behavior of C-Steel in Aqueous Solutions by the  
Weight Loss Measurements

3.1- Weight loss measurements.....	66
3.1.2.Effect of temperature on corrosion processes.....	82

## Part(B)

Studying the Corrosion Behavior of C-Steel in Aqueous Solutions by  
Galvanostatic polarization technique

3.2.Galvanostatic polarization technique.....	101
---	-----

## Part (C)

Studying the Corrosion Behavior of C-Steel in Aqueous Solutions by  
Potentiodynamic anodic polarization technique

3.3.1- Effect of NaCl concentration on the pitting curves of carbon steel in 1.0M HCl solution.....	117
3.3.2. Effect of addition of some polymer compounds on the pitting corrosion of carbon steel.....	123

## Part(D)

Studying the Corrosion Behavior of C-Steel in Aqueous Solutions by  
Impedance spectroscopy

3.4. The electrochemical impedance spectroscopy (EIS).....	133
--	-----

## Part (E)

3.5.Mechanism of inhibition and Adsorption Isotherm.....	149
--	-----

summary.....	154
--------------	-----

References.....	161
-----------------	-----

Arabic summary.....	173
---------------------	-----



## List of Figures

Figures title	page
Fig.(1.1): The basic corrosion cell consists of an anode, a cathode, an electrolyte, and a metallic path for electron flow. Note that the corrosion current ( $i$ ) enters the electrolyte at the anode and flows to the cathode	6
Fig.(2.1): Schematic diagram of Electrochemical cell.....	63
Fig.(2.2): Schematic diagram of the working electrode.....	64
Fig.(3.1):Weight loss-time curves for corrosion of carbon steel in 1.0 HCl solution containing various concentration of compound I.....	70
Fig.(3.2):Weight loss-time curves for corrosion of carbon steel in 1.0 HCl solution containing various concentration of compound II.....	71
Fig.(3.3):Weight loss-time curves for corrosion of carbon steel in 1.0 HCl solution containing various concentration of compound III...	72
Fig.(3.4):Weight loss-time curves for corrosion of carbon steel in 1.0 HCl solution containing various concentration of compound IV....	73
Fig(3.5):Weight loss-time curves for corrosion of carbon steel in 1.0 HCl solution containing various concentration of compound V.....	74
Fig(3.6):Weight loss-time curves for corrosion of carbon steel in 1.0 HCl solution containing various concentration of compound VI.....	75
Fig.(3.7):Weight loss-time curves for carbon steel in 1.0 M HCl solution containing 500 ppm of compound I at different temperatures.	85

Fig.(3.8):Weight loss-time curves for carbon steel in 1.0 M HCl solution containing 500 ppm of compound II at different temperatures.	86
Fig.(3.9):Weight loss-time curves for carbon steel in 1.0 M HCl solution containing 500 ppm of compound III at different temperatures.	87
Fig.(3.10):Weight loss-time curves for carbon steel in 1.0 M HCl solution containing 500 ppm of compound IV at different temperatures.	88
Fig.(3.11):Weight loss-time curves for carbon steel in 1.0 M HCl solution containing 500 ppm of compound V at different temperatures.	89
Fig.(3.12):Weight loss-time curves for carbon steel in 1.0 M HCl solution containing 500 ppm of compound VI at different temperatures.	90
Fig.(3.13):Arrhenius plots for corrosion of carbon steel in free and inhibited 1.0M HCl solution.	91
Fig.(3.14):Transtion state plot for corrosion of carbon steel in free and inhibited 1.0 M HCl solution.	92
Fig.(3.15):Galvanostatic polarization curves for C-steel in 1.0M HCl solution in presence and absence of various concentrations of compound I at 30°C. ppm (2)100 ppm (3)200 ppm (4)300 ppm (5)400 ppm 0.0(1) (6)500 ppm.	105
Fig.(3.16):Galvanostatic polarization curves for C-steel in 1.0M HCl solution in presence and absence of various concentrations of compound II at 30°C. (1)0.0 ppm (2)100 ppm (3)200 ppm (4)300 ppm (5)400 ppm (6)500 ppm. 104	106
Fig.(3.17):Galvanostatic polarization curves for C-steel in 1.0M HCl solution in presence and absence of various concentrations of compound III at 30°C. (1)0.0ppm (2)100 ppm (3)200 ppm (4)300 ppm (5)400 ppm (6)500 ppm.	107
Fig.(3.18):Galvanostatic polarization curves for C-steel in 1.0M HCl solution in presence and absence of various concentrations of compound IV at 30°C. (1)0.0 ppm (2)100 ppm (3)200 ppm (4)300 ppm (5)400 ppm (6)500 ppm.	108

Fig(3.19):Galvanostatic polarization curves for C-steel in 1.0M HCl solution in presence and absence of various concentrations of compound V at 30°C. (1)0.0ppm (2)100 ppm (3)200 ppm (4)300 ppm (5)400 ppm (6)500 ppm.	109
Fig(3.20):Galvanostatic polarization curves for C-steel in 1.0M HCl solution in presence and absence of various concentrations of compound VI at 30°C. (1)0.0ppm (2)100 ppm (3)200 ppm (4)300 ppm (5)400 ppm (6)500 ppm.	110
Fig.( 3.21): Potentiodynamic anodic polarization curves of C-steel in different concentrations of NaCl solutions at a scan rate $1\text{mV sec}^{-1}$ 1)0.5 M, 2) 0.1 M , 3)0.05M, 4) 0.01 M 5) 0.001M.	121
Fig.(3.22)The relation between $E_{\text{pitt}}$ and logarithm of chloride ion concentration.	122
Fig.(3.23) Potentiodynamic anodic polarization curves of C-steel in 1.0 M HCl + 0.1 M NaCl solution containing different concentrations of compound I at a scan rate of $1\text{mV sec}^{-1}$ . (1)0.0 ppm (2)100 ppm (3)200 ppm (4)300 ppm (5)400 ppm (6)500 ppm.	126
Fig.(3.24) Potentiodynamic anodic polarization curves of C-steel in 1.0 M HCl + 0.1 M NaCl solution containing different concentrations of compound II at a scan rate of $1\text{mV sec}^{-1}$ . (1)0.0 ppm (2)100 ppm (3)200 ppm (4)300 ppm (5)400 ppm (6)500 ppm.	127
Fig.(3.25) Potentiodynamic anodic polarization curves of C-steel in 1.0 M HCl + 0.1 M NaCl solution containing different concentrations of compound III at a scan rate of $1\text{mV sec}^{-1}$ . (1)0.0 ppm (2)100 ppm (3)200 ppm (4)300 ppm (5)400 ppm (6)500 ppm.	128
Fig.(3.26) Potentiodynamic anodic polarization curves of C-steel in 1.0 M HCl + 0.1 M NaCl solution containing different concentrations of compound IV at a scan rate of $1\text{mV sec}^{-1}$ . (1)0.0 ppm (2)100 ppm (3)200 ppm (4)300 ppm (5)400 ppm (6)500 ppm.	129

Fig.(3.27) Potentiodynamic anodic polarization curves of C-steel in 1.0 M HCl + 0.1 M NaCl solution containing different concentrations of compound V at a scan rate of $1\text{mV sec}^{-1}$ . (1)0.0 ppm (2)100 ppm (3)200 ppm (4)300 ppm (5)400 ppm (6)500 ppm.	130
Fig.(3.28) Potentiodynamic anodic polarization curves of C-steel in 1.0 M HCl + 0.1 M NaCl solution containing different concentrations of compound VI at a scan rate of $1\text{mV sec}^{-1}$ . (1)0.0 ppm (2)100 ppm (3)200 ppm (4)300 ppm (5)400 ppm (6)500 ppm.	131
Fig.(3.29) Variation of $E_{\text{pitt}}$ of carbon steel electrode versus $\log C_{\text{inh}}$	132
Fig.(3.30).Nyquist plot of C-steel in 1.0M HCl solution in absence and presence of different concentrations of compound I. (1) 0.00 ppm (2) 100 ppm (3) 200 ppm (4) 300 ppm (5)400 ppm.(6)500ppm	137
Fig.(3.31).Nyquist plot of C-steel in 1.0M HCl solution in absence and presence of different concentrations of compound II. (1) 0.00 ppm (2) 100 ppm (3) 200 ppm (4) 300 ppm (5)400 ppm.(6)500ppm	138
Fig.(3.32).Nyquist plot of C-steel in 1.0M HCl solution in absence and presence of different concentrations of compound III. (1) 0.00 ppm (2) 100 ppm (3) 200 ppm (4) 300 ppm (5)400 ppm.(6)500ppm	139
Fig.(3.33).Nyquist plot of C-steel in 1.0M HCl solution in absence and presence of different concentrations of compoundIV. (1) 0.00 ppm (2) 100 ppm (3) 200 ppm (4) 300 ppm (5)400 ppm.(6)500ppm	140
Fig.(3.34).Nyquist plot of C-steel in 1.0M HCl solution in absence and presence of different concentrations of compound V. (1) 0.00 ppm (2) 100 ppm (3) 200 ppm (4) 300 ppm (5)400 ppm.(6)500ppm	141
Fig.(3.35).Nyquist plot of C-steel in 1.0M HCl solution in absence and presence of different concentrations of compoundVI. (1) 0.00 ppm (2) 100 ppm (3) 200 ppm (4) 300 ppm (5)400ppm .(6)500ppm	142
Fig.(3.36) Freundlich isotherms for corrosion of carbon steel in inhibited 1.0 M HCl solution	152

## List of tables

Table title	page
Table(3.1): Corrosion parameters obtained from weight loss measurements of C-steel in a 1.0M HCl solution devoid of and contain different concentrations of compound I.	76
Table(3.2): Corrosion parameters obtained from weight loss measurements of C-steel in a 1.0M HCl solution devoid of and contain different concentrations of compound II.	77
Table(3.3): Corrosion parameters obtained from weight loss measurements of C-steel in a 1.0M HCl solution devoid of and contain different concentrations of compound III.	78
Table(3.4): Corrosion parameters obtained from weight loss measurements of C-steel in a 1.0M HCl solution devoid of and contain different concentrations of compound IV.	79
Table(3.5): Corrosion parameters obtained from weight loss measurements of C-steel in a 1.0M HCl solution devoid of and contain different concentrations of compound V.	80
Table(3.6): Corrosion parameters obtained from weight loss measurements of C-steel in a 1.0M HCl solution devoid of and contain different concentrations of compound IV.	81
Table(3.7):Variation of corrosion rate( $R_{corr}$ )of carbon steel in 1.0M HCl solution at different temperature.	93
Table(3.8):Variation of corrosion rate( $R_{corr}$ ),degree of surface coverage( $\Theta$ ),and percentage of inhibition efficiency (I.E%) of carbon steel in 1.0M HCl solution containing 500ppm of compound I at different temperatures.	94
Table(3.9):Variation of corrosion rate( $R_{corr}$ ),degree of surface coverage( $\Theta$ ),and percentage of inhibition efficiency (I.E%) of carbon steel in 1.0M HCl solution containing 500ppm of compound II at different temperatures.	95
Table(3.10):Variation of corrosion rate( $R_{corr}$ ),degree of surface coverage( $\Theta$ ),and percentage of inhibition efficiency (I.E%) of carbon steel in 1.0M HCl solution containing 500ppm of compound III at different temperatures.	96
Table(3.11):Variation of corrosion rate( $R_{corr}$ ),degree of surface coverage( $\Theta$ ),and percentage of inhibition efficiency (I.E%) of carbon steel in 1.0M HCl solution containing 500ppm of compound IV at different temperatures.	97

Table(3.12):Variation of corrosion rate( $R_{corr.}$ ),degree of surface coverage( $\Theta$ ),and percentage of inhibition efficiency (I.E%) of carbon steel in 1.0M HCl solution containing 500ppm of compound V at different temperatures.	98
Table(3.13):Variation of corrosion rate( $R_{corr.}$ ),degree of surface coverage( $\Theta$ ),and percentage of inhibition efficiency (I.E%) of carbon steel in 1.0M HCl solution containing 500ppm of compound VI at different temperatures.	99
Table(3.14):Activation thermodynamic parameters for carbon steel 1.0M HCl solution in the absence and presence of 500ppm of the studied inhibitors.	100
Table(3.15):Effect of increasing the concentration of compound I on the corrosion kinetic parameters obtained from galvanostatic polarization measurements of carbon steel in 1.0M HCl solution.	111
Table(3.16):Effect of increasing the concentration of compound II on the corrosion kinetic parameters obtained from galvanostatic polarization measurements of carbon steel in 1.0M HCl solution.	112
Table(3.17):Effect of increasing the concentration of compound III on the corrosion kinetic parameters obtained from galvanostatic polarization measurements of carbon steel in 1.0M HCl solution.	113
Table(3.18):Effect of increasing the concentration of compound IV on the corrosion kinetic parameters obtained from galvanostatic polarization measurements of carbon steel in 1.0M HCl solution.	114
Table(3.19):Effect of increasing the concentration of compound V on the corrosion kinetic parameters obtained from galvanostatic polarization measurements of carbon steel in 1.0M HCl solution.	115
Table(3.20):Effect of increasing the concentration of compound VI on the corrosion kinetic parameters obtained from galvanostatic polarization measurements of carbon steel in 1.0M HCl solution.	116

Table(3.21):Electrochemical parameters obtained by EIS measurements of carbon steel electrode in 1.0M HCl solution at different concentrations of compound I.	143
Table(3.22):Electrochemical parameters obtained by EIS measurements of carbon steel electrode in 1.0M HCl solution at different concentrations of compound II.	144
Table(3.23):Electrochemical parameters obtained by EIS measurements of carbon steel electrode in 1.0M HCl solution at different concentrations of compound III.	145
Table(3.24):Electrochemical parameters obtained by EIS measurements of carbon steel electrode in 1.0M HCl solution at different concentrations of compound IV.	146
Table(3.25):Electrochemical parameters obtained by EIS measurements of carbon steel electrode in 1.0M HCl solution at different concentrations of compound V.	147
Table(3.26):Electrochemical parameters obtained by EIS measurements of carbon steel electrode in 1.0M HCl solution at different concentrations of compound VI.	148
Table (3.27 ): The values $K_{ads}$ and $\Delta G^{\circ}_{ads}$ for C-steel in 1.0 M HCl solution in the absence and presence of 500 ppm of the studied polymer compounds.	153

**CHAPTER (1)**  
**INTRODUCTION**



بِسْمِ اللَّهِ الرَّحْمَنِ الرَّحِيمِ

## ***INTRODUCTION***

### **1.1. Definition of corrosion**

Corrosion can be defined as “an unwanted chemical attack on a metal from its surroundings”. Corrosion is an electrochemical process, including metals and electrolytes[1] . All corrosion reactions are obeying the thermodynamic laws. Except for noble metals such as gold and platinum, all other metals corrode and transform into substances like their mineral ores from which they are extracted. It is important to note that, the developed countries suffer an annual loss equivalent to 2-4% of their GNP due to corrosion[2] . Approximately 20-25% can be avoided by using appropriate anticorrosion technology. Various preventive measures are used against metallic corrosion.

### **1.2. Various forms of corrosion**

Corrosion can manifest itself in the following main forms:

#### **1.2.1-General and local electrochemical corrosion[3]**

When separate corrosion cells can be distinguished by variation of the electrode potential over the metal surface, or by the appearance of corrosion currents or of separate anodic and cathodic corrosion products, local electrochemical corrosion is said to occur.

General electrochemical corrosion occurs when separate anodic surfaces do not appear or are of small dimensions ( sub micro cells ) or fluctuate over the surfaces, the attack will be more uniform. Thus, there are possibilities for corrosion products to form a continuous film and delay the continuous attack. Therefore, general electrochemical corrosion leads to uniform attack whereas local electrochemical corrosion leads to localized attacks.

Many researchers [4,5] have demonstrated that galvanic corrosion is directly proportional to the ratio of the area of the cathode metal to the anode metal, and that galvanic corrosion is the maximum at the intersection of the two metals. The attack decreases as the distance from the intersection increases.

### **1.2.2-Galvanic corrosion or dissimilar metal corrosion**

Galvanic corrosion occurs when two or more dissimilar metals in electrical contact are placed in an electrolyte. This leads a potential difference between the metals which results in the flow of current between them.

### **1.2.3.Crevice corrosion[6,7]**

This has happened in some mineral environment combinations. Only metals and alloys that rely on oxide film for corrosion resistance subject to crevice corrosion. It is an intense localized corrosive attack that occurs within a narrow space or crevices caused by certain mechanical configurations. It is produced by surface deposits of corrosion products, scratches in paint films, etc.

### **1.2.4.Filiform corrosion [2]**

This is a special type of crevice corrosion that produces irregular developed hair- fine lines or filaments of corrosion products below coatings of paints, tin, silver, etc. It does not destroy the component, but it does affect the appearance of the surface.

### **1.2.5-Intergranular corrosion[8]**

Hence, localized attack occurs at adjacent to grain boundaries with relatively little corrosion of the matrix. This attack is usually rapid and penetrates deep into the metal resulting in loss of strength and causing catastrophic failures.

Most metals and alloys are subject to intergranular corrosion, when exposed to specific corrodents. The corrosion of iron, nickel and chromium alloys is mostly due to its commercial importance. Several reviews[9-11] have appeared on this topic.

#### **1.2.6-Pitting corrosion**

This is also a form of intensive localized attack, the rate of attack being nonuniform. It is most destructive form of corrosion and results in sudden failure of the equipment due to the formation of pits or holes. It is said to occur in the presence of chloride ions depending upon the concentration of chloride ions[11-14].

Loss of minerals as layers or sheets of solid metal or peeling alloy is called. This type is mostly observed in wrought products. Moreover, Al-Mg, Al-Cu, Al-Zn and Al-Mg-Si alloys are subjected to peeling.

#### **1.2.7-Exfoliation[15]**

The loss of metals as layers or leaves from a solid metal or alloy is called exfoliation. This type is observed mostly in wrought products. Further Al- Mg, Al- Cu, Al- Zn and Al- Mg- Si alloys undergo exfoliation.

#### **1.2.8-Stress corrosion cracking[16- 18]**

The cracking of metal or alloy due to the simultaneous presence of tensile stress and a specific corrosive environment is known as stress corrosion cracking.

#### **1.2.9-Corrosion fatigue cracking[18,19]**

Reduction in the fatigue strength due to the presence of a corrosive environment is known as corrosion fatigue cracking. It occurs due to the combined action of cyclic stress and corrosive environment.

### **1.2.10-Fretting corrosion[20]**

This type of corrosion occurs between two surfaces in contact with each other in dry or humid air when exposed to slight relative motion of small amplitude. Various alternate terms such as friction oxidation, wear oxidation, chafing. False brinelling are used to describe this phenomenon.

### **1.2.11-Erosion corrosion**

Erosion corrosion is defined as an increase in the rate of corrosion to the relative movement between the metal surface and the liquid or gaseous environments. This type of corrosion is also known as impingement corrosion[20]. This corrosion occurs in agitators, copper pipes, centrifuge etc. Localized attack due to erosion corrosion usually has bright surface from corrosion products. eg. Pits, rounded holes and valleys.

### **1.2.12-Cavitation corrosion[21]**

This is a special type of erosion corrosion caused by the formation of vapor bubbles in a corrosive environment near a metal surface and when a bubbles collapse attack arises. For example, hydraulic turbulence, ship propellers etc.

## **1.3.Theories of corrosion**

Corrosion of metals in aqueous solutions is an electrochemical process as established in the first half of the nineteenth century. Whitney[22]gave the most widely accepted electrochemical theory. the other theories such as acid theory[23] chemical attack theory, colloidal theory[24,25] and biological theory[26] have been established regardless of electrochemical theory

## Electrochemical theory of corrosion

An atom has a massive positively charged central nucleus surrounded by a cloud of negatively charged electrons. This electron cloud is absorbed in a series of shells. The outer shell must contain eight electrons in the case of the most stable element. If the electrons are insufficient to fill the outer most shell, the atom tends to obtain a cloud of complete shells by gaining or losing electrons to cause modified atoms called 'ions

Evans[27] explained the role of these ions in the corrosion of metals and alloys under the influence of the exchange of ionic charges. This has laid down the basis of the electrochemical theory of corrosion. When a metal object is immersed in a corrosive medium the metallic surface is divided into regions with different potentials under the influence of different metallic phases, grain boundaries stress and strain, impurities etc. in the electrolyte the metal under disintegration due to the displacement of a hydrogen ions in the electrolyte by those of the anode metal, resulting in the formation of a galvanic cell.

*a-* Corrosion occurs by an electrochemical process. the phenomenon is like that which takes place when a carbon-zinc “dry” cell generates a direct current. basically, an anode (negative electrode), a cathode (positive electrode), an electrolyte (environment), and a circuit connecting the anode and the cathode are required for corrosion to occur (see fig.(1.1)). dissolution of metal occurs at the anode where the corrosion current enters the electrolyte and flows to the cathode. the general reaction (reactions, if an alloy is involved) that occurs at the anode is the dissolution of metal as ions:

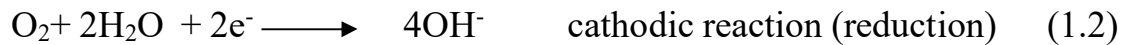


where

m = metal involved

n = valence of the corroding metal species

Examination of this fundamental reaction reveals that a loss of electrons, or oxidation, occurs at the anode. Electrons are lost at the anode, flow through the metallic circuit to the cathode and allow a cathodic reaction (or reactions) to occur. In alkaline and neutral aerated solutions, the predominant cathodic reaction is



the cathodic reaction that usually occurs in deaerated acids is

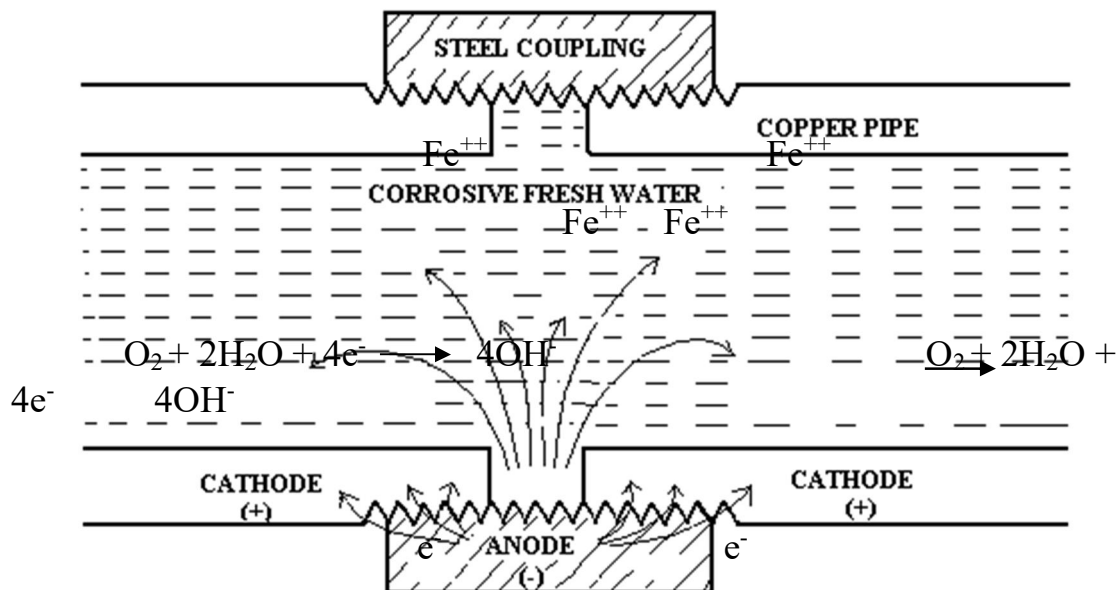


Fig.(1.1): The basic corrosion cell consists of an anode, a cathode, an electrolyte, and a metallic path for electron flow. Note that the

corrosion current ( $i$ ) enters the electrolyte at the anode and flows to the cathode.

In aerated acids, the cathodic reaction could be



All these reactions involve a gain of electrons and a reduction process.

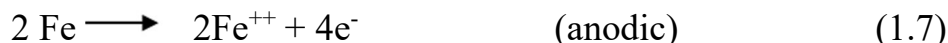
*b-* The number of electrons lost at the anode must equal the number of electrons gained at the cathode. For example, if iron (Fe) was exposed to an aerated, corrosive water, the anodic reaction would be



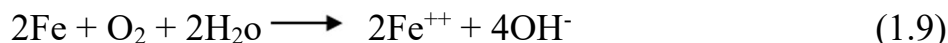
At the cathode, reduction of oxygen would occur



because there can be no net gain or loss of electrons, two atoms of iron must dissolve to provide the four electrons required at the cathode. thus, the anodic and cathodic reactions would be



these can be summed to give the overall oxidation reduction reaction



c- After dissolution, ferrous ions ( $\text{Fe}^{++}$ ) generally oxidize to ferric ions ( $\text{Fe}^{+++}$ ); these will combine with hydroxide ions ( $\text{OH}^-$ ) formed at the cathode to give a corrosion product called rust ( $\text{FeOOH}$  or  $\text{Fe}_2\text{O}_3 \cdot \text{H}_2\text{O}$ ).

## 1.4. Corrosion monitoring techniques.

### 1.4.1 Non-electrochemical techniques.

#### (i) Thermometric method:

A simple, fast and specific method for comparing the inhibition efficiency of different additional agent[28]. It was originally developed for iron and its alloys. According to this test, a piece of metal of specified area is dropped into a definite volume of a corrosive solution. The variation of the temperature of the system is followed by a function of time. After an initial period of approximately constant temperature, they rise rapidly to reach a maximum value, which in some cases approaches the boiling point of the solution. A reaction number, R.N., was defined by Mylius as follow:

$$\text{R.N.} = \frac{T_m - T_i}{t} \quad \text{K/min} \quad (1.10)$$

where:  $T_m$  = maximum temperature in K.

$T_i$  = initial temperature in K.

$t$  = time in minutes from the start of the experimental to attain  $T_m$ .

The reaction number is proportional to the rate of the corrosion of the metal. The extent of corrosion inhibition by a certain concentration of additive is evaluated from the percentage reduction in the reaction number.

$$\% \text{ Reduction in R.N.} = \frac{(\text{R.N.})_{\text{free}} - (\text{R.N.})_{\text{add}}}{(\text{R.N.})_{\text{free}}} \quad (1.11)$$

where,  $(\text{R.N.})_{\text{free}}$  = reduction in R.N. in the corrosive medium.

$(\text{R.N.})_{\text{add}}$  = reduction in R.N. in the presence of additive.



**(ii) Hydrogen evolution method:**

Reactions in which gases are given off or taken up can be monitored by studying the change of gas amount over time. This method is also limited. The efficiency of a given inhibitor can be evaluated as the percentage reduction in reaction rate (K), so the percentage inhibition efficiency (%IE) can be calculated as follows:

$$\% \text{ IE} = \frac{K_{\text{free}} - K_{\text{add}}}{K_{\text{free}}} \times 100 \quad (1.12)$$

where:  $K_{\text{free}}$  = specific reaction rate in the corrosive medium.

$K_{\text{add}}$  = specific reaction rate in the inhibited solutions.

and specific reaction rate constants (K) are calculated from the relation,

$V = K.t$ , where, (V) is the volume of hydrogen evaluated in  $\text{cm}^3$  and (t) is the time in minutes.

**(iii) Weight loss method:**

Weight loss measurements are comprehensive tests for laboratory and field [29-34]. It is useful for metals or alloys, which are not subjected to special types of attack and form, which corrosion products can be removed easily. To determine the inhibition efficiency of inhibitor using these measurements, the metal sample must be polished, degreased, weighed and then immersed in the corrosive medium with and without inhibitor for certain time intervals at fixed temperature. Weight loss is determined after removing corrosion products and then thoroughly wash the specimens by distilled water dry and weight.

The efficiency of inhibition is calculated from the weight loss values using the following equation:

$$\% \text{ IE} = \frac{W_{\text{free}} - W_{\text{add}}}{W_{\text{free}}} \times 100 \quad (1.13)$$

where,  $W_{\text{free}}$  = weight loss in the corrosive medium in  $\text{mg cm}^{-2}$ .

$W_{\text{add.}}$  = weight loss in the inhibited solutions in  $\text{mg cm}^{-2}$ .

Also, the corrosion rate is determined by the relationship:

$$\text{C. R. (mmpy)} = \frac{\text{wt. loss (mg)} \times 87.6}{\text{area (cm}^{-2}\text{)} \times \text{time (hrs)} \times \text{d (gm.c m}^{-3}\text{)}} \times 100 \quad (1.14)$$

***(iv) Electrical resistance method:***

This method involves the measurements of the change in the resistance of corroded metal by the equation:[29-33]

$$R_{\text{metal}} = \frac{\rho \times L}{A} \quad (1.15)$$

where,  $R_{\text{metal}}$  = resistance of metal.

$\rho$  = specific resistance.

$A$  = area of cross section.

On corrosion, the area of specimen ( $A$ ) is decreased. Hence the resistance ( $R$ ) is increased. This means that the change in  $R$  value is correlated to corrosion rate (Kelvin or Wheatstone bridge).

**1.4.2 Electrochemical techniques.**

***(i) Open circuit potential method:***

This method is used to measure the steady state potential ( $E_{\text{ocp}}$ ), of the metal or alloy in the absence and in the presence of additives[35]. In this method, the potential of the corroding material is measured against reference electrode at different time periods until a steady state is reached. The steady state represents an equilibrium state at which ( $I_{\text{ox.}}$ ) is equal ( $i_{\text{red}}$ ).

***(ii) Potentiodynamic polarization method:***

***(a) Tafel plots.***

In this method, corrosion current can be determined from polarization curves by intercept method based on anodic and / or cathodic Tafel curves[36-37]. The corrosion rate of the system involves the measurements of potential of the working electrode for various applied current densities.

The relation between (E) against log (i) gives polarization diagram (Tafel plot). The intercept of anodic and cathodic Tafel lines provides the corrosion current and Tafel slopes give anodic ( $b_a$ ) and cathodic ( $b_c$ ) Tafel slopes.

*(b) Linear polarization method.*

This technique is an accepted method of monitoring corrosion rate[37-41]. For a corroding electrode, the polarization resistance ( $R_p$ ), at small applied range of potential (5-20 mV) is related to the corrosion current density ( $i_{corr.}$ ) by the equation:

$$i_{corr} = \frac{b_a \cdot b_c}{2.3(b_a + b_c)} \times \frac{1}{R_p} = \frac{B}{R_p} \quad (1.16)$$

where,  $b_a$  and  $b_c$  are anodic and cathodic Tafel slopes respectively and  $R_p$  is the polarization resistance.

A controlled potential scan is applied over a small range, typically  $\pm 25$  mV with respect to  $E_{corr}$ . At a scan rate of 0.1 mV/sec, the resulting current is plotted against the potential. The slope of this linear potential-current plot at  $E_{corr}$  is identical with the polarization resistance which used together with the measured Tafel constants to determine the rate of corrosion.

The percentage inhibition efficiency (%IE) can be expressed as:

$$\% \text{ IE} = \frac{i_{\text{free}} - i_{\text{add}}}{i_{\text{free}}} \times 100 \quad (1.17)$$

where,

$i_{\text{free}}$  : corrosion current in the corrosive medium.

$i_{\text{add}}$  : corrosion current in the presence of additive.

### 1.4.3. Electrochemical impedance spectroscopy

The electrochemical impedance spectroscopy technique has been widely used to measure the rates of corrosion of metals [42-43]. The main advantage of this method is the complete elimination of the solution resistance. The equivalent circuit of a corrosive metal having anodic and cathodic reactions under activation controlled can be represented as a parallel combination of charge transfer resistance ( $R_t$ ), double layer capacitance ( $C_{dl}$ ) and the solution resistance ( $R_s$ ) in series.

From ( $R_t$ ) value, the  $i_{\text{corr}}$  is obtained from the relationship:

$$i_{\text{corr}} = \frac{b_a \cdot b_c}{2.303(b_a + b_c)R_t} \quad (1.18)$$

An alternating voltage of 10-20 mV is applied, the resulting current and the phase angle ( $\theta$ ) is measured for various frequencies where, the impedance [ $Z = \text{voltage/a.c}$ ] is resolved to a real part [ $z' = z \cos(\theta)$ ] and imaginary part [ $z'' = z \sin(\theta)$ ]. Plots of  $z'$  against  $z''$  is a semicircle which cuts the real axis at high frequency corresponds to ( $R_s$ ) and at low frequencies corresponds to ( $R_s + R_t$ ) and the difference between the two values gives ( $R_t$ ).

#### **1.4.4 Surface examination techniques.[44-45]**

##### ***(i) Scanning electron microscopy (SEM):***

SEM is used to examine and analyze the microscopic surface.. It gives resolution of about (25Å). It is useful for a quantitative identification of phases especially, for assessing the geometry of microscopic structures by image analysis

Corrosion is studied by scanning electron microscopy to distinguish the type of corrosion and the kinetic of the processes. Degradation of microstructures during the morphological changes such as grain growth, particle coarsening and recrystallization are also investigated using (SEM).

The combination of x-ray, mapping and (SEM) is used to quantify the fractured areas in the ductile and brittle phases, the depth of dimples, and the size of the process zone in front of the crack and the mode of crack propagation to establish a quantitative model for fracture of the material.

##### ***(ii) Optical microscopy:***

It is the most important tool for microstructure studies. Identifying unknown constituents may be aided noting their rigidity relative to the matrix, and their natural color, by their response to polarized light and by their response to selective etchants. These notes are compared to known details about the physical metallurgy of the examined material. The basic components of the optical microscope are illumination system, condenser, light filter, objective lenses and eye piece. Three types of illumination are used which they are:

- Bright field for the observations of microstructure.
- Oblique for the three dimensional appearance.
- Dark field for strong image contrast.

**(iii) X-ray analysis:**

It is used to study the crystal perfection, crystal structure, and dimension of phase diagrams, order-disorder transformation and chemical composition. Quantitative analysis is also possible because the intensities of the diffraction lines due to one constituent of a mixture depend on the proportion of that constituent in the specimen.

**(iv) Auger electron spectroscopy (AES):**

AES together with x-ray photoelectron spectroscopy (XPE) are the two major surface analysis techniques. (XPS) is more sensitive and gives more useful chemical information's while, AES has the advantages of greater speed and the potential of high speed resolution. The idea of the two techniques depends on the ejection of electron from an inner shell, where the energy released appears either as an x-ray photon or transferred to another electron, which is ejected, from the atom with energy. The basic components of an (AES) are electron gun, electron spectrometer and electron detector.

**(v) X-ray photoelectron spectroscopy (XPS):**

It has wide applications in the case of polymers organics, biological specimens, fibers films, powders and particles. In this technique the specimen is excited by the excitation source and its subsequent response in the form of an emission of some species is observed by some types of microscopy.

### 1.5. Corrosion inhibitor.

Among the methods for corrosion control and prevention, certain types of chemicals can be added to the environment to reduce the aggressiveness of the environment or to slow down the corrosion process.

Inhibitors function by adsorption of ions or molecules onto the surface of the metal. They reduce the corrosion rate by

- (i) Increasing or decreasing the anodic and/or cathodic reaction
- (ii) Reducing the diffusion rate for reactants to the surface of the metal
- (iii) Reducing the electrical resistance of the metal surface

The types of environment that can be modified include aqueous, partly aqueous and gaseous. Aqueous and partly aqueous conditions are often found in at near neutral pH range such as natural waters, cooling water systems and in acidic range such as acid pickling to remove the rolling scale as well as in oil and gas production and refining.

Inhibitors are often easy to apply and provide the advantage of in-situ application without causing any significant disruption to the process. However, there are several considerations when choosing an inhibitor:

- Cost of the inhibitor can be sometimes very high when the material involved is expensive or when the amount demanded is huge.
- Toxicity of the inhibitor can cause jeopardizing effects on human beings, and other living species.

- Availability of the inhibitor will determine the selection of it as if the availability is low, the material is often expensive.
- Environmental friendliness

### **1.5.1 Types of Inhibitors**

There are several types of inhibitors available to the industries now. They are:

#### **(i) Volatile Inhibitors: [46,47]**

This type of inhibitors is also known as vapour phase inhibitors. As corrosion can also occur in vapour environment, it is useful to carry corrosion inhibitors into the system, which then need to be, themselves, volatile. When the inhibitor molecules in the vapour come into contact with the surface of a metal, the adsorption of the inhibitor will occur. The moisture then hydrolyses it; hence protective ions may be released. These include species like amines and nitrites for inhibition of ferrous metal.

#### **(ii) Passivating (Anodic) Inhibitors [48]**

Passivating inhibitors are anodic inhibitors. They cause the anodic curve of polarization to shift such that less current flows. They have the ability to passivate the metal surface. There are two categories of passivating inhibitors, namely oxidizing anions and non-oxidizing anions. Oxidizing anions such as chromate, nitrite and nitrate can passivate metal in the absence of oxygen. Typical oxidizing anions are chromate, nitrite and nitrate. Non-oxidizing ones such as phosphate, tungstate and molybdate require oxygen to perform passivation.



This type of inhibitor is the most widely used and possesses higher efficiency than others. However, one major drawback of this is that in order to maintain adequate passivation of the metal and thus provide sufficient inhibition, the concentration of the inhibitor must remain significantly above the critical or minimum concentration. If the concentration is below the minimum value, it is likely that the metal, which must be protected in the first place, will suffer from localized corrosion such as pitting.

### **(iii) Precipitation Inhibitors [49]**

These inhibitors are often film-forming in nature, for instance silicates and phosphates. They are effective at blocking anodic and cathodic sites. They precipitate on the metal surface, forming a protective barrier layer. Hard water is rich in magnesium and calcium. When these salts precipitate on the metal surface, for example at the cathode where the pH is higher, they establish a protection layer on the metal. Film-forming types of inhibitors are often distinguished by two classes. The first one works by slowing down the corrosion without stopping it completely. The second ceases the attack completely.

Therefore, the efficiency of this inhibitor depends on the pH value and saturation index. The saturation index is then in turn determined by the water composition and temperature.

### **(iv) Cathodic Inhibitors [49,50]**

Cathodic inhibitors reduce the rate of cathodic reaction which is the reduction of oxygen in near neutral environments and the evolution of hydrogen in acidic solutions, respectively. These types are deposited in the cathodic sites, thus increasing the surface impedance and reducing the

diffusion rate. The inhibiting action of cathodic inhibitors works by three mechanisms:

- Cathodic poisons

In this case, the cathodic reduction process is suppressed, for example by impeding the hydrogen recombination and discharge. But it may increase the tendency of the metal to be susceptible to hydrogen induced cracking. Hydrogen can be absorbed into the metal during this process. It is essential to keep hydrogen in atomic form. Typical types of cathodic poisons are arsenic and antimony.

- Cathodic precipitates

Compounds such as calcium, magnesium will precipitate as oxides to form a protective layer which acts as a barrier on the metal surface.

- Oxygen scavenger

This mechanism functions by the removal of oxygen in the system to reduce corrosion. The compounds of oxygen scavenger react with oxygen presenting the system to form a product.

#### **(v) Organic Inhibitors [49]**

This type of inhibitors too, is formed by the nature of the film. It forms a form a hydrophobic layer on the surface of the metal to prevent dissolution of the metal. The efficiency of this inhibitor depends on the chemical composition and molecular structure of the inhibitor as well as its association with the metal. They are used often when environmental issues are taken into account. It is categorized into organic anions and cations. Inhibitors like sulphonates and

phosphonates fall into the anions category. Chemicals with active groups such as aliphatic and aromatic and positively charged amine groups are organic cations. This type of organic inhibitor is often in the form of liquid or wax-like.

#### **(vi) Inorganic Inhibitors [50]**

Common inorganic inhibitors used are crystalline salts, for example, sodium chromate and molybdate. The only active groups of these compounds that reduce corrosion are the negative anions they carry.

#### **(vii) Mixed Inhibitors [47]**

Corrosion inhibitors are rarely used as just one compound. The formulation can be can consist of two or more inhibitors which all carry different characters. This is due to three factors:

- A single inhibitor can only inhibit a few numbers of metals. When the environments involve multi-metal system, the inhibitive action may sometimes cause dangerous effects to other metals.
- The advantages of anodic and cathodic inhibitors can be combined and optimized for best performance.
- The addition of halide ions improves the action of the organic inhibitor in acid solutions.

## **1.6-Literature survey for corrosion inhibition of carbon steel in aqueous solution.**

### **1.6.1-Organic compound as corrosion inhibitor:**

Selected triazole derivatives were synthesized and evaluated as corrosion inhibitors for carbon steel in neutral aqueous environment by weight loss, potentiodynamic polarization and AC impedance methods [51]. All the condensed products showed good inhibition efficiency. The effect of changing functional groups of some triazole derivatives on their inhibition efficiency was also studied. 3-salicylalidene amino-1,2,4-triazole phosphonate was found to be the best corrosion inhibitor compare to the other compounds. Surface analysis was performed to determine the mechanism of corrosion inhibition of carbon steel in neutral aqueous media.

The inhibition effect of three amino acids namely, alanine, glycine and leucine against the corrosion of steel in HCl solutions was investigated by potentiodynamic polarization methods [52]. Corrosion parameters such as corrosion current ,corrosion rate, corrosion potential and polarization resistance ( $R_p$ ) were determined by extrapolation of the cathodic and anodic Tafel region. The inhibition efficiency depended on the type of amino acid and its concentration. The inhibition effect ranged from 28 to 91%. The amino acids act as a corrosion inhibitor in HCl solution through adsorption on the surface of steel and adsorption follows Langmuir isotherm.

4-Phenylazo-3-methyl-2-pyrazolon-5-one and three of its derivatives was investigated as corrosion inhibitors for carbon steel in 2 M hydrochloric acid solution using weight loss and galvanostatic

[53].The inhibition efficiency increases with increasing inhibitor concentration but decreases with increasing temperature. The synergistic effect of the pyrazolone derivatives and KBr, KSCN and KI were also studied. The apparent activation energy ( $E_a^*$ ) and some thermodynamic parameters for the corrosion process were also calculated. The galvanostatic polarization data indicated that the inhibitors were of a mixed type, but the cathode is more polarized than the anode. The adsorption of these compounds on C- steel surface was found to obeys Frumkin's adsorption isotherm. The mechanism of inhibition was discussed in the light of the chemical structure of the undertaken inhibitors.

The effect of some aminopyrimidine derivatives on the corrosion of 1018 carbon steel in 0.05M  $\text{HNO}_3$  .solution was studied using weight loss and polarization techniques [54]. The percentage inhibition efficiency was found to increase with increasing concentration of inhibitor and with decreasing temperature. The addition of KI to aminopyrimidine derivatives enhanced the inhibition efficiency due to synergistic effect. The inhibitors are adsorbed on the steel surface according to Temkin isotherm. Some thermodynamic functions were computed and discussed. It was found that the aminopyrimidine derivatives provide a good protection to steel against pitting corrosion in chloride containing solutions.

The inhibition efficiency of n- decylamine on the corrosion of low carbon steel in 1N sulphuric acid at different temperatures was investigated potentiokinetically [55]. Various parameters such as corrosion potential, corrosion current, polarization resistance, transfer coefficient, standard free energy of adsorption, enthalpy and entropy as well as the activation energy were calculated. It has been found that the

adsorption of n- decylamine on the steel surface follows Langmuir isotherm. The mechanism of carbon steel dissolution and the hydrogen evolution reaction does not change in the presence of the inhibitor used.

Selected triazole derivatives have been synthesized and evaluated as corrosion inhibitors for carbon steel in neutral aqueous environment by weight loss, potentiodynamic polarization and AC impedance methods [56]. All intensive products showed good inhibition efficiency. The effect of changing functional groups of some triazole derivatives on the efficacy of their inhibition was also reported. 3-salicylalidene amino-1,2,4-triazole phosphonate was found to be the best corrosion inhibitor compare to the other compounds. Surface analysis was performed to determine the mechanism of corrosion inhibition of carbon steel in a neutral aqueous media.

The effect of some pyridine derivatives on the corrosion of carbon steel in 2M HCl solution was studied using electrochemical polarization method (potentiodynamic-Tafel extrapolation) as well as weight loss method [57]. The inhibition efficiency of the tested compounds dependent on the concentration and nature of the inhibitor. Results obtained from both potentiodynamic polarization and weight loss techniques reveal that, these compounds are good inhibitors. The presence of substituent's in pyridine ring plays an important role in the percentage inhibition of the compounds under investigation. The adsorption of these compounds on the carbon steel follows Langmuir adsorption isotherm.

Four azoles compounds, namely, imidazole, benzoimidazole, benzotriazole and benzothiazole were investigated as inhibitors for corrosion of mild steel in 1M HCl solution [58]. Impedance spectroscopy, polarization resistance, gravimetric and polarization

methods were used. A suitable structural model is provided for the interface in the presence of inhibitors and the corresponding parameter values are calculated.. The apparent activation energy of the process that occurs in the presence of an inhibitor was determined on the ground of five temperature values in the range from 20°C to 60°C. Using the data obtained by two independent methods comparative investigations were carried out in 1M H<sub>2</sub>SO<sub>4</sub> aiming to demonstrate the effect of the acid's anion. The generalization of the data obtained provided to make conclusions concerning the mechanism of the inhibitor's adsorption.

The effect of succinic acids (SA) on the corrosion inhibition of a low C-steel (LCS) was investigated in aerated non-stirred 1.0 M HCl solutions in the pH range (2-8) at 25°C [59]. Weight loss, potentiodynamic polarization and electrochemical impedance spectroscopy (EIS) techniques was applied to study the steel corrosion behavior in the absence and presence of different concentrations of SA under the influence of various experimental conditions. Measurements of open circuit potential as a function of time till steady-state potential ( $E_{st}$ ) were also established. Surface analysis using energy dispersive X-ray and scanning electron microscope allowed to clarify the mechanistic aspects and evaluate the relative inhibition efficiency. Results obtained showed that SA is a good inhibitor for LCS in HCl solution. The polarization curves showed that SA behaves mainly as an anodic type inhibitor. The inhibition efficiency increases with increase in SA concentration. Maximum inhibition efficiency (97.5%) at SA concentration >0.01 M at pH 8. The effect of SA concentration and pH on the potential of zero charge (PZC) of the LCS electrode in 1.0 M HCl solutions was studied and the mechanism of adsorption is discussed. The

results obtained from weight loss, polarization and impedance measurements are in good agreements.

The corrosion behavior of carbon steel in a wide range of concentrations (0.1-1M) of gluconate and tartarate was studied by potentiodynamic and open circuit measurements [60]. The results showed a high rate of corrosion with an increase in the concentration of organic acid salt. The results indicate that low carbon steel displays typical active to passive transition behavior in absence of chloride ions. The effect of scan rate, temperature and chloride ions on the behavior of carbon steel in gluconate and tartarate solutions was also studied. The corrosion of carbon steel in tartarate was higher than that in gluconate solutions.

Some tertiary amines in the series of 1,3-di-amino-propan-2-ol, referred as 1,3-di-morpholin-4-yl-propan-2-ol (DMP) and 1,3-bis-diethylamino-propan-2-ol (DEAP), had been synthesized by alkylation reaction [61]. These compounds were examined by MS, IR, HNMR and  $^{13}\text{C}$  NMR. The electrochemical performance of these products was investigated by potentiodynamic polarization measurement and electrochemical impedance spectroscopy (EIS) under thin electrolyte layer and their inhibition efficiencies were measured using gravimetric methods. These compounds, retarding the anodic dissolution of iron by forming protective layer on the metal surface. Polarization data indicated that the inhibitive performance of DMP for carbon steel was improved with the increasing of concentration, while DEAP showed a maximum inhibiting power at  $2.5 \times 10^{-2}$  M was 95%. Adsorption on the carbon steel surface follows the Langmuir isotherm model. A Fourier transform spectrometer (FTIR) was used to analyze adsorbed surface film.



The effect of some synthesized pyrazole compounds on the corrosion of carbon steel in 1M H<sub>2</sub>SO<sub>4</sub> solution was investigated [62]. The investigation involved electrochemical polarization methods (potentiodynamic, Tafel extrapolation and the determination of the polarization resistance). A significant decrease in the corrosion rate of carbon steel was observed in the presence of the investigated compounds. The results show that these compounds act as mixed type inhibitors, but the cathode is more preferentially polarized. The relative inhibition efficiency of these compounds depends on both the nature and concentrations of the investigated compounds. Compounds are found to adsorb on the carbon steel surface according to the Langmuir adsorption isotherm.

1,12-bis(1,2,4-triazole) dodecane (dtc12) is an excellent corrosion inhibitor for carbon steel in deaerated 1M HCl solution [63]. Electrochemical and analytical techniques were used to study the inhibition of corrosion of carbon steel in acidic medium. The corrosion inhibition of carbon steel with dtc12 was attributed to the synergistic effect between chloride anion and quaternary ammonium ion. The protective efficiency of the film was higher than 90%, indicating that corrosion of carbon steel in 1M HCl solution is reduced by dtc12. The effect of dissolved oxygen on the inhibition efficiency was also investigated. The results showed that the inhibition efficiency increases at an early stage and decreases during immersion.

Quinine was tested as a corrosion inhibitor for low carbon steel in 1.0 M HCl solution [64]. Electrochemical impedance spectroscopy (EIS) and potentiodynamic polarization were used to study the inhibiting effect of quinine in the temperature range (20°-50°C). The corrosion of steel was controlled by a charge transfer process at the prevailing

conditions. The electrochemical results showed that quinine is an an effective inhibitor of low carbon steel. Efficiency up to 96% was obtained at 20°C. The inhibition efficiency increases with increasing the inhibitor concentration and reaches a near constant value in the concentration range 0.48 mM and above. Application of the Langmuir adsorption isotherm enabled a study of the extent and the mode of adsorption.

The effect of some mercaptotriazole derivatives synthesized in the laboratory containing different hetero atoms and substituent in the organic structure on the corrosion and hydrogen permeation of mild steel in 1.0M HCl solution was investigated by weight loss and various electrochemical techniques [65]. The obtained results showed that all the mercaptotriazol derivatives work perfectly as corrosion inhibitors for mild steel in 1.0 M HCl solution. Potentiodynamic polarizations showed that all of these compounds inhibit both the anodic and cathodic process and act as mixed-type inhibitors. Double layer capacitance and charge transfer resistance values were derived from Nyquist plots obtained from AC impedance of these compounds on the metal surface. The inhibition efficiency was mainly dependent on the nature of the investigated compounds. The values of the inhibition efficiency calculated from these techniques are in reasonably good agreement. The extent of reduction of hydrogen permeation current through mild steel surface was studied by the hydrogen electro permeation technique. The adsorption of these compounds on mild steel surface is found to obey Langmuir adsorption isotherm. The free energy of adsorption for inhibiting process was determined based on Langmuir adsorption isotherm.

The inhibiting effect of three compounds of pyrazolo[3,4-*d*]pyrimidnone derivatives toward the corrosion of carbon steel in 1.0M

HCl solution was investigated using galvanostatic and potentiodynamic anodic polarization techniques [66]. The rise of the concentration of the inhibitors and decreasing the temperature led to the greater of inhibition efficiency. The inhibiting action of these compounds was explicated on the basis of its adsorption on the carbon steel surface. The adsorption operation of these compounds was obeyed Langmuir isotherm. There is only one anodic peak during the anodic cyclic voltammogram. This peak was elucidated due to the active dissolution of Fe as  $\text{Fe}^{2+}$ . The percentage inhibition efficiency was computed from the values of peak current density. There is a good convention between the values of the percentage inhibition efficiency gained from the diverse techniques. These compounds inhibit the pitting corrosion of carbon steel by shifting the pitting corrosion potential to more noble direction. The effect of elevation of temperature on the rate of corrosion in devoid of and containing these compounds was studied and some activated thermodynamic parameters were computed.

Seven homologous imidazoline inhibitors, derivatives of cyclopentyl and cyclohexyl naphthenic acids, were synthesized [67]. The effectiveness of these compounds as inhibitors for carbon steel and austenitic stainless steel was tested using the impedance method in 2% NaCl solution in the presence of a hydrocarbon phase. The solution was saturated with hydrogen sulphide. It was found that the inhibitors and their mixture displayed high inhibition efficiencies, reaching 93% for carbon steel and 94% for the austenitic steel. Inhibitors with the shortest hydrocarbon side chains on the imidazoline ring were found to offer the lowest level of protection, the inhibition efficiency increasing with the length of the side chain. The capacitance measured on the surface was decreased linearly as the coverage of the steel surface by inhibitors increased. The results of impedance measurements with commercial

inhibitors have confirmed the conclusions from the tests on the pure chemical species.

The corrosion inhibitor 2,5 - bis (4- dimethyl aminophenyl)-1,3,4-thiodiazole (DAPT) was synthesized and its inhibiting action on the corrosion of mild steel in 1 M HCl and 0.5 M H<sub>2</sub>SO<sub>4</sub> solution at 30°C was investigated by various corrosion monitoring techniques [68]. A preliminary screening of the inhibition efficiency was carried out using weight loss measurements. At constant acid concentration, the inhibition efficiency increases with concentration of DAPT and it founds to be more efficient in 0.5 M H<sub>2</sub>SO<sub>4</sub> than in 1 M HCl. Potentiodynamic polarization studies showed that DAPT is a mixed type inhibitor. The effect of temperature on the corrosion behavior of mild steel in 1 M HCl with addition of DAPT was studied in the temperature range from 25° to 60°C. It was shown that the adsorption is constant with the Langmuir's adsorption isotherm at 30°C. The negative free energy of adsorption in the presence of DAPT suggests chemisorptions of the thiodiazole molecules on the steel surface.

The inhibition ability of benzimidazole and its derivatives against the corrosion of mild steel in 1M HCl solution was studied using galvanostatic polarization and electrochemical impedance spectroscopy [69]. The change of impedance parameters observed by variation of inhibitors concentration within the range of 50–250 ppm was an indication of their adsorption. The thermodynamic adsorption parameters proposed that these inhibitors retard both cathodic and anodic processes through physical adsorption and blocking the active corrosion sites. The adsorption of these compounds obeyed the Langmuir's adsorption isotherm. The inhibition efficiency was increased with increasing the inhibitor concentration according to the

order of 2-mercaptobenzimidazole > 2-methylbenzimidazole > benzimidazole, which is in accordance with the variation of apparent activation energy of corrosion.

The oxo-triazole derivative (DTP) was synthesized and its inhibiting action on the corrosion of mild steel in sulphuric acid was investigated [70]. The results obtained from weight loss, potentiodynamic polarization, electrochemical impedance spectroscopy and scanning electron microscope. The results revealed that DTP was an excellent inhibitor and the inhibition efficiencies obtained from weight loss and electrochemical experiment were in good agreement. Potentiodynamic polarization studies clearly revealed that DTP acted essentially as the mixed-type inhibitor. Thermodynamic and kinetic parameters were obtained from weight loss of the different experimental temperatures, which suggested that at different temperatures (298–333 K) the adsorption of DTP on metal surface obeyed Langmuir adsorption isotherm model.

The inhibitive effect of two Schiff bases namely, 2-[[[(4-methoxyphenyl) imino) methyl] phenol [SB-1] and 1-[[[(4-methoxyphenyl) imino) methyl]-2-naphthol [SB-2], on the corrosion of carbon steel in 0.1 M and 1M H<sub>2</sub>SO<sub>4</sub> was studied by polarization methods [71]. Corrosion parameters and adsorption isotherms were determined from current- potential curves. It was found that the percentage inhibition efficiencies and surface coverage increase with an increase in the concentration of inhibitors. The results showed that these compounds act as good corrosion inhibitors especially at high concentrations. The adsorption of used compounds on the steel surface follows Langmuir isotherm.

The effect of azathiones as corrosion inhibitors for the corrosion of carbon steel (0.14%C) in  $H_2SO_4$  and in HCl was investigated by weight loss and potentiostatic polarization techniques [72]. Potentiostatic data showed that these inhibitors are of mixed type. Azathiones can exist as cations species like other amino compounds. These cationic species are adsorbed on the cathodic sites of the steel and decrease the evolution of hydrogen. The adsorption of azathione molecules on the anodic sites takes place through the lone pair of electrons of nitrogen and sulphur atoms which decreases the anodic dissolution of steel. Azathiones gives better inhibition in 1M HCl than that of 1  $MH_2SO_4$ . This is explained based on synergistic mechanism, according to which  $Cl^-$  ions and azathiones molecules can jointly be adsorbed on the steel surface giving higher efficiency.

The inhibition effect of two compounds of Schiff base namely, N, N-bis (salicylidene) -2- hydroxyl-1,3- propanediamine (LOH) and N,N-bis(2-hydroxyaceto-phenylidene)-2-hydroxyl- 1,3-propanediamine (LACOH) toward the corrosion of mild steel in 2M HCl solution was studied at 303K [73]. It has been determined using weight loss, polarization and electrochemical impedance spectroscopy (EIS) methods. It was found that the corrosion rates decrease, percentage inhibition efficiencies and the degree surface coverage increase with increasing additive concentration. The inhibitors appear to function through the Langmuir's adsorption isotherm. The results showed that LACOH has the highest inhibition efficiency among the two studied compounds.

The inhibition effect of 1-methyl-4[4'(-X)-styryl] pyridinium iodides (X:H,  $CH_3$  and  $OCH_3$ ) toward the corrosion of mild steel in 1.5 M HCl [74] was studied by hydrogen evolution and weight loss

measurements. It was found that the studied compounds exhibit a very good performance as inhibitors for mild steel corrosion in 1.5 M HCl. Results show that the inhibition efficiency increases with decreasing temperature and increasing concentration of inhibitors. Good agreement between the results obtained from hydrogen evolution and weight loss measurements was appeared. It has been determined that the adsorption for the studied inhibitors on mild steel complies with the Langmuir adsorption isotherm at all studied temperatures. The kinetic and thermodynamic parameters for mild steel corrosion and inhibitor adsorption, respectively, were determined and discussed. On the bases of thermodynamic adsorption parameters, comprehensive adsorption (physisorption and chemisorptions) for the studied inhibitors on mild steel surface was suggested. A good correlation between the substituent type and the inhibition efficiency of inhibitors through the application of Hammett relationship was obtained. Results show that with increasing the donor property of the substituent, the inhibition efficiency of the inhibitor is increased in the sequence:  $H < CH_3 < OCH_3$ .

4-Phenylazo-3-methyl-2-pyrazolon-5-one and three of its derivatives was investigated as corrosion inhibitors for carbon steel in 2 M HCl solution using weight loss and galvanostatic polarization techniques [75]. The inhibition efficiency increases with the increase in the inhibitor concentration but decrease with a rise in temperature. The conjoint effect of the pyrazolone derivatives and KBr, KSCN and KI has also been studied. The apparent activation energy ( $E_a^*$ ) and some thermodynamic parameters for the corrosion process have also been calculated. The galvanostatic polarization data indicated that the inhibitors were of mixed type, but the cathode is more polarized than the anode. The adsorption of these compounds on C- steel surface has been found to obeys Frumkin's

adsorption isotherm. The mechanism of inhibition was discussed in the light of the chemical structure of the undertaken inhibitors.

5-Amino-3-methyl-1-phenyl-1*H*-pyrazole-4-carbonitrile (**1**) was used as a precursor for preparation of 3-methyl-1-phenyl-1,5-dihydro-pyrazolo[3,4-*d*]pyrimidin-4-one (**2**) and its derivatives **3–10**. The produced compounds were separated, purified, and characterized by FT-IR, <sup>1</sup>H NMR, <sup>13</sup>C NMR, and mass spectroscopy [76]. The surface properties were studied by measuring the surface tension. The surface tension, critical micelle concentration (CMC), and surface activities were determined. The surface parameters such as surface excess concentration ( $\Gamma_{\max}$ ), the area per molecule at interface ( $A_{\min}$ ), and the effectiveness of surface tension reduction ( $\pi\text{CMC}$ ) were determined from the adsorption isotherms of the prepared compounds. Furthermore, the corrosion inhibition performance of the prepared compounds was evaluated by chemical methods (weight loss) at different inhibitor concentrations and different temperatures. The corrosion inhibition efficiency increased with increase in inhibitor concentration, but decreased with increase in temperature. Thermodynamic activation parameters were computed and discussed to reach the mechanism of the corrosion inhibition process.

Electrochemical techniques were used for investigating of carbon steel by thiomorpholin-4-ylmethyl-phosphonic acid (TMPA) and morpholin-4-methyl-phosphonic acid (MPA) in natural sea water [77]. The free corrosion potential was observed to shift in the noble direction which indicated that the phosphoric acids tested inhibit the corrosion of carbon steel in seawater. Potentiodynamic polarization curves show clearly the fact that the addition of these molecules is associated with corrosion current density decrease and a corresponding reduction of the corrosion rate. The phosphonic acids tested as corrosion inhibitors of carbon steel in natural sea water are effective even with small



concentration. Fourier transform infrared spectroscopy was used to obtain information on bonding mechanism between the metallic surface and the inhibitors. The morphology of the metal surface in the uninhibited and inhibited solution was examined using the scanning electron microscope coupled with an energy dispersive X-ray analysis system.

New compounds of alkylamides derived from amino acids were tested as corrosion inhibitors for carbon steel in aqueous solution of HCl. The chemical synthesis of these amides performed by aminolysis of amino acid methyl esters resulted in good yields [78]. Electrochemical measurements were performed using polarization scans and weight loss measurements. Polarization scans indicated that these compounds act as mixed corrosion inhibitors with an efficiency of 80-90% when dissolved in the testing solution at  $\geq 50$  ppm, whereas gravimetric results displayed a similar tendency. Microtox testing indicated a correlation with the molecular structure of inhibitors. Apparently, a long aliphatic chain ( $C > 12$ ) promoted not only higher corrosion efficiency, but also a higher toxicity. The higher efficiency of dodecyl amine of tyrosine was apparently derived from its longer aliphatic chain, with some contribution from its phenyl ring, which reinforces the molecular interactions of  $n$  type bonding to the  $d$  orbital metal favouring film formation.

Some Azole derivatives were used as inhibitors for corrosion irradiated and non-irradiated carbon steel in 0.5 M  $\text{HNO}_3$  solution using weight loss and potentiodynamic polarization measurement [79] the inhibition efficiency increased with increase in the concentration of the inhibitors but decreased with an increase in temperature. The inhibition was explained in terms of adsorption of these compounds on the steel

surface. The inhibition efficiency increased in the case of irradiated carbon steel than for the non irradiated one. The  $\gamma$ -radiation improved the passive film and increases its resistance to the nucleation of pits. This phenomenon is termed a photo inhibition effect.

The use of new biocide, antimicrobial corrosion inhibitor namely, 8-hydroxy-N-(2-(quinolin-8-yloxy)acetyl)-quinoline-5-sulfonohydrazide (HQS) to inhibit the corrosion of mild steel in salty water environment were studied using weight loss, electrochemical measurements, and microorganism tests [80]. The results obtained study show that, the new inhibitor can decrease corrosion and microbial growth under the conditions tested. The mass loss for the protected mild steel coupons shows lower corrosion rate compared to the unprotected one. Cyclic polarization test reveals that, the biocide minimizes the pitting area (hysteresis). The nature of protective film formed on mild steel was studied by scanning electron microscopy (SEM). SEM images revealed that, the corrosion inhibition by the HQS on the mild steel surface significantly improved in the presence of biocide.

N-3-hydroxyl-2-naphthoyl hydrazone derivatives were used as inhibitors for corrosion of carbon steel in 0.5 M  $H_2SO_4$  solution using weight loss and polarization measurements [81]. The inhibiting action of these compound, depends primarily on their concentration and molecular size. These compounds acted as mixed type inhibitors and function via adsorption on carbon steel surface, which follows Frumkin adsorption isotherm. The addition of KI, KBr and KSCN to these compounds had a synergistic effect in enhancing the efficiency of corrosion inhibitors.

The inhibiting effect of N-[4-(diethylamino)benzylidene]-3-[[8-(trifluoromethyl)-quinolin-4-yl]thio}propano hydrazide (DEQTPH)

toward the corrosion for carbon steel in HCl and H<sub>2</sub>SO<sub>4</sub> solutions using weight loss method, electrochemical impedance spectroscopy (EIS) and potentiodynamic polarization method [82]. The corrosion inhibition efficiencies measured by all the above three techniques were in good agreement with each other. The carbon steel samples were also analyzed by scanning electron microscopy (SEM). The results showed that DEQTPH is an excellent inhibitor for mild steel in acid media. The inhibition efficiency in different acid media was found to be in the order, 0.5M H<sub>2</sub>SO<sub>4</sub> > 1.0M HCl > 2.0M HCl > 1.0M H<sub>2</sub>SO<sub>4</sub>. The inhibition was assumed to occur via adsorption of the inhibitor molecule on the carbon steel surface. It acts as an anodic inhibitor. In the 30–60 °C temperature range, the DEQTPH adsorption follows Langmuir isotherm model. The protection efficiency increased with increasing inhibitor concentration in the range  $0.2 \times 10^{-4}$  to  $10.5 \times 10^{-4}$ M and slightly increased with increasing temperature.

Tris-hydroxymethyl-(2-hydroxybenzylidenamino)-methane (THHM) was synthesized. The effect of THHM on the corrosion of cold rolled steel (CRS) in 0.1M HCl solution was studied using Tafel polarization measurements and electrochemical impedance spectroscopy (EIS) [83]. Polarization curve results clearly reveal the fact that THHM is a good cathodic type inhibitor. EIS results confirm its corrosion inhibition ability. The inhibition efficiency increases with increasing THHM concentration but decreases with immersion time. Atomic force microscopy (AFM) reveals that a protective film forms on the surface of the inhibited sample. The adsorption of this inhibitor is found to follow the Langmuir adsorption isotherm. THHM adsorbs on the sample probably by chemisorption's.

The corrosion behavior of mild steel (SS400) and stainless steels (types 430 and 304) in  $\text{H}_2\text{SO}_4$  and  $\text{CH}_3\text{COOH}$  solutions containing KF was investigated with corrosion tests, electrochemical measurement, surface analysis and solution pH analysis [84]. The corrosion rate of SS400 steel in 0.01 M aqueous solution containing KF decreased with increasing the concentration of KF. The SS400 and type 430 stainless steels were corroded in boiling 50% aqueous  $\text{CH}_3\text{COOH}$  and non-aqueous  $\text{CH}_3\text{COOH}$  solution containing high concentration of KF. The corrosion rate of these two steels was decreased. This is due to decrease in corrosive ions such as  $\text{H}^+$  in  $\text{CH}_3\text{COOH}$  by contrast, type 304 steel was scarcely corroded in the boiling 50% aqueous and non-aqueous  $\text{CH}_3\text{COOH}$  solutions containing KF because of the formation of a stable oxide film.

The inhibiting effect of imidazole derivative 1,7-dimethyl-2-propyl-1 H, 3'-2,5'-bibenzo imidazole (DPBI) against mild steel corrosion in 1M HCl solution was evaluated using the conventional mass loss method, potentiodynamic polarization, linear polarization, and electrochemical impedance spectroscopy [85]. The mass loss results showed that DPBI is an excellent corrosion inhibitors, electrochemical impedance spectroscopy showed that the change in the impedance parameters, charge transfer resistance, and double layer capacitance with change in the concentration of the inhibitor is due to the adsorption of the molecule leading to the formation of protective layer on the surface of mild steel. The inhibition action of this compound was assumed to occur via adsorption on the steel surface through the active centers of the molecule.

### 1.6.2-Inorganic as corrosion inhibitor:

The effect of the sodium salts of molybdate, tungstate and monovanadate as well as some derivatives of Neville-Winter acid azo dyes on the corrosion of carbon steel in 3.5 percent NaCl solution was studied [86]. Open circuit potential measurements and potentiostatic polarization techniques was used. It was found that all the compounds have inhibition effects on carbon steel dissolution. The inhibition efficiency increased with increase in inhibitor concentration. The process of inhibition was attributed to the formation of an adsorbed film on the metal surface which protects the metal against the corrosive medium. The adsorption of these compounds on the steel/chloride interface was found to follow Freundlich adsorption isotherm.

The corrosion of carbon steel in three kinds of artificial potable waters containing different concentrations of aggressive anions, e.g.  $\text{Cl}^-$  and  $\text{SO}_4^{2-}$  open to air in the temperature range from  $5^\circ\text{C}$  to  $60^\circ\text{C}$  were conducted using weight loss and electrochemical methods [87]. The corrosion rate was increased with increasing the concentration of aggressive anions and with increasing temperature. At lower concentration of aggressive anions and temperatures, the corrosion rate was lower and the corrosion potential was higher, at intermediate concentrations and temperatures, the corrosion rate increased logarithmically with decreasing potential, and at higher concentrations and temperatures, the corrosion rate was higher and the potential was lower. The corrosion behavior in potable water can be determined by the balance between inhibitive action of oxygen (passive film formation) and aggressive action of  $\text{Cl}^-$  and  $\text{SO}_4^{2-}$  ions.

The corrosion resistance of carbon steel in caustic-containing sulfide solutions was found to depends on the formation of a stable passive film

on the surface of the metal [88]. The effects of rising temperature up to 170°C and the concentrations of sulfide and hydroxide on the corrosion rate to determine environmental limits for the reliable operation of carbon steel. The results indicate that, carbon steel can exhibit high corrosion rates with increased hydroxide or sulfide concentrations at temperatures above 100 ° C and change the open circuit potential to values below -1.00V(SCE).

Potential-time curves are constructed for the steel electrode in naturally aerated Ca(OH)<sub>2</sub> solutions simulating the corrosion behavior in concrete. Cl<sup>-</sup> and SO<sub>4</sub><sup>2-</sup> ions cause the destruction of passivity and initiation of pitting corrosion [89]. The rate of oxide film growth by Ca(OH)<sub>2</sub> and oxide film destruction by Cl<sup>-</sup> and SO<sub>4</sub><sup>2-</sup> ions follows a direct logarithmic law as evident from the linear relationships between the open-circuit potential and the logarithm of immersion time. Chromate, phosphate, nitrite, tungstate and molybdate ions inhibit the pitting corrosion of steel. The rate of oxide film healing and thickening increases with their concentrations. In presence of constant inhibitor concentration, the efficiency of pitting inhibition increases in the order: (weak) CrO<sub>4</sub><sup>2-</sup> < HPO<sub>4</sub><sup>2-</sup> < NO<sub>2</sub><sup>-</sup> < WO<sub>4</sub><sup>2-</sup> < MoO<sub>4</sub><sup>2-</sup> (strong).

The inhibition effect of [Cu<sup>+2</sup> cation + 3,5-dimethylpyrazole] mixture of different molar ratios on the corrosion of carbon steel in a 0.5 M H<sub>2</sub>SO<sub>4</sub> solution was investigated using both weight loss and galvanostatic polarization techniques [90]. The inhibiting solutions were analyzed using UV- visible spectrophotometric before and after polarization measurements. The results revealed a complex formation between the two components, which was much more effective than the inhibiting action of each additive separately. The inhibition mechanism was explained depending on the results derived from both corrosion and

UV-visible spectrophotometric measurements as well as conductometric measurement

The effect of  $\text{Ni}^{2+}$ , imidazol and mixtures of them on the corrosion behavior of carbon steel in 0.5M  $\text{H}_2\text{SO}_4$  solution was studied using galvanostatic, potentiodynamic anodic polarization and weight loss techniques[91].  $\text{Ni}^{2+}$  cation, imidazole and mixtures of them provide a good protection to carbon steel against pitting corrosion in chloride containing solutions. The inhibiting solutions were analyzed using UV-vis spectrophotometry. The inhibition was explained in the basis of formation of a complex between the two components[92]. The inhibition mechanism was discussed in terms of the results derived from corrosion and UV-vis spectrophotometric measurements as well as conductometric investigation.

### **1.6.3- Drugs as corrosion inhibitors:**

The inhibiting effect of four sulfa drugs compounds (e.g. sulfaguanidine, sulfamethoxazole and sulfadiazine) on mild steel corrosion in 1.0M HCl were evaluated using both galvanostatic polarization and weight loss techniques [93]. All the examined sulfa drugs compounds reduce the corrosion of mild steel. Among the compound studied; sulfadiazine exhibits the best inhibition efficiency and sulfaguanidine the lowest. The inhibition efficiency goes through a maximum for sulfaguanidine while it increases continuously with concentration to a limit with sulfadiazine, sulfamethoxazole and sulfamethazine, respectively. Galvanostatic polarization measurements indicate that all the examined compounds are a mixed inhibitor type with predominant cathodic effectiveness. Moreover, the results revealed a better performance for these compounds as corrosion inhibitors in HCl.

The corrosion inhibition of carbon steel in 1M HCl solution by cefotaxime was studied using Tafel polarization, electrochemical impedance spectroscopy (EIS) and weight loss measurement [94]. The inhibitor showed 95.8 % inhibition efficiency at optimum concentration 300 ppm. Results obtained revealed that inhibition occurs through adsorption of the cefotaxime on the steel surface without modifying the mechanism of corrosion process. Potentiodynamic polarization studies suggest that it is a mixed type of inhibitor. Electrochemical impedance spectroscopy techniques were also used to investigate the mechanism of corrosion inhibition.

The inhibition efficiencies of ampicillin and flucloxacillin expired drugs on mild steel (MS) corrosion in 1.0 M sulfuric acid medium was examined at 20°C using weight loss (WL), and electrochemical potentiodynamic polarization (PDP) and electrochemical impedance spectroscopy (EIS) techniques [95]. Examined expired drugs are set to be efficient inhibitors for MS corrosion in sulfuric acid medium. The experimental outcomes of weight loss technique displayed that the inhibition performances of the investigated expired drugs augmented with increasing concentrations of such drugs and reduced by raising the temperature. The observed high inhibition efficiencies of the studied expired drugs may be owing to powerful adsorption of the drug species on MS surface resulting in formation of protective layers. Adsorption of the tested expired drugs on the MS surface was set to accord with Langmuir adsorption isotherm. The assessed thermodynamic parameters supported the mechanism of physical adsorption of the inhibitors.



#### **1.6.4-Surfactant as corrosion inhibitors:**

The adsorption behavior of dodecylamine and its effect on the wettability and corrosion of carbon steel in hydrochloric acid solution were studied [96]. Polarization data indicated that the inhibitions of carbon steel corrosion are due to geometric blocking effect of adsorbed dodecylamine molecules on the metal surface which leads to the formation of monolayer on the metal. Phase images measured by tapping mode atomic force microscopy (AFM) reveal different properties of the surface with and without various concentrations of dodecylamine. AFM force- distance curves indicate that sample surface exhibits adhesion characteristic after the adsorption of dodecylamine. Contact angle measurements show that dodecylamine reduces surface wettability obviously.

The corrosion behavior of carbon steel in 1M HCl solution in absence and presence of three compounds of ethoxylated fatty amide was studied using weight loss and galvanostatic polarization techniques [97]. The percentage inhibition efficiency was found to increase with increasing the additive concentration, number of ethylene oxide unit and with decreasing temperature. The inhibition action of these compounds was explained in term of adsorption on the steel surface through ethylene oxide unit while the hydrocarbon parts protrude brush-like into the solution. The adsorption process follows Langmuir adsorption isotherm.

Novel cationic Gemini surfactants compounds were synthesized, characterized and tested as corrosion inhibitors for carbon steel in 1M HCl solution [98]. The corrosion inhibition efficiency was measured by using electrochemical impedance spectroscopy, potentiodynamic polarization and weight loss methods. The obtained results showed that, the synthesized compounds are excellent inhibitors for

carbon steel in 1M HCl solution. The inhibition efficiency decreased in the temperature range 30-40°C and then increased in the temperature range 40-60°C. The prepared inhibitors act as mixed inhibitors. Thermodynamic and activation parameters were discussed. Adsorption of the synthesized inhibitors was found to follow Langmuir's adsorption isotherm. Mixed physical and chemical adsorption mechanism is proposed. The morphology of carbon steel samples was investigated by scanning electron microscopy (SEM).

The inhibiting power of three synthesized amino acids based-surfactant molecules, namely, sodium N-dodecylasparagines (AS), sodium N-dodecylhistidine (HS) and sodium N-dodecyltryptophan (TS) on the dissolution of carbon steel was inspected in 0.5 M NaCl and 05 M NaOH solutions at 25 °C [99] The methods employed in this work were weight-loss (WL), potentiodynamic polarization (PP) and electrochemical impedance spectroscopy (EIS). The chemical structures of the synthesized surfactants were confirmed by FT-IR and <sup>1</sup>H NMR. The inhibition efficiencies were found to increase as the surfactants concentrations increase, while decreasing with increasing the concentration of the corrosive media (NaCl & NaOH) and temperature. Results obtained from the different techniques revealed that the inhibition efficiency of the compound TS was higher than those of both AS and HS. The inhibition efficiencies of the synthesized surfactants were declined in terms of strong adsorption of surfactants on the surface of carbon steel and forming a protective film and such adsorption was found to obey Langmuir isotherm. Both thermodynamic and kinetic parameters were evaluated which support the mechanism of physical adsorption of the inhibitors. The tested surfactants were found to act as mixed-type inhibitors with anodic predominance. The surface morphology of the carbon steel surface was examined by scanning electron microscopy (SEM). The

inhibitory mechanism of carbon steel corrosion was suggested. Results obtained from allemployed methods are consistent with each other.

### **1.6.5-Natural compound as corrosion inhibitor:**

Synthetic organic inhibitors are in most times toxic materials, and considered as source of pollution and their synthesis costs a lot of money. Therefore, natural products act as easy and cheap way to forbidden or retarding the electrochemical corrosion reaction. They can be gained or extracted by simple aqueous media from many wastes of agriculture plants and seeds without any over much cost with the comparison of synthetic organic materials. So, the use natural occurring substance as corrosion inhibitors for metals and alloys is very effective.

Rosemary oil was used as corrosion inhibitor for carbon steel in 0.5M  $H_2SO_4$  solution using weight loss, potentiodynamic polarization and electrochemical impedance spectroscopy [100].The inhibition efficiency increases with an increase in the concentration of oil and a decrease of the temperature. The inhibiting effect of this oil is due to its adsorption on the surface of the steel with formation of a complex with charge transfer between the phenol groups in the inhibitor molecule and the surface of steel. The adsorption process obeys Langmuir's isotherm.

The inhibitive action of natural honey on the corrosion of C- steel, used in manufacturer of petroleum pipelines in high saline water was evaluated [101].The inhibition efficiency was calculated using weight loss measurements and potentiostatic polarization technique. It was found that, natural honey exhibited a very good performance as inhibitor for steel corrosion in high saline water. The inhibition efficiency increases with an increase in natural honey concentration. After some time, the inhibition

efficiency decreased due to the growth of fungi in the medium. The adsorption of honey on the C- steel was found to follow the Langmuir adsorption isotherm.

The inhibitive effect of the aqueous extract of the root of shirsh el zallouh (*Ferula harmonis*) toward the corrosion of C-steel in HCl solution was investigated [102]. The inhibition efficiency was measured using weight loss and potentiostatic polarization techniques. The electrochemical behavior of the extract was investigated using cyclic voltammetry. It was found that the addition of the extract reduces the corrosion rate of C-steel. The inhibition efficiency increases with increasing extract concentration. The inhibitive effect of the tested extract was discussed in view of adsorption of its components on the steel surface. The adsorption of the extract components on the C-steel surface obeys Langmuir isotherm. The inhibition efficiency decreases as the temperature is increased. The presence of extract increases the activation energy of the corrosion process of C-steel. The curves of cyclic voltammetry technique showed that the adsorbed molecules reduce the charge density on the steel surface.

Saleh et al. [103]. was studied the inhibitive effects of aqueous extracts of *Opuntia ficus indica* and *Aloe vera* (leaves) and of orange, mango and pomegranate (fruit-peels) on the corrosion of mild steel, aluminum, zinc and copper in HCl and H<sub>2</sub>SO<sub>4</sub> solutions using weight loss and polarization measurements. The extracts reduce the dissolution reactions to an extent dependent on the metal used, the concentration of the additive and the type, concentration and temperature of the attacking acid. The additives provide adequate protection to steel in 5% HCl at 25°C and in 10% HCl at 25°C and 40°C. In the presence of a sufficient concentration of the extracts in 5% HCl at 25°C, the inhibitory efficiency towards steel decreases in the order: Mango (82%), Orange and *Aloe vera* (80%), *Opuntia ficus* (75%),

pomegranate (65%). These order of efficiency differs for the different metals, but extract of mango peels is still the most effective for Al (82%) and Zn (80%). The most effective extract for Cu is that of pomegranate fruit-shells (73%). The extracts are generally more effective in HCl than in H<sub>2</sub>SO<sub>4</sub> pomegranate measurements prove that all the extracts increase the polarization of steel and Zn, while orange and aloe have no effect on the anodic reaction of Al and only pomegranate has any effect on the anodic polarization of Cu. The results indicate that the extracts generally act as mixed inhibitors.

The effect of extracts of chamomile (*chamaemelum mixtum* L.), halfbar (*cymbopogon proximus*), black cumin (*Nigella sativa* L.), and kidney bean (*phaseolus vulgaris* L.) plants on the corrosion of carbon steel in aqueous 1M H<sub>2</sub>SO<sub>4</sub> solution were investigated by electrochemical impedance spectroscopy (EIS) and potentiodynamic polarization techniques [104] EIS measurements showed that the dissolution process of steel occurs under activation control. Potentiodynamic polarization curves indicate that the plant extracts behave as mixed-type inhibitors. The corrosion rates of steel and the inhibition efficiencies of the extracts were calculated. The results obtained show that the extract solution of the plant could serve as an effective inhibitor for the corrosion of steel in 1M H<sub>2</sub>SO<sub>4</sub> solution. Inhibition was found to increase with increasing concentration of the plant extract up to a critical concentration. The inhibitive actions of plant extracts are discussed based on adsorption of stable complex at the steel surface. Theoretical fitting of different isotherms, Langmuir, Flory-Huggins, and the kinetic-thermodynamic model, were tested to clarify the nature of adsorption.

The effect of eugenol (Eug) and its derivative acetyleneugenol (AcEug) extracted from the nail of giroflier on the corrosion of steel in

molar hydrochloric acid was studied using weight loss measurements, electrochemical polarization and EIS methods [105]. The naturally substances reduce the corrosion rate. It was found that the inhibition efficiency increased with the content of acetylogenol to 91% at 0.1737 g/l. Eugenol compounds act as mixed type inhibitors. The effect of temperature on the corrosion behavior of steel indicates that the inhibition efficiency of the natural substance increases with increasing temperature.. The adsorption of natural product on the steel is found to follow the Langmuir isotherm

Natural oil extracted from pennyroyal Mint (*Mentha pulegium*, PM) was examined as corrosion inhibitor of steel in 1.0M HCl solution using weight loss measurements, electrochemical polarization and EIS methods [106]. The naturally oil was found to reduce the corrosion rate of steel. The inhibition efficiency was found to increase with oil content to attain 80% at 2.76 g; PM oil acts as a cathodic inhibitor. The increase in temperature leads to an increase in the inhibition efficiency of the natural substance. The adsorption isotherm of natural product on the steel has been determined.

The inhibitive effect of the extract of khillah (*Ammi visnaga*) seeds, on the corrosion of SX 316 steel in HCl solution was determined using weight loss measurements as well as potentiostatic technique [107]. It was found that the presence of the extract reduces markedly the corrosion rate of steel in the acid solution. The inhibition efficiency increases as the extract concentration is increased. The inhibitive effect of khillah extract was discussed based on the adsorption of its components on the steel surface. Negative values were calculated for the energy of adsorption indicating the spontaneity of the adsorption process. The formation of insoluble

complexes as a result of interaction between iron cations and khellin, which present in the extract, was also discussed.

The aqueous extract of the leaves of henna (*lawsonia*) is tested as corrosion inhibitor of C-steel, nickel and zinc in acidic, neutral and alkaline solutions, using the potentiostatic polarization technique [108]. It was found that the extract acts as a good corrosion inhibitor for the three tested electrodes in all tested media. The inhibition efficiency increases as the added concentration of extract is increased. The degree of inhibition depends on the nature of metal and the type of the medium. For C-steel and nickel, the inhibition efficiency increases in the order: alkaline < neutral < acid, while in the case of zinc it increases in the order: acid < alkaline < neutral. The extract acts as a mixed inhibitor. The inhibitive action of the extract is discussed in view of adsorption of *lawsonia* molecules on the metal surface. It was found that this adsorption follows Langmuir adsorption isotherm in all tested systems. The formation of complex between metal cations and *lawsonia* is also proposed as additional inhibition mechanism of C-steel and nickel corrosion. Also, vanillin [109] was investigated for the corrosion of mild steel in acid media. Berberine an alkaloid isolated from *Captis* was studied for its anticorrosion effect for mild steel corrosion in  $H_2SO_4$  medium by Yan Li et al [110].

The inhibitive action of the extent of *ficus nitida* leaves toward general and pitting corrosion of C-steel, nickel and zinc in different aqueous media was investigated [111]. Weight loss measurements, potentiodynamic polarization techniques were used. It is found that the presence of *ficus* extract in the corrosive media (acidic, neutral or alkaline) decreases the corrosion rates of the three tested metals. The inhibition efficiency increases as the extract concentration is increased. The inhibition efficiency depends on the type of corroded metal and on the corrosive

solution. It was also found that the presence of ficus extract in the chloride containing solution shifts, the pitting potential of the tested metals toward the noble direction. The inhibitive action of the ficus extract is discussed in view of adsorption of its components, the poly aromatic compounds, friendeln, epifriedelanol and nit idol, on the metal surface. It was found that such adsorption follows Langmuir adsorption isotherm. The calculated values of the free energy of adsorption indicated that the adsorption process is spontaneous.

The inhibitory effect of henna extract (*Lawsonia inermis*) and its main constituents (lawsone, gallic acid,  $\alpha$ -D-Glucose and tannic acid) on corrosion of mild steel in 1M HCl solution was investigated by electrochemical techniques and surface analysis (SEM/EDS) [112]. Polarization measurements indicate that all the screening compounds act as a mixed inhibitor and inhibition efficiency increases with inhibitor concentration. Maximum inhibition efficiency (92.06%) is obtained at 1.2 g/l Henna. Inhibition efficiency increases in the order: lawsone>henna extract>gallic acid> $\alpha$ -D-Glucose> tannic acid. Also, the mechanism of inhibition and parameters of thermodynamics is discussed

The inhibitor effect of the naturally occurring biological molecule caffeic acid toward the corrosion of mild steel in 0.1 M H<sub>2</sub>SO<sub>4</sub> solution was investigated using weight loss, potentiodynamic polarization, electrochemical impedance and Raman spectroscopy [113]. The different techniques confirmed the adsorption of caffeic acid onto the mild steel surface and consequently the inhibition of the corrosion process. Caffeic acid acts by reducing the available cathodic reaction area and modifying the activation energy of the anodic reaction. A



mechanism is proposed to explain the inhibitory action of the corrosion inhibitor.

The inhibitive and adsorption prosperities of ethanol extract of phyllanthus amarus for the corrosion of mild steel in  $H_2SO_4$  were investigated using gravimetric, thermometric and gasometric methods [114]. Ethanol extract of phyllanthus amarus leaves is a good adsorption inhibitor for the corrosion of mild steel in  $H_2SO_4$ . Thermodynamic consideration indicates that the adsorption of the extract is exothermic and spontaneous. Also, the adsorption characteristic of the inhibitor is consistent with the assumptions of Langmuir adsorption isotherm. From the results and findings of the study, physical adsorption mechanism is proposed for the adsorption of ethanol extract of phyllanthus amarus on mild steel surface.

The inhibitive action of lupine (*Lupinus albus* L.) extract on the corrosion of carbon steel in aqueous solution of 1M  $H_2SO_4$  and 2M HCL solutions was investigated by potentiodynamic polarization and electrochemical impedance spectroscopy (EIS) techniques [115]. Potentiodynamic polarization curves indicate that the lupine extract acts as a mixed- type inhibitor. EIS measurements showed that the corrosion process is under activation control. The inhibition efficiency of extract obtained from impedance and polarization measurements was in good agreement and it was found to increase with the increase in the extract concentration .The obtained results showed that, the lupine extract could serve as an effective inhibitor for the corrosion of steel in the acidic medium and the extract was more effective in case of HCl solution. Theoretical fitting of the corrosion data to the kinetic.

Galvanostatic and potentiodynamic anodic polarization methods were used to study the inhibiting effect of parsley, lettuce and radish oils on the corrosion of carbon steel (L-52) used in Egyptian manufacturing pipelines in 0.5M NaOH solution [116]. The inhibition efficiency increases with an increase in the concentration of these oils. This is due to the adsorption of the basic component of these oils on the surface of the steel. The adsorption process is described by a Langmuir isotherm. It was found that incorporation of chloride ion in the 0.5M solution of NaOH accelerates pitting corrosion of the steel as a result of moving the pitting potential toward more negative values. The investigated oils added to the solution containing chloride ions protect steel from pitting corrosion by shifting the pitting potential to more positive direction.

#### **1.6.6-Polymer as corrosion inhibitor:**

Guar gum was tested as corrosion inhibitor for carbon steel in 1M H<sub>2</sub>SO<sub>4</sub> solution using weight loss, Tafel polarization techniques [117]. The result showed that, the inhibition efficiency increases with the increasing of guar gum concentration, which act as an inhibitor of the mixed type. The inhibition action of guar gum was discussed in terms of its horizontal adsorption on the metal surface. The adsorption follows Langmuir adsorption isotherm. The effect of the presence of chloride ion in pitting corrosion was analyzed by the potentiodynamic anodic polarization technique. The pitting corrosion potential changes with the concentration of Cl<sup>-</sup> ion according to a sigmoid S- shaped curve. This behavior was explained on the basis of the formation of passivable active and continuously propagated pits.

Biodegradation and environmental toxicity of products used in the oil industry are of great importance and the corrosion inhibitor cannot be an exception [118]. Chitosan and some derivatives were evaluated as corrosion inhibitors at acidic pH, mainly due to the solubility of the polymer. An eco-friendly corrosion inhibitor with water solubility in all pH range must be ideal and can work under the high salinity of the oilfield environment. Thus, the performance of water-soluble carboxymethyl chitosan (CMC) is presented here as a corrosion inhibitor of carbon steel in the presence of 3.5% NaCl without any acid or base addition. CMC showed good properties as corrosion inhibitor in media containing  $\text{Cl}^-$ , and behaved as an anodic inhibitor. CMC exhibited inhibitory efficiency of about 80% and 67%, according to Tafel curve and electrochemical impedance, respectively, which are attributed to chemisorption mechanism ( $\Delta G_{\text{ads}} \approx -45 \text{ kJ/mol}$ ).

The inhibition efficiency of the antibacterial cephalosporin e.g. cefotaxime, cefalexin, cefradine and cefazolin toward the corrosion of iron in 1.0 M HCl was investigated using electrochemical techniques. [119] The results of these techniques indicated that the inhibition efficiency increased with the concentration of inhibitor but decreased with temperature. Potentiodynamic studies proved that the inhibitors act as mixed mode of inhibition and the inhibitor molecules adsorb on the metal-solution interface. The adsorption of the inhibitors on iron surface obeys the Langmuir adsorption isotherm equation. All impedance spectra in EIS tests exhibit one capacitive loop which indicates that the corrosion reaction is controlled by charge transfer process. Inhibition efficiencies obtained from Tafel polarization, charge transfer resistance ( $R_{\text{ct}}$ ) is consistent.

The corrosion inhibition efficiency of aniline, formaldehyde and piperazine based polymer (ADPD) on N80 steel in 3.5% NaCl solution saturated with carbon dioxide was investigated using electrochemical impedance spectroscopy (EIS), potentiodynamic polarization, weight loss, scanning electrochemical microscopy (SECM), scanning electron microscopy (SEM) measurements, density functional theory (DFT) and molecular dynamics simulation (MD) [120]. The adsorption of polymer onto N80 steel surface follows Langmuir adsorption isotherm model. Potentiodynamic polarization study confirmed that inhibitor is mixed type with cathodic predominance. SECM study reveals the current values decreases with the increasing concentration of polymer. SEM study supports the smooth metal surface texture. DFT and MD calculations are in agreement with the experimental findings.

A new class of corrosion inhibitors, namely, polyamino-enzoquinone (PAQ) has been synthesized and its inhibiting action on the corrosion of mild steel in 1M H<sub>2</sub>SO<sub>4</sub> and 1M HCl solutions has been investigated by various corrosion monitoring techniques[121]. A preliminary screening of the inhibition efficiency of the polymer was carried out by self corrosion studies. PAQ is found to behave better in 1M H<sub>2</sub>SO<sub>4</sub> than 1M HCl solution . Potentiodynamic polarization studies clearly reveal the fact that PAQ is a mixed-type inhibitor. PAQ is able to reduce considerably the permeation current through the steel surface in both the acids. Changes in impedance parameters ( $R_{ct}$  and  $C_{dl}$ ) are indicative of adsorption of PAQ on the metal surface leading to the formation of a protective film which grows with increasing exposure time. The adsorption of this polymer is also found to obey Temkin's adsorption isotherm in both acids thereby indicating that the main process of inhibition is by adsorption. UV spectral studies were also carried out to establish the actual mechanism of inhibition of corrosion

The corrosion inhibition of mild steel in  $\text{H}_2\text{SO}_4$  in the presence of gum arabic (GA) (naturally occurring polymer) and polyethylene glycol (PEG) (synthetic polymer) was studied using weight loss, hydrogen evolution and thermometric methods at 30–60 °C[122]. PEG was found to be a better inhibitor for mild steel corrosion in acidic medium than GA. The effect of addition of halides (KCl, KBr and KI) was also studied. Results obtained showed that inhibition efficiency increased with increase in GA and PEG concentration, addition of halides and with increase in temperature. Increase in inhibition efficiency and degree of surface coverage was found to follow the trend  $\text{Cl}^- < \text{Br}^- < \text{I}^-$  which indicates that the radii and electronegativity of the halide ions play a significant role in the adsorption process. GA and PEG alone and in combination with halides were found to obey Temkin adsorption isotherm. Phenomenon of chemical adsorption is proposed from the trend of inhibition efficiency with temperature and values  $\Delta G^\circ_{\text{ads}}$  were obtained. The synergism parameter evaluated is found to be greater than unity indicating that the enhanced inhibition efficiency caused by the addition of halides is only due to synergism

## Aim of the Present Work

Carbon steel is used as an essential part in the manufacturing of a lot of things in our life. The choice of carbon steel is due to its availability and low cost. Carbon steel surface server corrosion in aggressive media like HCl .Corrosion inhibitors are widely used in industry to reduce the corrosion of carbon steel .Many studied have been carried out to find asuitable compound to use as corrosion inhibitors . Among of these compounds the organic polymer compounds successively used as corrosion inhibitors .The present study aims to examine some polymer compounds e.g polyvinyle alcohol ,synperonic, maltodextrine ,alginic acid, pectin and chitosan to be used as corrosion inhibitors for carbon steel.

Thus ,the present work involves the following :

- 1) Investigation of the inhibiting effect of some polymer compounds towards the corrosion of carbon steel in 1M HCl.
- 2) Determination of the inhibition efficiencies of these compounds using different techniques e.g.
  - a .Weight loss measurements.
  - b. Galvanostatic polarization technique.
  - c. potentiodynamic anodic polarization at  $1 \text{ m V sec}^{-1}$ .
  - d. Electrochemical impedance spectroscopy (EIS).
- 3) Studying the effect of increasing temperature on the rate of corrosion.
- 4) Study the initiation of the pitting corrosion of carbon steel in chloride containing solutions and its inhibition by the examined polymer compounds.
- 5) Explanation the mechanism of the inhibition of polymer compounds

6) Finally, the arrangement of polymer compounds according to their percentage inhibition efficiency from the results obtained by all methods used.

**CHAPTER (2)**  
**EXPERIMENTAL TECHNIQUES**



## ***EXPERIMENTAL TECHNIQUES***

### **2.1-Chemical composition of carbon steel.**

The experiments were conducted using carbon steel that contains the chemical compositions mentioned in Table.(2.1)

<b>Element</b>	C	Mn	S	P	Si	Al	Fe
<b>Weight (%)</b>	0.110	0.450	0.050	0.040	0.250	0.039	balance

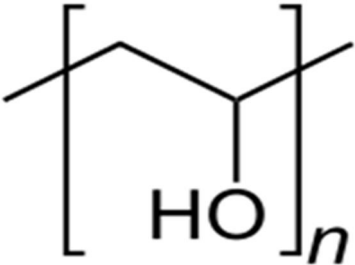
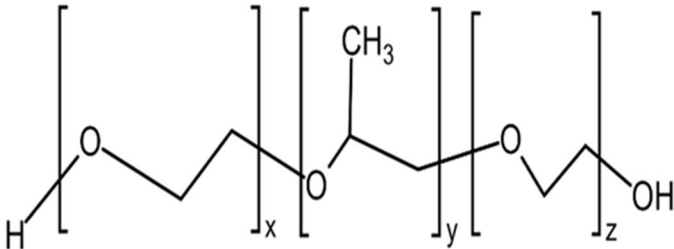
### **2.2- Chemical additives and solution.**

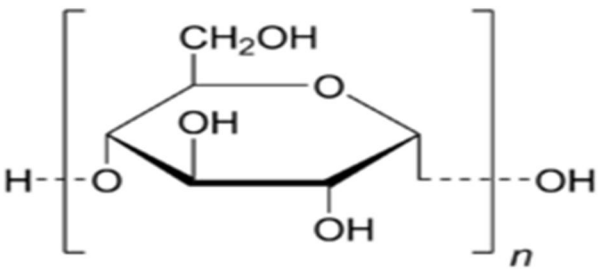
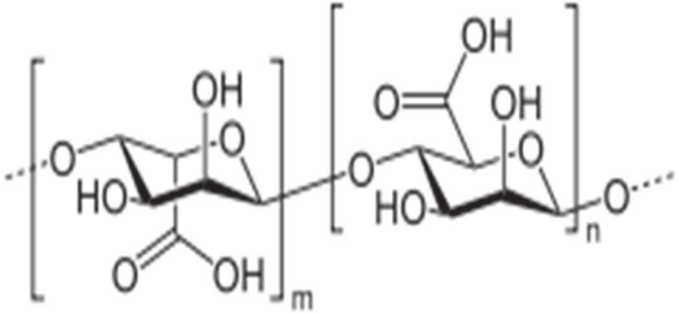
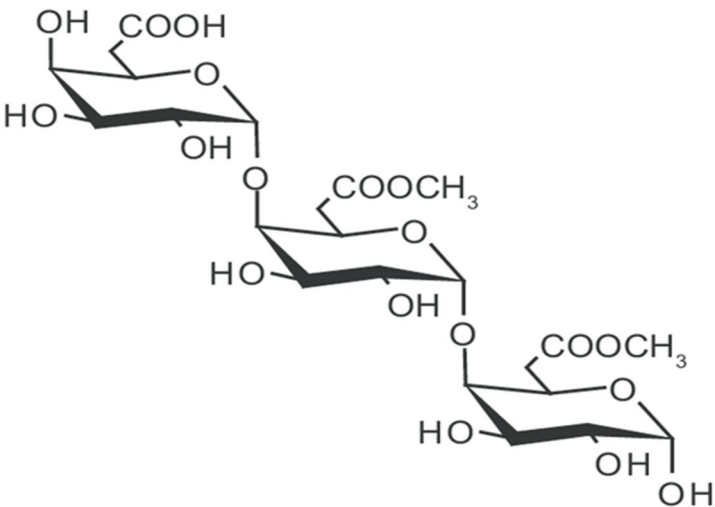
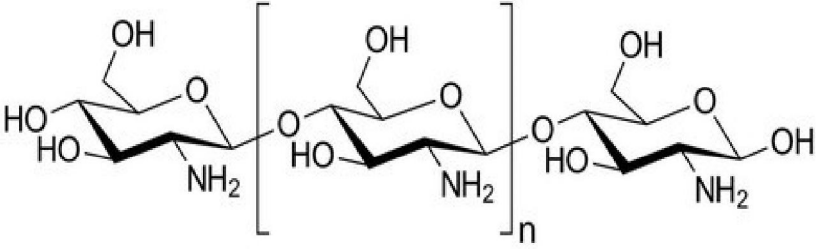
All solutions employed in this work are freshly prepared from Merck or Aldrich chemicals using bidistilled water. Stock solutions of the corrosive medium (HCl) were prepared by dilution of 37% HCl (Merck) using bidistilled water. The concentration range of the polymer (inhibitors) used was 100-500 ppm. The polymer solutions were prepared by dissolving the required quantities of samples in bidistilled water and the desired concentrations were obtained by appropriate dilution. Each experiment was performed in aerated stagnant solutions and was repeated at least three times under the same conditions to check the reproducibility and the average of the three replicated values was used for further processing of the data.

### 2.3. The chemical structure of polymer and uses.

#### 2.3.1. The chemical structure of polymer:

**Table(2.2)** The names and chemical structures of polymer used.

Name	Chemical structure	Molecular weight
<p>(i) compound I <u>Poly vinyl Alcohol</u></p>	 <p>The diagram shows a repeating unit of Polyvinyl Alcohol (PVA) enclosed in large square brackets with a subscript 'n'. The backbone consists of two carbon atoms connected by a single bond. The left carbon is bonded to a hydrogen atom (H) and another carbon atom that continues the chain. The right carbon is bonded to a hydroxyl group (HO) and another carbon atom that continues the chain.</p>	44g/mol
<p>(ii) compound II <u>synperonic</u></p>	 <p>The diagram shows a copolymer chain with three repeating units enclosed in large square brackets. The first unit is a polyethylene glycol (PEG) unit: -[CH2-CH2-O]-. The second unit is a poly(methyl methacrylate) (PMMA) unit: -[C(CH3)(COO-)]-. The third unit is another PEG unit: -[CH2-CH2-O]-. The units are connected by oxygen atoms, and the chain ends with a hydrogen atom (H) on the left and a hydroxyl group (OH) on the right. Subscripts x, y, and z are placed below the brackets for each unit respectively.</p>	164g/mol

<p><u>(iii)Compound III</u> <u>Maltodextrin</u></p>		178g/mol
<p><u>(iv)compound IV</u> <u>Alginate</u></p>		176g/mol
<p><u>(v)compound V</u> <u>pectin</u></p>		193g/mol
<p><u>(vi)compound VI</u> <u>chitosan</u></p>		201g/mol

### **2.3.2.Uses of polymer compound[133-135].**

#### **(i) Poly vinyl alcohol:**

Poly vinyl alcohol is used in a variety of medical applications because of its biocompatibility, low tendency for protein adhesion, and low toxicity. Specific uses include cartilage replacements, contact lenses, and eye drops. Polyvinyl alcohol is used as an aid in suspension polymerizations. Its largest application in China is its use as a protective colloid to make polyvinyl acetate dispersions. In Japan its major use is the production of vinylon fiber.

#### **(ii) Synperonic:**

It is widely used around the world as an industrial surfactant primarily for the cleaning of textiles but with a variety of other uses.

#### **(iii) Maltodextrin:**

It is a white powder that is relatively tasteless and dissolves in water. It is an additive in a wide range of foods, as it can improve their texture, flavor, and shelf life.

#### **(iv)Alginic acid:**

Alginate absorbs water quickly, which makes it useful as an additive in dehydrated products such as slimming aids, and in the manufacture of paper and textiles. It is also used for waterproofing and fireproofing fabrics, in the food industry as a thickening agent for drinks, ice cream and cosmetics, and as a gelling agent for jellies.[citation needed] Alginate is used as an ingredient in various pharmaceutical preparations, such as Gaviscon, in which it combines with bicarbonate to inhibit reflux. Sodium alginate is used as an impression-making material in dentistry, prosthetics, lifecasting and for creating positives for small-scale casting.

**(v) Pectin:**

The main use for pectin is as a gelling agent, thickening agent and stabilizer in food. The classical application is giving the jelly-like consistency to jams or marmalades, which would otherwise be sweet juices. Pectin also reduces syneresis in jams and marmalades and increases the gel strength of low-calorie jams. For household use, pectin is an ingredient in gelling sugar (also known as "jam sugar") where it is diluted to the right concentration with sugar and some citric acid to adjust pH. In some countries, pectin is also available as a solution or an extract, or as a blended powder, for home jam making .

For conventional jams and marmalades that contain above 60% sugar and soluble fruit solids, high ester pectins are used. With low ester pectins and amidated pectins, less sugar is needed, so that diet products can be made. Water extract of aiyu seeds is traditionally used in Taiwan to make aiyu jelly, where the extract gels without heating due to low-ester pectins from the seeds and the bivalent cations from the water.

**(vi) Chitosan:**

It can be used as a fining agent, also helping to prevent spoilage. In industry, it can be used in a self-healing polyurethane paint coating. In medicine, it may be useful in bandages to reduce bleeding and as an antibacterial agent; it can also be used to help deliver drugs through the skin. More controversially, chitosan has been asserted to have used in limiting fat absorption, which would make it useful for dieting, but there is evidence against this. Other uses of chitosan that have been researched include use as a soluble dietary fibre. Used as the biopesticide, Antifungal and Antibacterial agent.

## 2.4. Experimental techniques.

Four different techniques have been employed for studying the corrosion behavior of carbon steel in 1.0 M HCl solution in absence and presence of the synthesized surfactants. There are as the following:

- 1- Chemical technique e. g., Weight loss measurements(WL)
- 2- Electrochemical techniques such as,
  - i- Galvanostatic polarization method(GPM)
  - ii- Potentiodynamic anodic polarization(PAP)
  - iii-Electrochemical impedance spectroscopy (EIS)

### 2.4.1. Weight loss method.

Prior to each experiment the surface of carbon steel samples was mechanically polished with different grades of emery paper ranging from 200 to 1600 and rinsed with distilled water bilaterally and dried between two filter papers. The cleaned carbon steel was weighed before and after immersion in 100 ml of the test solution for a period up to hours .The average weight loss for each two identical experiments was taken and expressed in mg/cm<sup>2</sup>. The temperature was adjusted to 25±1°C using a thermostat. Inhibition efficiencies were calculated from the weight loss data using the relation (2.1):

$$IE\% = \left[ \frac{W_f - w_i}{w_f} \right] \times 100 \quad (2.1)$$

Where IE% is the percentage inhibition efficiency, W<sub>f</sub> and W<sub>i</sub> are the weight loss in absence and presence of inhibitors, respectively.

### 2.4.2. Electrochemical techniques.

#### i) Galvanostatic polarization method:

Galvanostatic polarization method was used to determine the anodic and cathodic polarization curves of carbon steel in 1 M HCl in absence and presence of different concentrations of polymer compounds. E vs. log I curves recorded. The corrosion kinetic parameters such as corrosion current ( $I_{\text{corr}}$ ), corrosion potential ( $E_{\text{corr}}$ ), cathodic Tafel slope ( $\beta_c$ ), and anodic Tafel slope ( $\beta_a$ ) were derived from the Tafel curves. The polarization was Galvanostatic tracked at a scan rate of 2 mV/ s.

Galvanostatic anodic polarization measurements were performed at scan rate 1mV/s to measure the pitting corrosion potentials.

The two polarization were measurements were performed using a PS remote potentiosta with PS6 software for the determination of some corrosion parameters

The corrosion rate was calculated by polarization method as the current corresponds to the intercept between cathodic and anodic lines. Inhibition efficiency was

$$IE\% = \left[ \frac{I_f - I_i}{I_f} \right] \times 100 \quad (2.2)$$

Where  $I_f$  and  $I_i$  are the corrosion rates in absence and presence of the extract.

The parameter ( $\theta$ ) which represents the fraction of surface covered by adsorbed molecules is calculated using the following equation:

$$\theta = \left[ \frac{IE\%}{100} \right] \quad (2.3)$$

## ii) Electrochemical impedance spectroscopy (EIS)

The EIS spectra were recorded at open circuit potential, OCP after immersion the electrode for 30 min. The AC signal was 5 mV peak to peak and the frequency range studied was between 50 kHz and 0.1 Hz by using same Potentiostat/Galvanostat as in polarization with EIS 300 software for calculations.

### 2.5-Electrochemical cell

The complete polarization cell is shown in Fig. (2.1). It is a multi-necked flat bottom 250 ml round flask. The multiple necks were used to introduce the working and auxiliary electrodes through ground glass joints. This latter was installed in a compartment separated from the main bulk of the electrolyte by means of a sintered glass to ensure the separation of the anode and cathode reaction products, gas inlet and gas outlet tubes and Luggin probe entered the cell through a clamped ball and socket joint. The arrangement allows the flexibility necessary to align the Luggin capillary from a saturated calomel reference electrode adjacent to the working electrode. During polarization measurements, it was important to use the correct position for the Luggin probe tip.

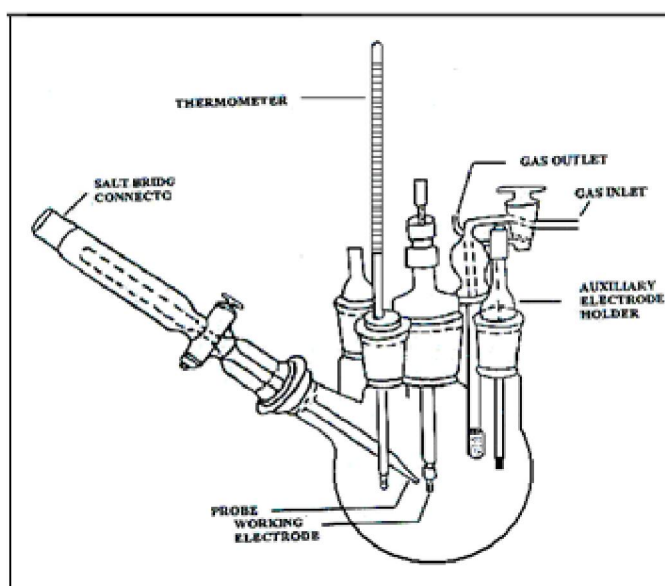




Fig.(2.1): Schematic diagram of Electrochemical cell

If the probe tip is placed close to the working electrode, it tends to screen current from the electrode, if it was placed too far away, appreciable resistance or IR drop may be introduced in the possible measurements. In general, the Luggin probe tip is placed between one and five millimeters the surface of the electrode. The polarization cell and its components were carefully cleaned after each experiment to remove any foreign residues, especially the metal products that formed during the measurement. All the glass-water used in polarization measurements was dried by keeping them in an oven at about 100 °C prior to use.

## 2.6. Electrodes.

### 2.6.1. The working electrode:

The working electrode (WE) of the same composition of carbon steel embedded in epoxy holder exposes only only a 0.75 cm<sup>2</sup> surface to the solution shown in in Figure (2.2). The exposure surface was polished successively with various grades emery paper until 1600 grades, degreased with acetone and then rinsed with distilled water ,before inserting it directly into the electrolytic cell

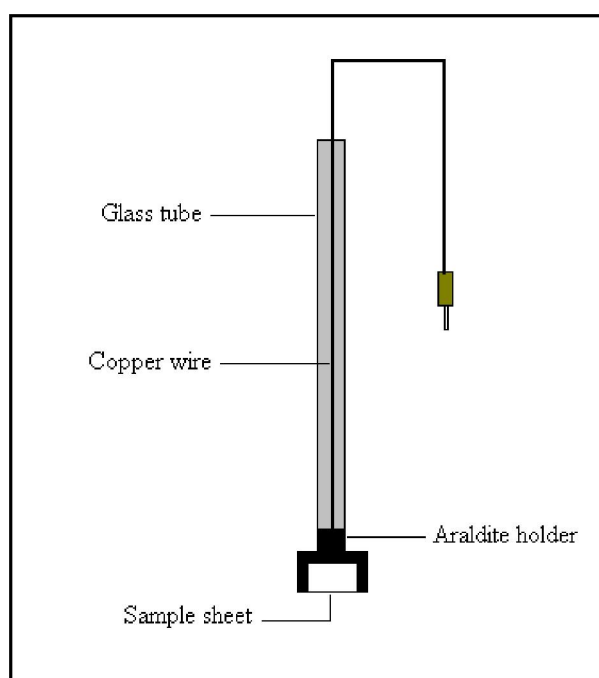


Fig. (2.2): Schematic diagram of the working electrode.

### 2.6.2-Reference electrode:

A saturated calomel electrode (SCE) was used during all polarization measurements. The electrical contact with the electrolyte solution was maintained by insertion through the Luggin-probe, care was always taken during the insertion, so that the probe should be free from any bubbles. The saturated calomel electrode was periodically calibrated and checked.

### 2.6.3-Auxiliary electrode:

The cell must A platinum foil sealed in a glass tube acted as a counter electrode. The main requirements in the cell for the electrochemical measurements are:

- 1) The cell must be air tight
- 2) Greased taps should be avoided
- 3) The cell must allow the adjustment of the anode in order to touch the tip of the luggin probe.

The polarization cells and its components were carefully cleaned after each experiment to remove any residues, especially the metal products that formed during the measurement. All glassware used in polarization measurements was dried by keeping them in an oven at 100 ° C before use

The complete electrochemical cell is shown in Fig. (2:1). It is multi-necked flat bottom 250 ml. round flask. The multiple necks were used to introduce the electrode-working and auxiliary electrodes

The polarization cells and its components were carefully cleaned after each experiment to remove any residues especially the metallic products that formed during the measurement. All the glass-wares used in polarization measurements was dried by keeping them in an oven at a boot 100°C before use.

**CHAPTER (3)**  
**RESULTS AND DISCUSSION**

***PART (A)*****Studying the Corrosion Behavior of C-Steel in Aqueous Solutions by the Weight Loss Measurements.****3.1. Weight loss measurements.**

The corrosion behavior of carbon steel (C-steel) in an aqueous environment is characterized by the extent to which it dissolves in the solution. The degree of dissolution, of course, depends on the surface area of the metal exposed and the time of exposure; thus the amount of corrosion is given with respect to area and time. The resulting amount, corrosion rate, is thus a fundamental measurement in the science of corrosion. Corrosion rates can be evaluated by measuring either the concentration of the dissolved metal in solution by chemical analysis or by measuring weight of a sample before and after exposure and applying the following equation:

$$\Delta w = (w_1 - w_2) \quad (3.1)$$

where,  $\Delta w$  is the weight of C-steel loss in the corrosive solution.

$W_1$  : is the weight of C-steel before exposure to the corrosive solution.

$W_2$  : is the weight of C-steel after exposure to the corrosive solution.

The degree of dissolution, of course, depends on the surface area of the exposed metal and the immersion; thus, the amount of corrosion is given in relation to the area and time. The resulting amount of corrosion rate, is thus a fundamental measurement in the science of corrosion. The corrosion rate can be assessed by measuring either the concentration of the dissolved metal in solution by chemical analysis or by measuring weight of specimen before and after exposure and applying equation (3.1). The latter most common method. The weight loss method is usually preferred because the the measured amount is directly related to the extent of corrosion and does not depend on any assumptions about the reactions that occur during corrosion.

Figures (3.1-3.6) represent the effect of addition of increasing concentrations of six polymer compounds on the weight loss -immersion time curves of C-steel in 1.0M HCl solutions. As shown in these figures, it is evident that with an increase in the concentration of these polymer compounds, the weight loss of C-steel sample is reduced. This means that the presence of these polymer compounds retards the corrosion of C-steel in 1.0M HCl solution. The linear variation of weight loss with immersion time in uninhibited and inhibitive 1.0M HCl solution indicates the absence of insoluble surface films during corrosion. In the absence of any surface films, the inhibitors are first adsorbed on to the metal surface and there after impeding corrosion either by merely blocking the reaction sites (anodic and cathodic) or by altering the mechanism of the anodic and cathodic partial processes [123]

The rate of corrosion ( $R_{\text{corr}}$ ) is calculated as  $\text{mg.cm}^{-1}.\text{min}^{-1}$ , as following (3.2):

$$R_{\text{corr}} = \frac{\Delta w}{A.t} \quad (3.2)$$

Where,  $\Delta w$ : is weight loss in milligrams.

A: is the surface area in square centimeters of the coupon.

t: is the immersion time in minutes.

The percentage inhibition efficiency (I.E%) and parameter ( $\theta$ ) which signifies the part of metal surface covered by the polymer molecules were calculated from the weight loss data using the following equations:

$$\%I.E = \left[ 1 - \frac{R_{\text{corr.inh}}}{R_{\text{corr.free}}} \right] \times 100 \quad (3.3)$$

$$\theta = \left[ 1 - \frac{R_{\text{corr.inh}}}{R_{\text{corr.free}}} \right] \quad (3.4)$$

where  $R_{\text{corr.inh}}$  and  $R_{\text{corr.free}}$  are the corrosion rates of carbon steel in the presence and absence of additives, respectively.

The values of inhibition efficiency (%IE) and the surface coverage ( $\theta$ ) for various concentrations of polymer compounds are inserted in Tables (3.1-

3.6). Inspection of these Tables, it clear that, the obtained values of IE % and  $\theta$  and increased by increased the concentration of polymer compounds.

The order of IE% decreases in following sequences:

Comp.VI > Comp. V > Comp. IV > Comp. III >Comp.II >Comp.I

The mechanism of inhibition process will be discussed later in the section inhibition mechanism .

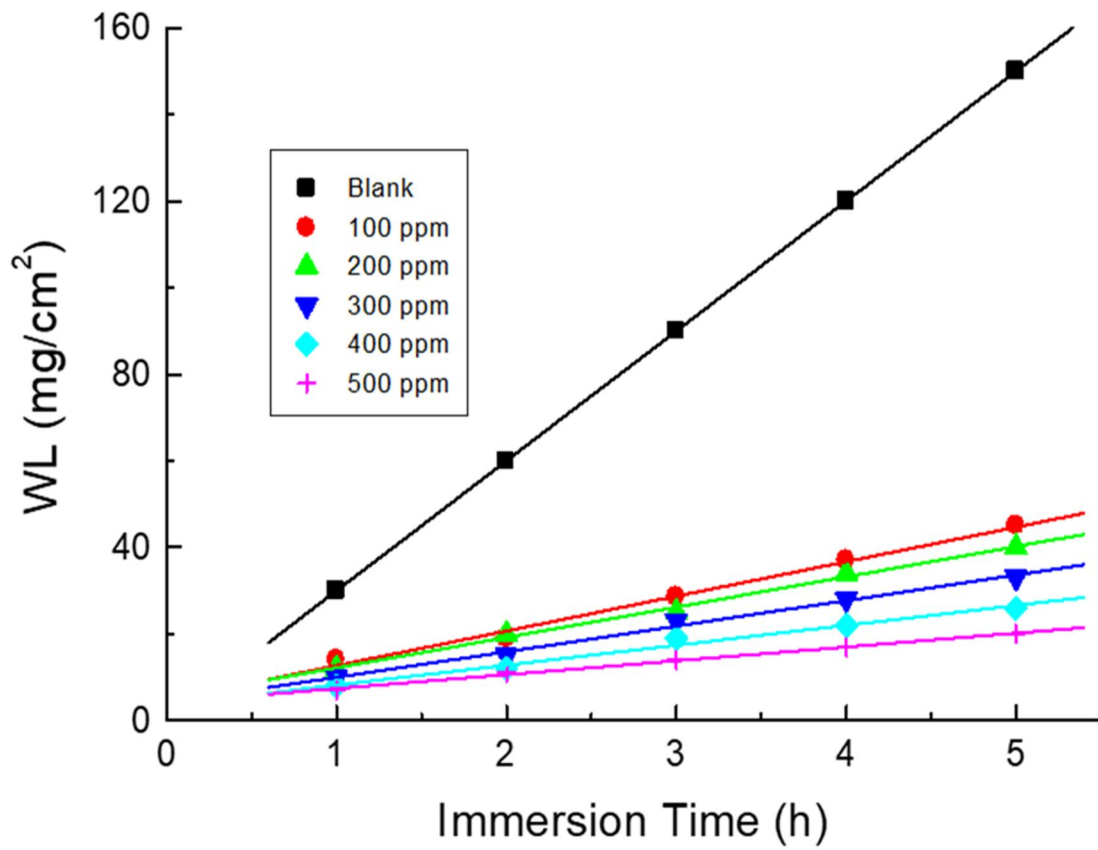


Fig.(3.1):Weight loss-time curves for corrosion of carbon steel in 1.0 M HCl solution containing various concentrations of compound I.



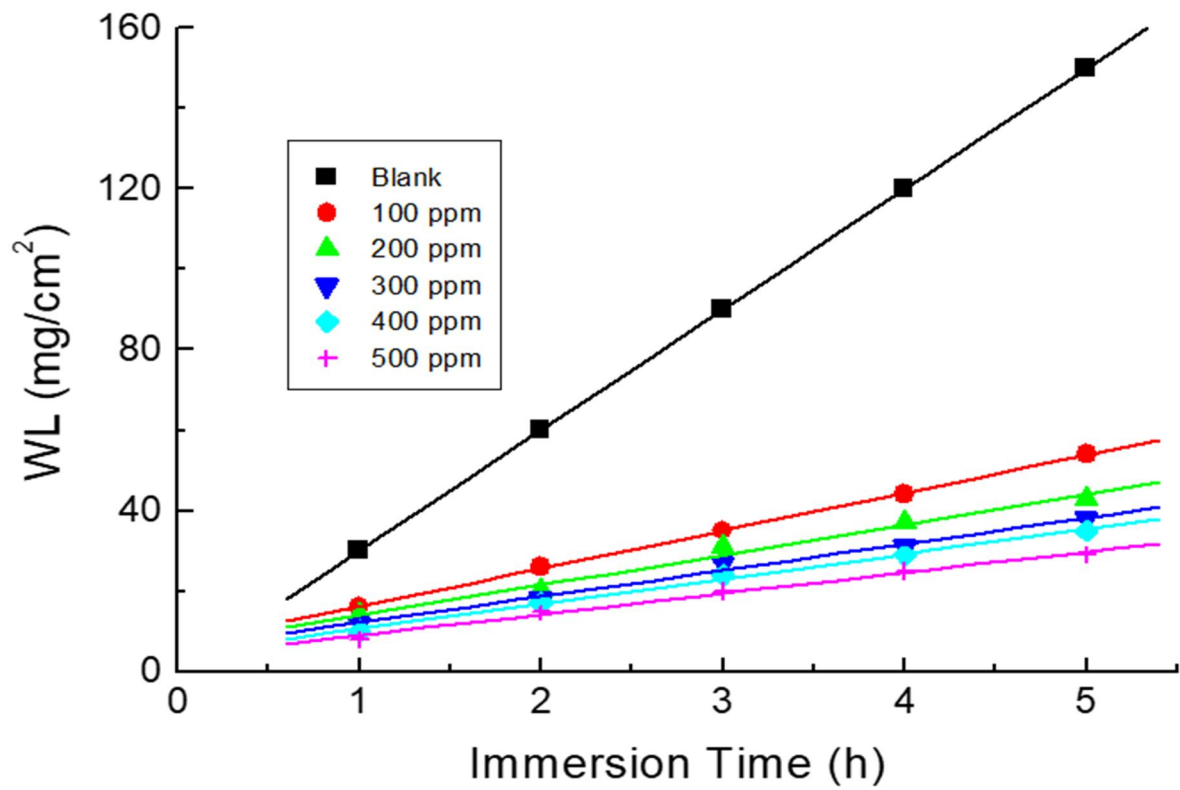


Fig.(3.2):Weight loss-time curves for corrosion of carbon steel in 1.0 M HCl solution containing various concentrations of compound II.

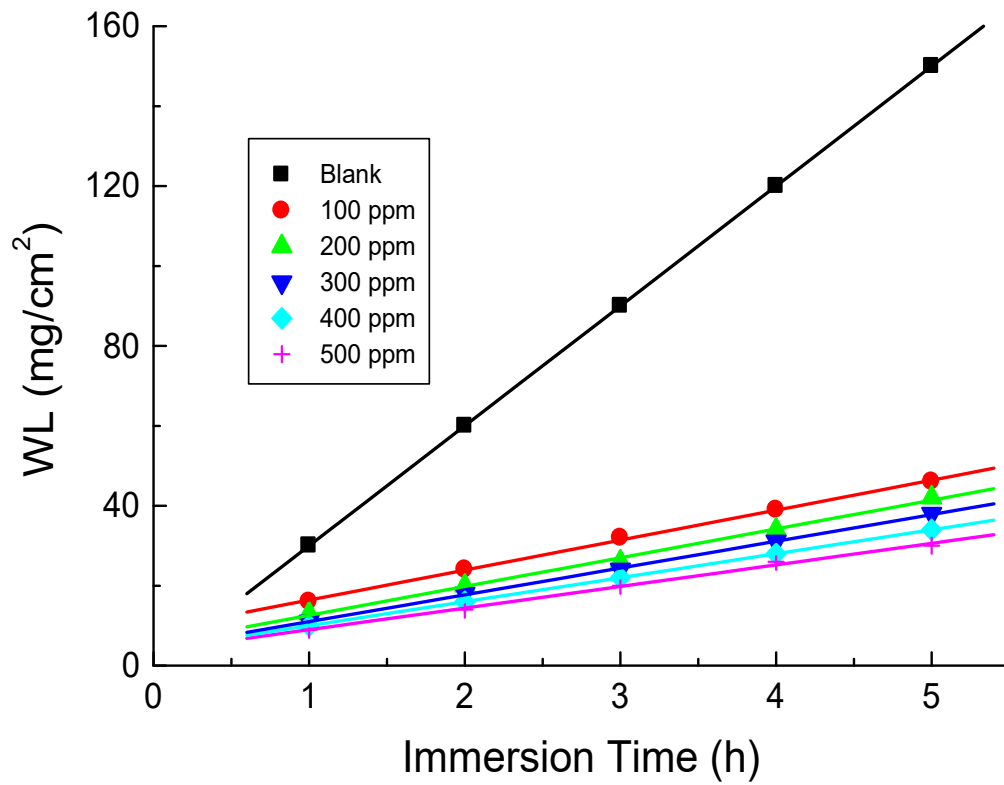


Fig.(3.3):Weight loss-time curves for corrosion of carbon steel in 1.0 M HCl solution containing various concentrations of compound III.

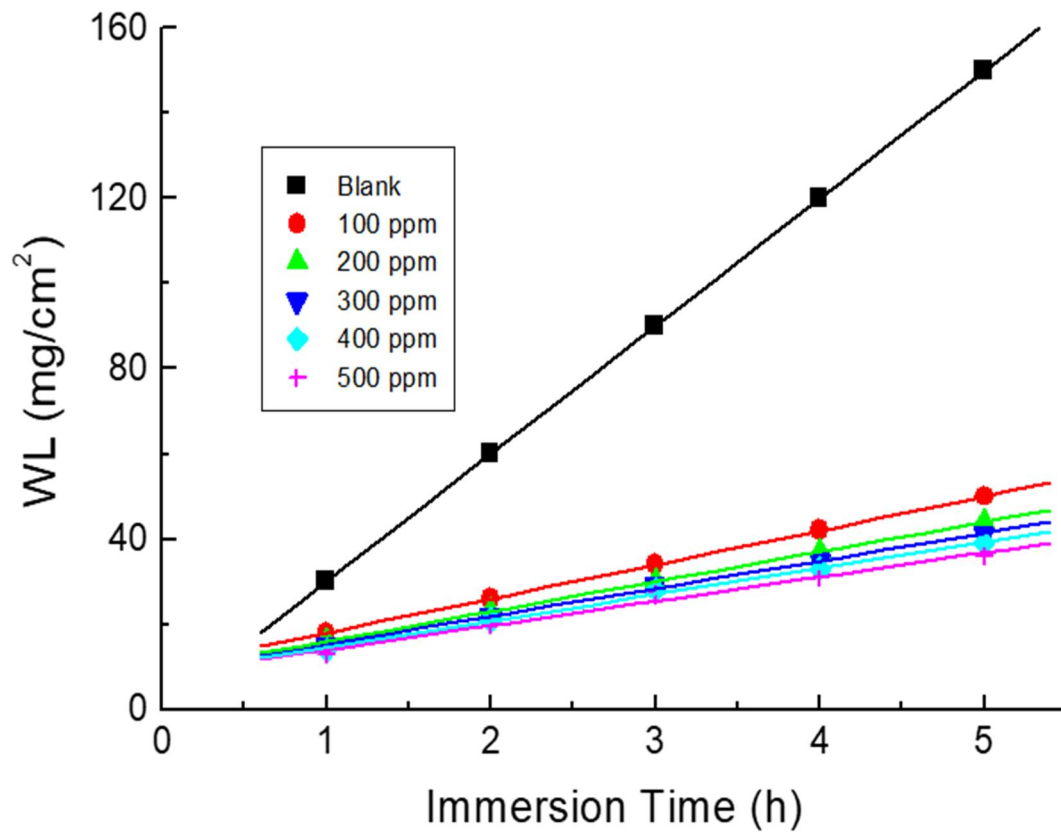


Fig.(3.4):Weight loss-time curves for corrosion of carbon steel in 1.0 M HCl solution containing various concentrations of compound IV

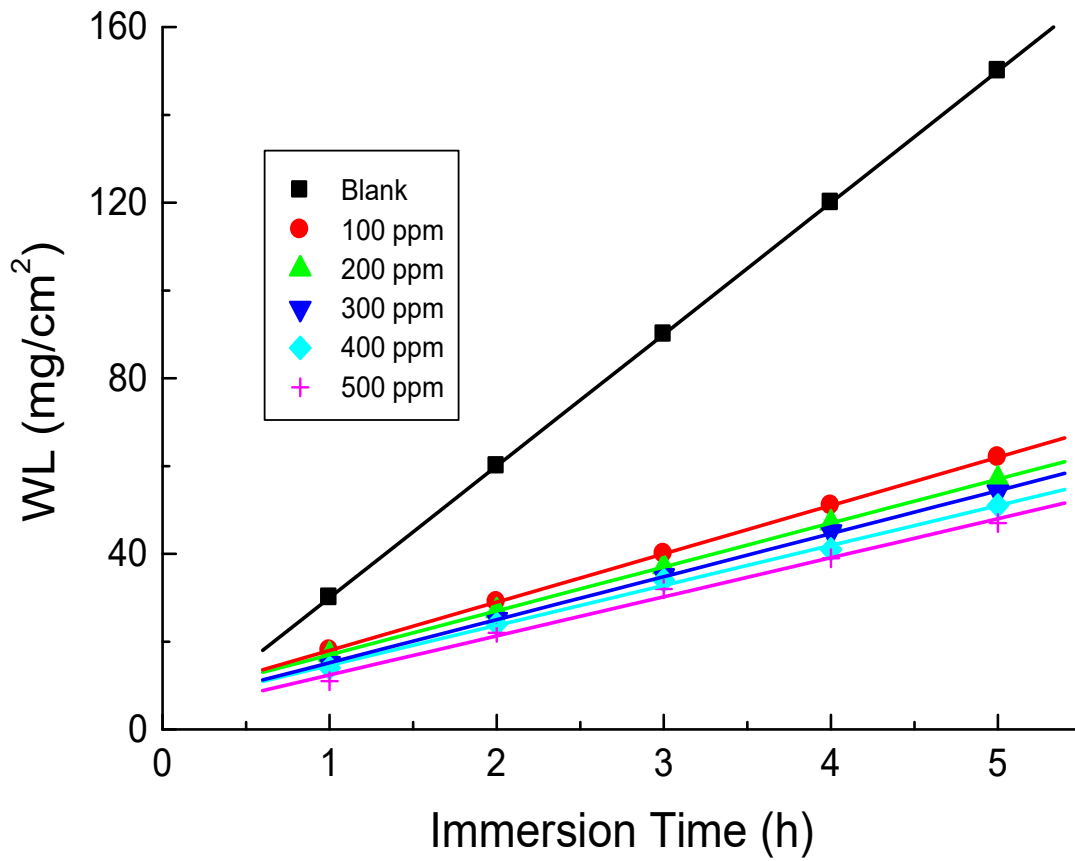


Fig.(3.5):Weight loss-time curves for corrosion of carbon steel in 1.0 M HCl solution containing various concentrations of compound V.

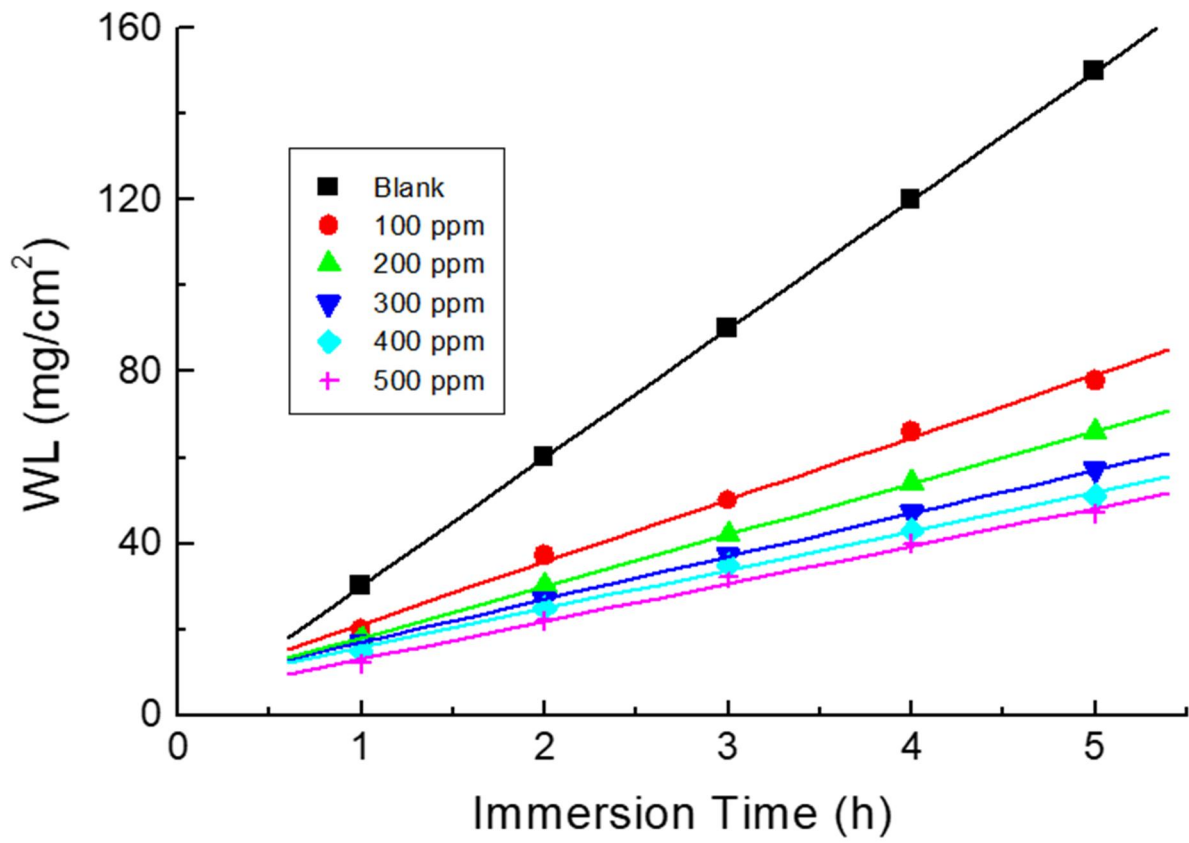


Fig.(3.6):Weight loss-time curves for corrosion of carbon steel in 1.0 M HCl solution containing various concentrations of compound VI.

Table(3.1): Corrosion parameters obtained from weight loss measurements of C-steel in a 1.0M HCl solution devoid of and contain different concentrations of compound I.

<b>Inhibitor</b>	<b>Conc. (ppm)</b>	<b>K (mg.cm<sup>-2</sup>.min<sup>-1</sup>)</b>	<b>θ</b>	<b>%I.E</b>
<b>Compound I</b>	0.00	0.5800	-	-
	100	0.2080	0.6414	64.14
	200	0.1375	0.7629	76.29
	300	0.1187	0.7953	79.53
	400	0.1145	0.8026	80.26
	500	0.1080	0.8138	81.38

Table(3.2): Corrosion parameters obtained from weight loss measurements of C-steel in a 1.0M HCl solution devoid of and contain different concentrations of compound II.

<b>Inhibitor</b>	<b>Conc. (ppm)</b>	<b>K (mg.cm<sup>-2</sup>.min<sup>-1</sup>)</b>	<b><math>\theta</math></b>	<b>%<i>I.E</i></b>
<b>Compound II</b>	0.00	0.5800	-	-
	100	0.1290	0.7776	77.76
	200	0.1180	0.7965	79.65
	300	0.1150	0.8017	80.17
	400	0.1125	0.8060	80.60
	500	0.1080	0.8138	81.38

Table(3.3): Corrosion parameters obtained from weight loss measurements of C-steel in a 1.0M HCl solution devoid of and contain different concentrations of compound III

<b>Inhibitor</b>	<b>Conc. (ppm)</b>	<b>K (mg.cm<sup>-2</sup>.min<sup>-1</sup>)</b>	<b>θ</b>	<b>%I.E</b>
<b>Compound III</b>	0.00	0.5800	-	-
	100	0.0800	0.7400	74.00
	200	0.0700	0.7700	77.00
	300	0.0680	0.7800	78.00
	400	0.0600	0.8100	81.00
	500	0.0500	0.8400	84.00



Table(3.4): Corrosion parameters obtained from weight loss measurements of C-steel in a 1.0M HCl solution devoid of and contain different concentrations of compound IV.

<b>Inhibitor</b>	<b>Conc. (ppm)</b>	<b>K (mg.cm<sup>-2</sup>.min<sup>-1</sup>)</b>	<b>θ</b>	<b>%I.E</b>
<b>Compound IV</b>	0.00	0.5800	-	-
	100	0.1040	0.8204	82.04
	200	0.0910	0.8431	84.31
	300	0.0890	0.8466	84.66
	400	0.0875	0.8491	84.91
	500	0.0850	0.8534	85.34

Table(3.5): Corrosion parameters obtained from weight loss measurements of C-steel in a 1.0M HCl solution devoid of and contain different concentrations of compound V.

<b>Inhibitor</b>	<b>Conc. (ppm)</b>	<b>K (mg.cm<sup>2</sup>.min<sup>-1</sup>)</b>	<b>θ</b>	<b>%IE</b>
<b>Compound V</b>	0.00	0.5800	-	-
	100	0.0958	0.6517	65.17
	200	0.0791	0.8636	86.36
	300	0.0750	0.8707	87.07
	400	0.0708	0.8779	87.79
	500	0.0660	0.8862	88.62

Table(3.6): Corrosion parameters obtained from weight loss measurements of C-steel in a 1.0M HCl solution devoid of and contain different concentrations of compound VI.

<b>Inhibitor</b>	<b>Conc. (ppm)</b>	<b>K (<math>\text{mg.cm}^{-2}.\text{min}^{-1}</math>)</b>	<b><math>\theta</math></b>	<b><math>\%I.E</math></b>
<b>Compound VI</b>	0.00	0.5800	-	-
	100	0.1210	0.7913	79.13
	200	0.0780	0.8655	86.55
	300	0.0750	0.8710	87.10
	400	0.07080	0.8779	87.79
	500	0.0660	0.8862	88.62

### 3.1.2. Effect of temperature on corrosion processes.

The study of the influence of rising temperature on the inhibition efficiency of different polymer compounds is important in the clarifying of the mechanism and the kinetics of their work and ultimately the proper selection of these inhibitors for specific practical situations. Accordingly, the effect of temperature on the corrosion medium on the reaction of carbon steel in pure acids has been reported by many authors [124,125].

In this part the effect of rising temperature ranging from 25 °C to 55°C on the corrosion rate of carbon steel in 1.0M HCl solutions in devoid of and containing 500ppm of the studied six polymer compounds using weight loss measurements as illustrated in Figures (3.7-3.12)

It is also clear from these figures that the rate of corrosion increases as the temperature increases. This indicates that the rising of temperature decrease the inhibition processes and the best inhibition efficiency is at room temperature 25 °C which indicates that the adsorption of inhibitors on the surface of C-steel is physical.

The apparent activation energy ( $E_a^*$ ) of the corrosion of carbon steel in 1.0M HCl solutions in absence and presence of polymer compounds at different temperatures were calculated from the Arrhenius equation [126-128]:

$$R_{\text{corr}} = A \exp\left(\frac{-E_a}{RT}\right) \quad (3.5)$$

And the logarithmic form:

$$\text{Log } R_{\text{corr}} = \log A - \frac{E_a}{2.303 RT} \quad (3.6)$$

Where  $R_{\text{corr}}$  is the corrosion rate

A is Arrhenius constant.

R is the gas constant and T is the absolute temperature.

Figure(3.13) shows the relationship between  $\log R_{\text{corr}}$  vs.  $1/T$  (Arrhenius plots) for carbon steel corrosion in free 1.0 M HCl solution and contains 500ppm of polymer compounds . Straight lines were obtained . From the slope of the straight lines, the values of  $E_a^*$  were computed for the different polymer compounds and given in Table(3.14)

It is obvious that the values of  $E_a^*$  in the presence of polymer compounds are higher than the free 1.0 M HCl solution .These

results indicate that these polymer compounds act as inhibitors through increasing activation energy of carbon steel dissolution by making a barrier to mass and charge transfer by their adsorption on carbon steel surface. This indicates The adsorption of the polymer compounds on the C-steel surface is physical

The enthalpy changes of activation ( $\Delta H^*$ )and the entropy change of activation ( $\Delta S^*$ ) for corrosion of carbon steel in 1.0M HCl solution devoid of and containing of each used polymer compounds are obtained by transition state equation:

$$R_{\text{corr}} = \frac{RT}{Nh} \exp(\Delta S^*/R) \exp(-\Delta H^*/RT) \quad (3.7)$$

Where  $N$  is Avogadro number and  $h$  is the plank constant.

Fig(3.14) Transtion state plot of  $\log (R_{\text{corr}} /T)$  vs  $1000/T$  for uninhibited C-steel electrode in free 1.0 M HCl solution and contains 500ppm of polymer compounds .The plots give a straight lines with a slope of  $(-\Delta H^*/ 2.303 R)$  and an intercept of  $[\log (R /Nh) + \Delta S^*/2.303 R]$ .The computed values of  $\Delta H^*$ and  $\Delta S^*$  are listed in Table (3.14).

Inspection of this Table it is evident that the values of  $\Delta H^*$  are positive reflect that the process of adsorption of the polymer compounds on the C-steel surface is an endothermic process. The values of  $\Delta S^*$  are determined from the intercepts of the straight lines are negative signs of  $\Delta S^*$  . This implies that the activation complex is a rate-determining step that represents a correlation rather than separation which indicates a decrease in turbulence when moving from the reactants to the activated compound [128].

The order of the inhibition efficiencies of polymer compounds as gathered from the increase in  $E_a^*$  and  $\Delta H^*$  values and decrease in  $\Delta S^*$  values is as follow:

Comp.VI > Comp. V > Comp. IV > Comp. III >Comp.II >Comp.I

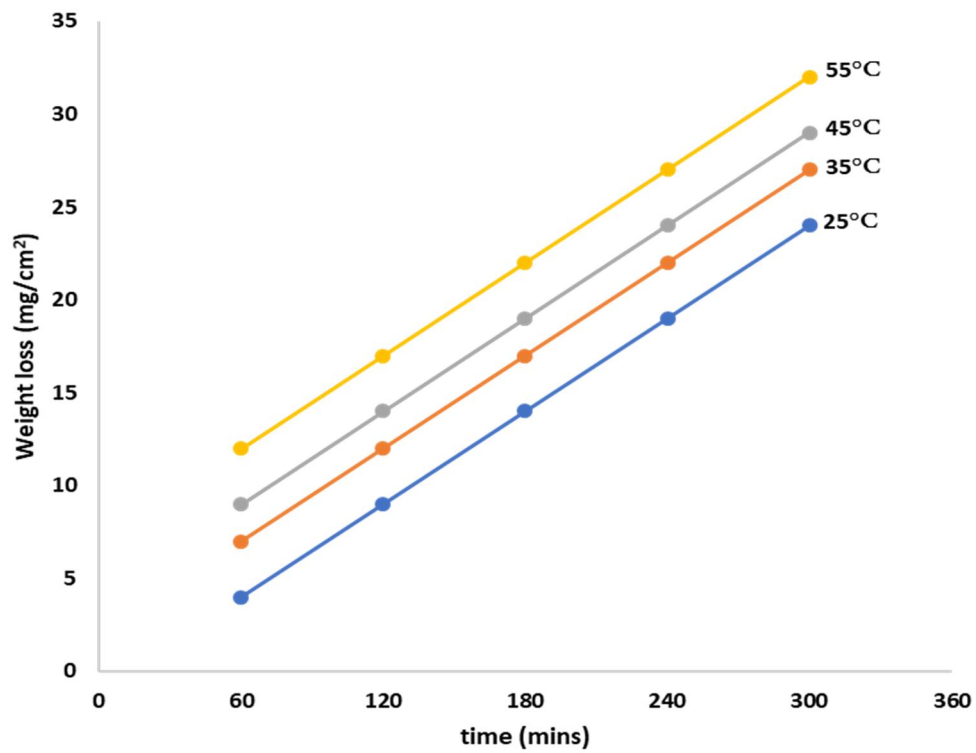


Fig.(3.7):Weight loss-time curves for carbon steel in 1.0 M HCl solution containing 500 ppm of compound I at different temperatures.

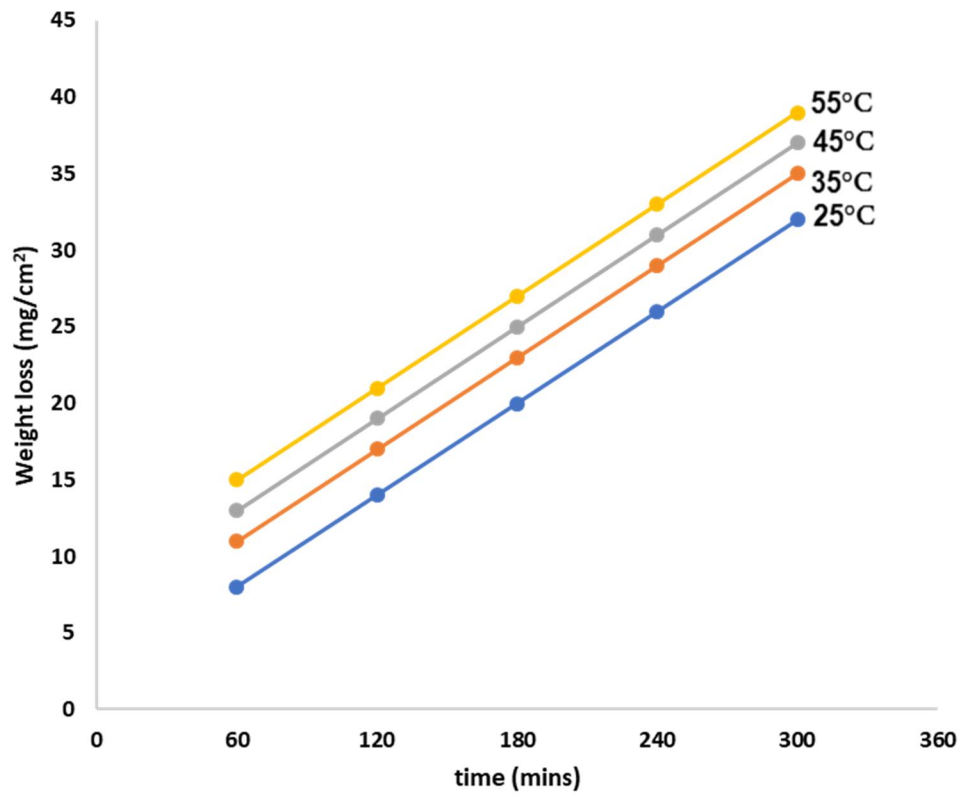


Fig.(3.8):Weight loss-time curves for carbon steel in 1.0 M HCl solution containing 500 ppm of compound II at different temperatures.



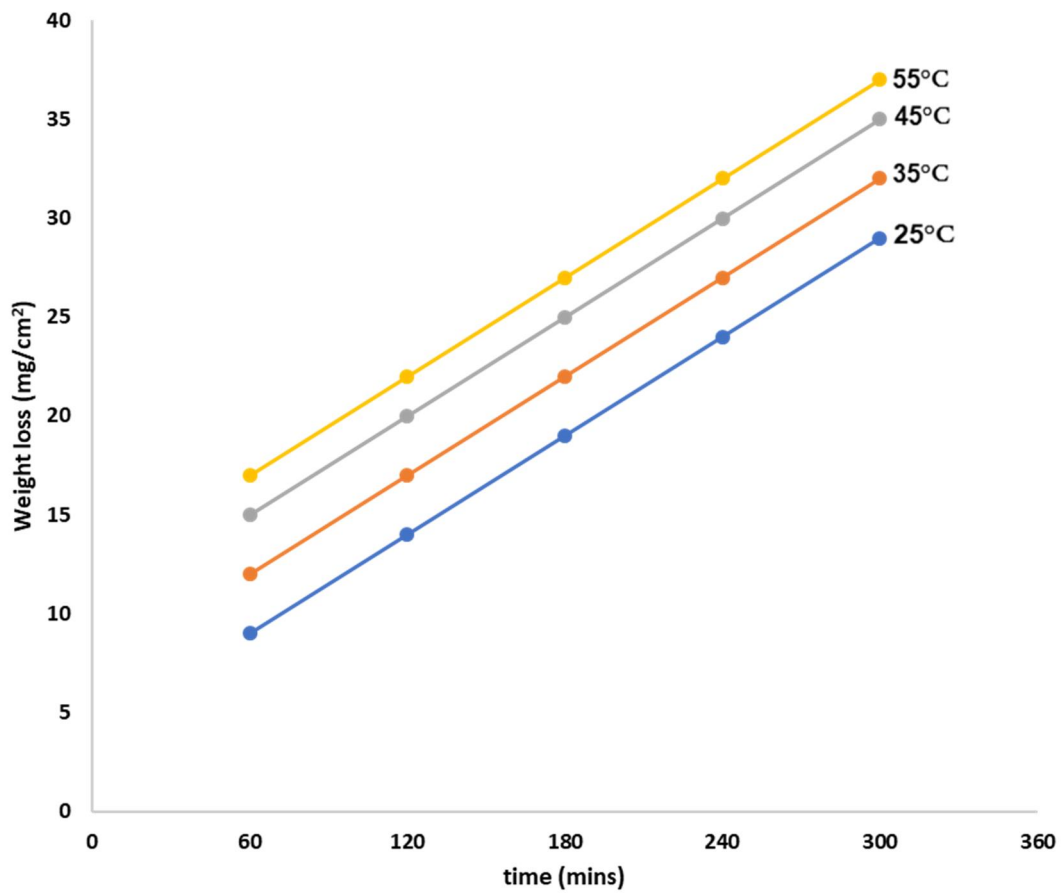


Fig.(3.9):Weight loss-time curves for carbon steel in 1.0 M HCl solution containing 500 ppm of compound III at different temperatures.

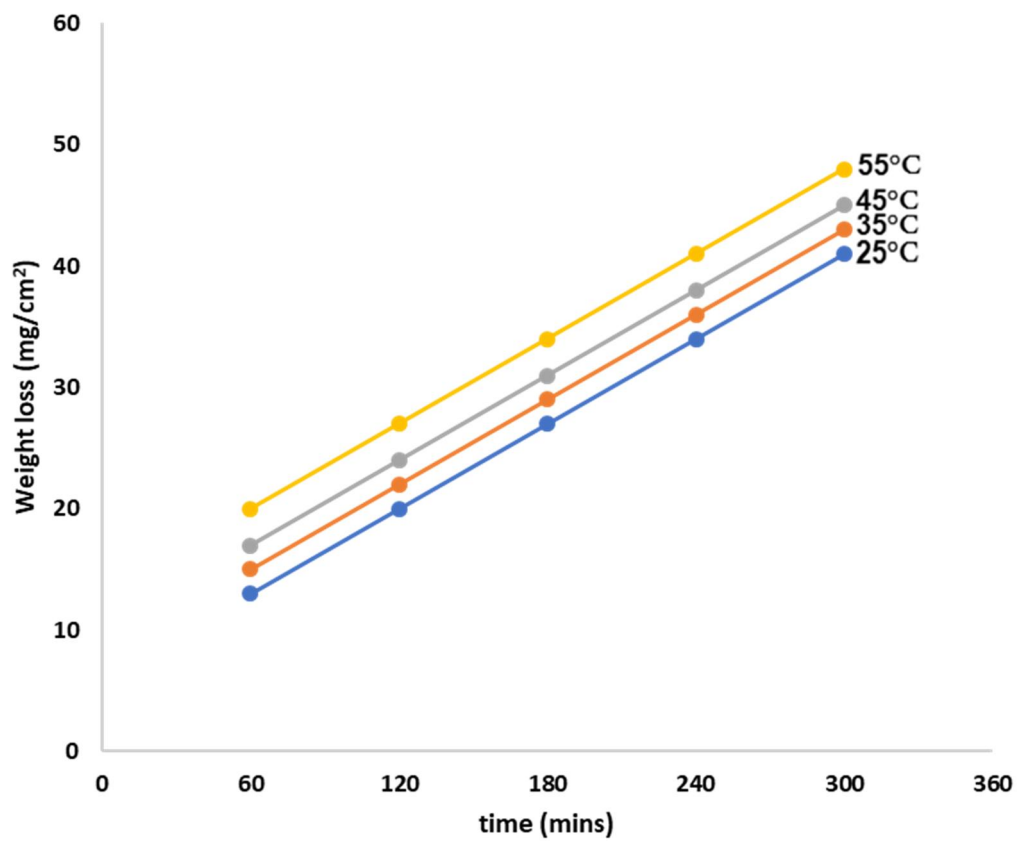


Fig.(3.10):Weight loss-time curves for carbon steel in 1.0 M HCl solution containing 500 ppm of compound IV at different temperatures.

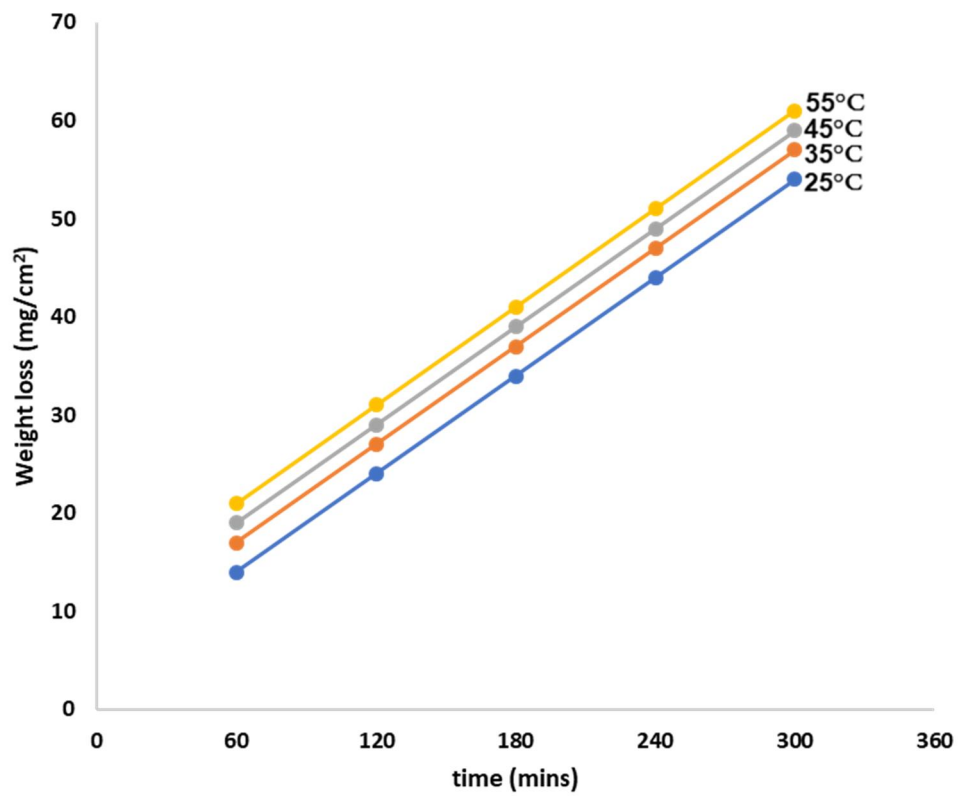


Fig.(3.11):Weight loss-time curves for carbon steel in 1.0 M HCl solution containing 500 ppm of compound V at different temperatures.

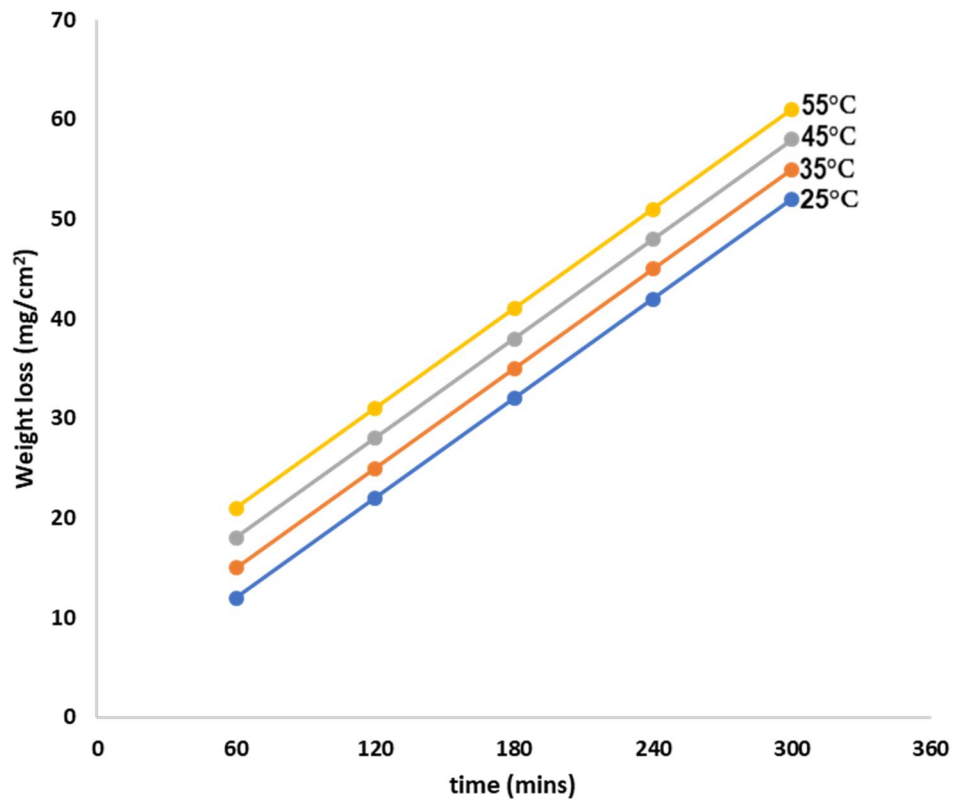


Fig.(3.12):Weight loss-time curves for carbon steel in 1.0 M HCl solution containing 500 ppm of compound VI at different temperatures.

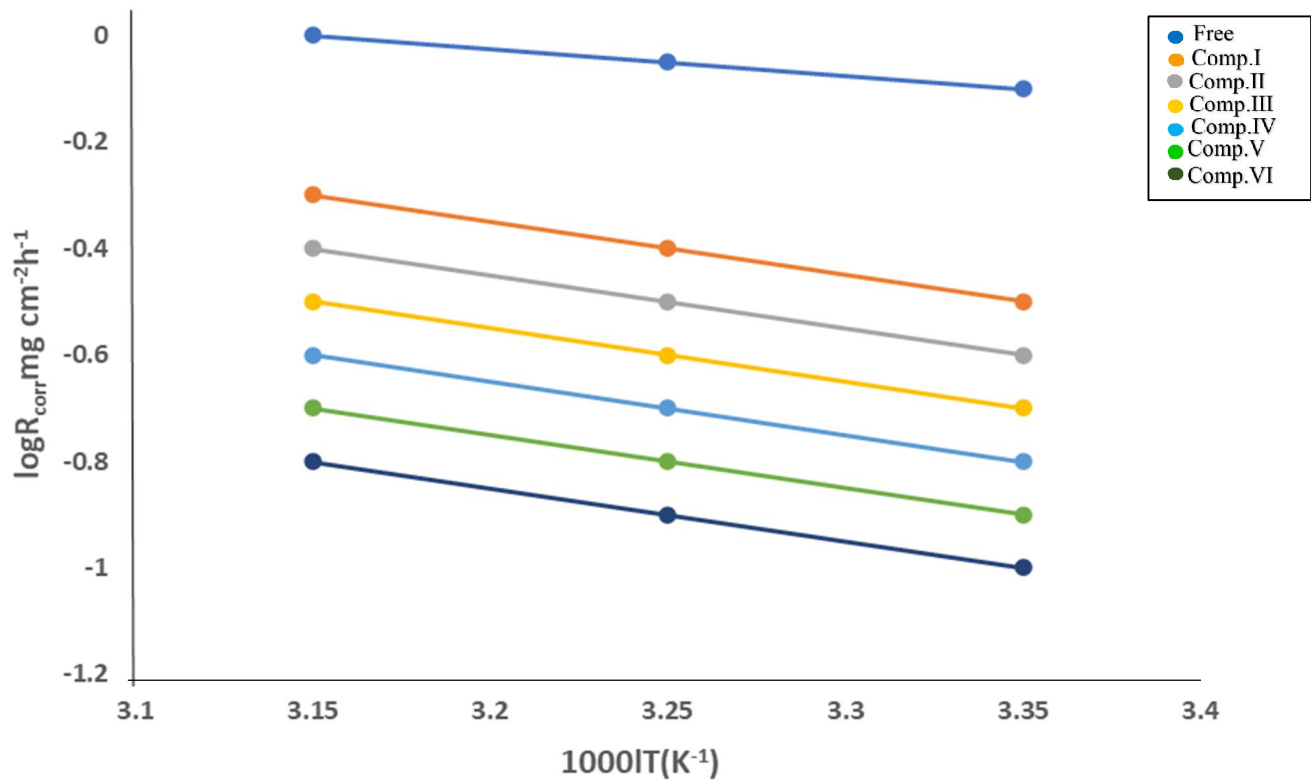


Fig.(3.13):Arrheneius plots for corrosion of carbon steel in free and inhibited 1.0 M HCl solution.

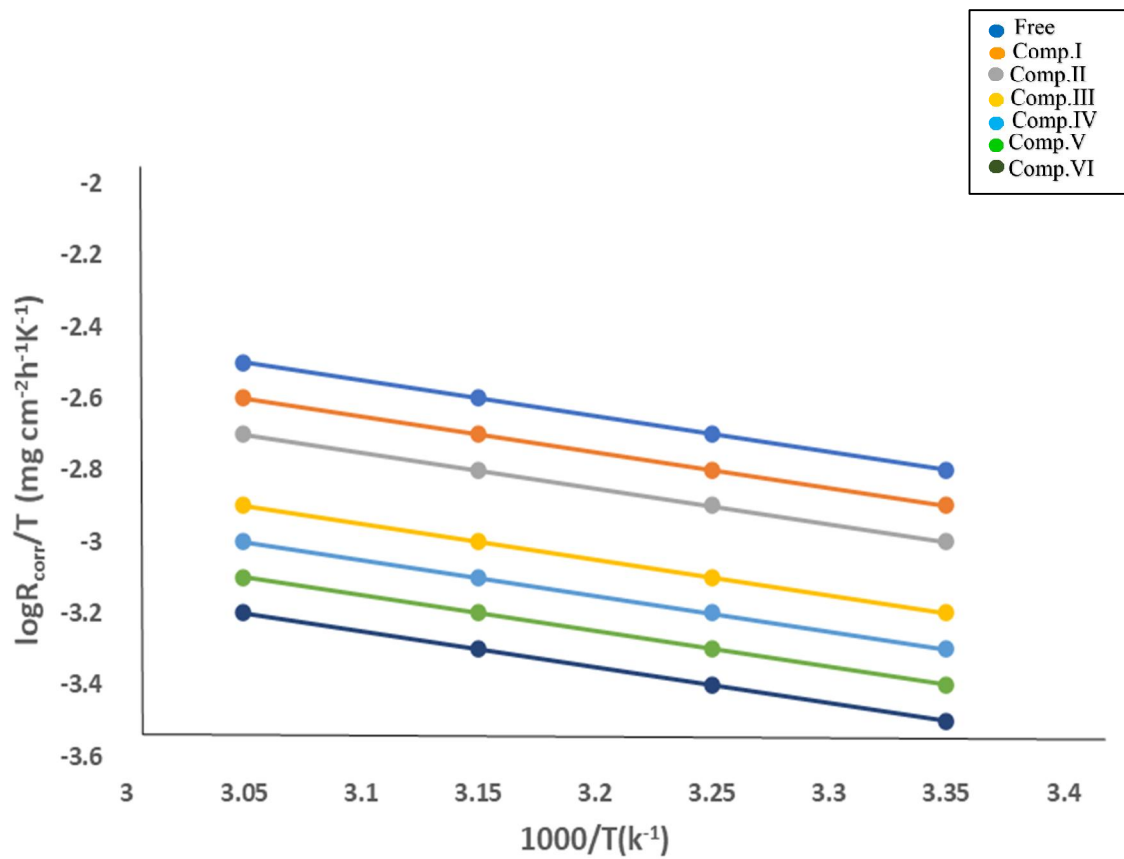


Fig.(3.14):Transition state plot for corrosion of carbon steel in free and inhibited 1.0 M HCl solution.

Table(3.7): Variation of corrosion rate( $R_{\text{corr}}$ ) of carbon steel in 1.0 M HCl solution at different temperature.

Temperature(K)	$K_{\text{corr.free}}$ ( $\text{mg cm}^{-2} \text{h}^{-1}$ )
298	0.68
308	0.84
318	1.02
328	1.14

Table(3.8): Variation of corrosion rate( $R_{\text{corr.}}$ ), degree of surface coverage( $\Theta$ ), and percentage of inhibition efficiency (%I.E) of carbon steel in 1.0 M HCl solution containing 500 ppm of compound I at different temperatures.

Inhibitor	Temperature $^{\circ}\text{C}$	K $(\text{mg}\cdot\text{cm}^{-2}\cdot\text{min}^{-1})$	$\Theta$	%I.E
Compound I	298	0.108	0.8411	84.11
	308	0.153	0.8178	81.78
	318	0.210	0.7941	79.41
	328	0.250	0.7807	78.07



Table(3.9): Variation of corrosion rate( $R_{\text{corr.}}$ ), degree of surface coverage( $\Theta$ ), and percentage of inhibition efficiency (%I.E) of carbon steel in 1.0 M HCl solution containing 500 ppm of compound II at different temperatures.

<b>Inhibitor</b>	<b>Temperature <math>c^{\circ}</math></b>	<b>K <math>(\text{mg.cm}^{-2}\text{min}^{-1})</math></b>	<b><math>\Theta</math></b>	<b>%I.E</b>
<b>Compound II</b>	298	0.077	0.8867	88.67
	308	0.098	0.8833	88.33
	318	0.130	0.8725	87.25
	328	0.15	0.8684	86.84

Table(3.10): Variation of corrosion rate( $R_{\text{corr.}}$ ), degree of surface coverage( $\Theta$ ), and percentage of inhibition efficiency (%I.E) of carbon steel in 1.0 M HCl solution containing 500 ppm of compound III at different temperatures.

Inhibitor	Temperature $^{\circ}\text{C}$	K ( $\text{mg.cm}^{-2}\text{min}^{-1}$ )	$\Theta$	%I.E
Compound III	298	0.128	0.8138	81.38
	308	0.198	0.7700	77.24
	318	0.286	0.7196	71.96
	328	0.374	0.6807	68.07

Table(3.11):Variation of corrosion rate( $R_{\text{corr}}$ ), degree of surface coverage( $\Theta$ ), and percentage of inhibition efficiency (%I.E) of carbon steel in 1.0 M HCl solution containing 500 ppm of compound IV at different temperatures.

Inhibitor	Temperature $^{\circ}\text{C}$	K ( $\text{mg.cm}^{-2}\text{min}^{-1}$ )	$\Theta$	%I.E
Compound IV	298	0.085	0.8750	87.50
	308	0.120	0.8571	85.71
	318	0.150	0.8529	85.29
	328	0.180	0.8421	84.21

Table(3.12):Variation of corrosion rate( $R_{\text{corr.}}$ ), degree of surface coverage( $\Theta$ ), and percentage of inhibition efficiency (%I.E) of carbon steel in 1.0 M HCl solution containing 500 ppm of compound V at different temperatures.

Inhibitor	Temperature $c^{\circ}$	K ( $\text{mg.cm}^{-2}\text{min}^{-1}$ )	$\Theta$	%I.E
Compound V	298	0.088	0.8705	87.05
	308	0.110	0.8690	86.90
	318	0.140	0.8627	86.27
	328	0.165	0.8552	85.52

Table(3.13):Variation of corrosion rate( $R_{\text{corr}}$ ), degree of surface coverage( $\Theta$ ), and percentage of inhibition efficiency (%I.E) of carbon steel in 1.0 M HCl solution containing 500 ppm of compound VI at different temperatures.

Inhibitor	Temperature $^{\circ}\text{C}$	K ( $\text{mg.cm}^{-2}\text{min}^{-1}$ )	$\Theta$	%I.E
Compound VI	298	0.096	0.8862	88.62
	308	0.168	0.8069	80.69
	318	0.242	0.7627	76.27
	328	0.316	0.7315	73.15

Table(3.14): Activation thermodynamic parameters for carbon steel 1.0M HCl solution in the absence and presence of 500ppm of the studied inhibitors.

<b>Inhibitor</b>	<b>E<sub>a</sub><sup>*</sup></b> kJ mol <sup>-1</sup>	<b>ΔH<sup>*</sup></b> kJ mol <sup>-1</sup>	<b>ΔS<sup>*</sup></b> JK <sup>-1</sup> mol <sup>-1</sup>
<b>1.0M HCl</b>	18.22	16.86	-102.3
<b>Compound I</b>	21.66	19.45	-111.4
<b>Compound II</b>	23.14	21,97	-118.1
<b>Compound III</b>	25.66	23.56	-120.9
<b>Compound IV</b>	27.72	25.74	-131.6
<b>Compound V</b>	29.32	27.65	-142.8
<b>Compound VI</b>	30.85	28.44	-155.6

## ***PART (B)***

### **Studying the Corrosion Behavior of C-Steel in Aqueous Solutions by Galvanostatic polarization technique.**

#### **3.2. Galvanostatic polarization technique(GPM).**

The technique of anodic and cathodic polarization of metals is used to study the phenomenon of metal corrosion and passivation. It yields useful information on the electrode behavior, action of inhibitive and aggressive anions and the effect of environmental conditions. In this technique, the corrosion current( $I_{\text{corr}}$ ) is determined from polarization curves by intercept method based on the intersection of anodic and /or cathodic Tafel lines with steady state(corrosion) potential( $E_{\text{corr}}$ ).The corrosion rate of the system involves the measurements of potential of working electrode for various applied current densities.when the Tafel equation is applicable for both anodic and cathodic polarization, the point of intersection of the two Tafel lines is corresponding to the stationary conditions of corrosion.

Thus, the function of the additive substance may be as an inhibitor or stimulator due to its effect on polarization curves, and the resulting displacement of the intersection point

The percentage inhibition efficiency (%IE) was evaluated from the values of  $I_{\text{corr}}$ . obtained from extrapolation Tafel Lines using the relationship[129]

$$\%IE = \frac{I_{\text{corr}} - I_{\text{inh}}}{I_{\text{corr}}} \times 100 \quad (3.8)$$

Where  $I_{\text{inh}}$ .and  $I_{\text{corr}}$ .are the corrosion current densities in the presence and absence of polymer compounds.

The effect of increasing concentration of polymer compounds on the Galvanostatic polarization curves of carbon steel in 1.0M HCl solution at 25°C are represented in Figures (3.15 – 3.20)

Inspection of the curves of these figures, one can observe at first a transition region in which the potential increases (anodic polarization) or decreases (cathodic polarization) slowly with current density following the region there is a rapid linear build up of potential with current density (Tafel region).

Transition region [130] that begins from the free corrosion potential and extends to the beginning of the Tafel region is characterized by the simultaneous occurrence of cathodic hydrogen evolution and anodic dissolution of steel. The former leads to coverage of fraction  $\Theta_H$  of the electrode surface by adsorbed OH groups  $Fe(OH)_{ads}$ . Having no common kinetics.

Mc Cafferty et.al., [131] considered that at the corrosion potential almost the whole electrode surface is covered by  $(Fe\ OH)_{ads}$  consequently, the coverage fraction  $\Theta$  close to 1 at cathodic potentials, and decreases when anodic polarization is increased.

Further inspection of the curves of Figures (3.15-3.20) reveals that. The presence of increasing concentrations of polymer compounds causes a decrease in the rate of anodic dissolution reaction of carbon steel i.e. shifting the anodic current potential curves in the anodic direction. This may be ascribed to a parallel adsorption of the polymer molecules over the

From the cathodic polarization curves shown in in Figs (3.15-3.20), it's clear that the increase of the polymer concentration shifts the current potential curves towards less cathodic potentials. Polymer compounds like other adsorption inhibitors are known to undergo specific adsorption i.e. they



adsorb in the inner part of the double layer. In doing so the adsorbed species replace some of the  $\text{H}_3\text{O}^+$  ion i.e. the additives block part of the surface and hence decrease the rate of hydrogen evolution reaction and consequently the rate of the overall corrosion reaction is produced.

The numerical values of variation of corrosion current density ( $i_{\text{corr}}$ ), corrosion potential ( $E_{\text{corr}}$ ), Tafel slopes ( $\beta_a$  and  $\beta_c$ ), degree of surface coverage ( $\Theta$ ) and protection efficiency (%IE) are given in Tables (3.15-3.20)

The results of these tables indicate the following:

1-The cathodic and anodic curves obtained exhibit Tafel-type behavior.

The addition of polymer compounds increased both cathodic and anodic overvoltage and mainly caused parallel displacement to the more negative and positive values, respectively.

2-. The values of Tafel slopes ( $\beta_a$  &  $\beta_c$ ) were changed slightly in the presence of the polymer compounds indicating these compounds are considered as mixed type inhibitors [130]. That is, these compounds influenced both cathodic hydrogen evolution and anodic steel corrosion reactions

3-The corrosion current density ( $i_{\text{corr}}$ ) decreases with increasing the concentration of polymer compounds, indicating that the presence of these compounds retards the dissolution of carbon steel in 1.0M HCl solution and the degree of inhibition depends on concentration and type of the inhibitor present.

4-The corrosion potential ( $E_{\text{corr}}$ ) values shifted to less negative values by increasing the concentration of polymer compounds.

5-At one and the same inhibitor concentration, the degree of inhibition efficiency increasing in the following sequence:

Comp. VI > Comp. V > Comp. IV > Comp. III > Comp. II > Comp. I

The values of inhibition efficiencies were evaluated using the Galvanostatic polarization and weight loss measurements show an agreement and conformity of experimental results. However, there are small differences in the values obtained from two techniques. These differences may be due to the short time taken by the electrochemical measurements.

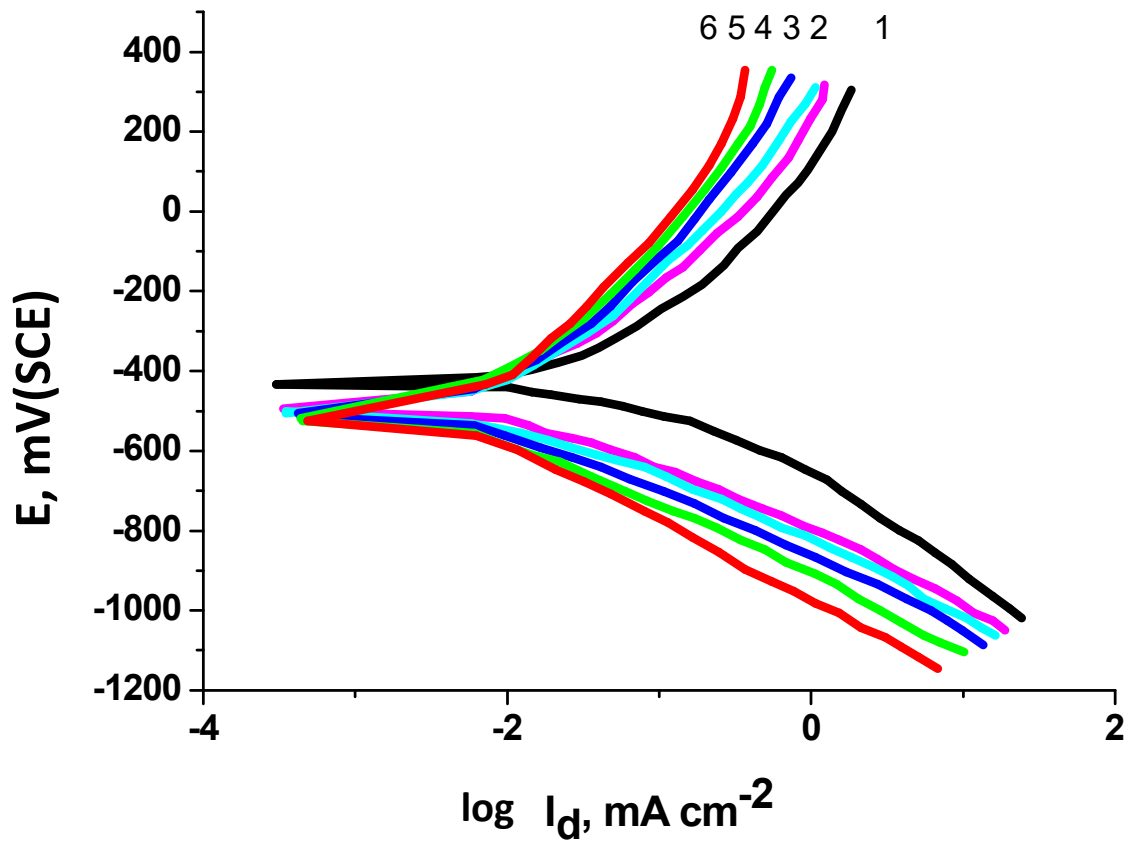


Fig.(3.15): Galvanostatic polarization curves for the dissolution of C-steel in 1.0M HCl solution in presence and absence of various concentrations of compound I at 30°C.  
(1)0.0 ppm (2)100 ppm (3)200 ppm (4)300 ppm (5)400 ppm (6)500 ppm.

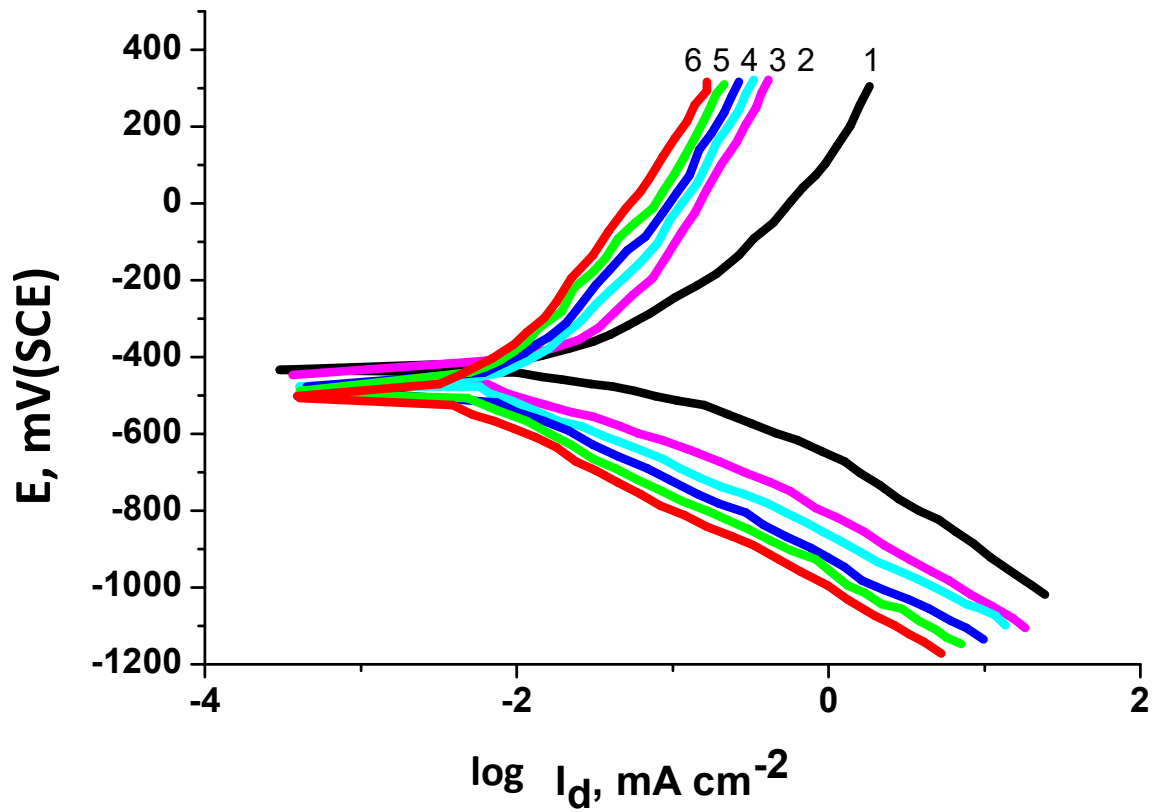


Fig.(3.16): Galvanostatic polarization curves for the dissolution of C-steel in 1.0M HCl solution in presence and absence of various concentrations of compound II at 30°C.  
(1)0.0 ppm (2)100 ppm (3)200 ppm (4)300 ppm (5)400 ppm  
(6)500 ppm.

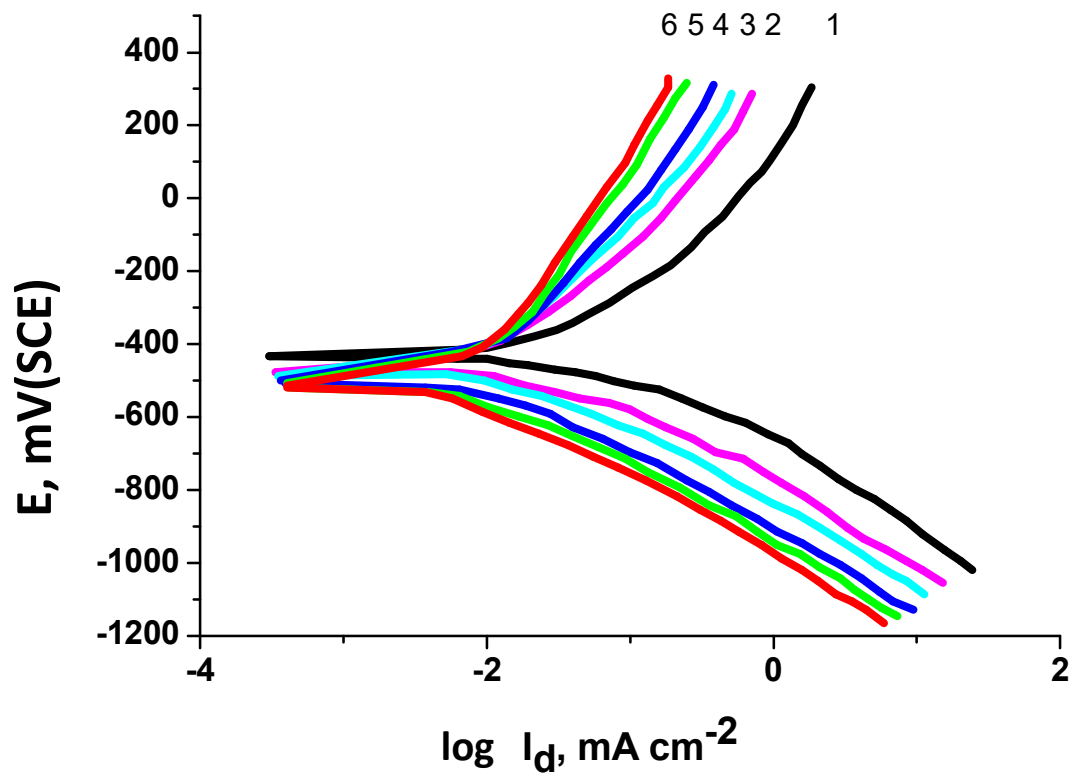


Fig.(3.17): Galvanostatic polarization curves for the dissolution of C-steel in 1.0M HCl solution in presence and absence of various concentrations of compound III at 30°C.

(1)0.0 ppm (2)100 ppm (3)200 ppm (4)300 ppm (5)400 ppm  
(6)500 ppm.

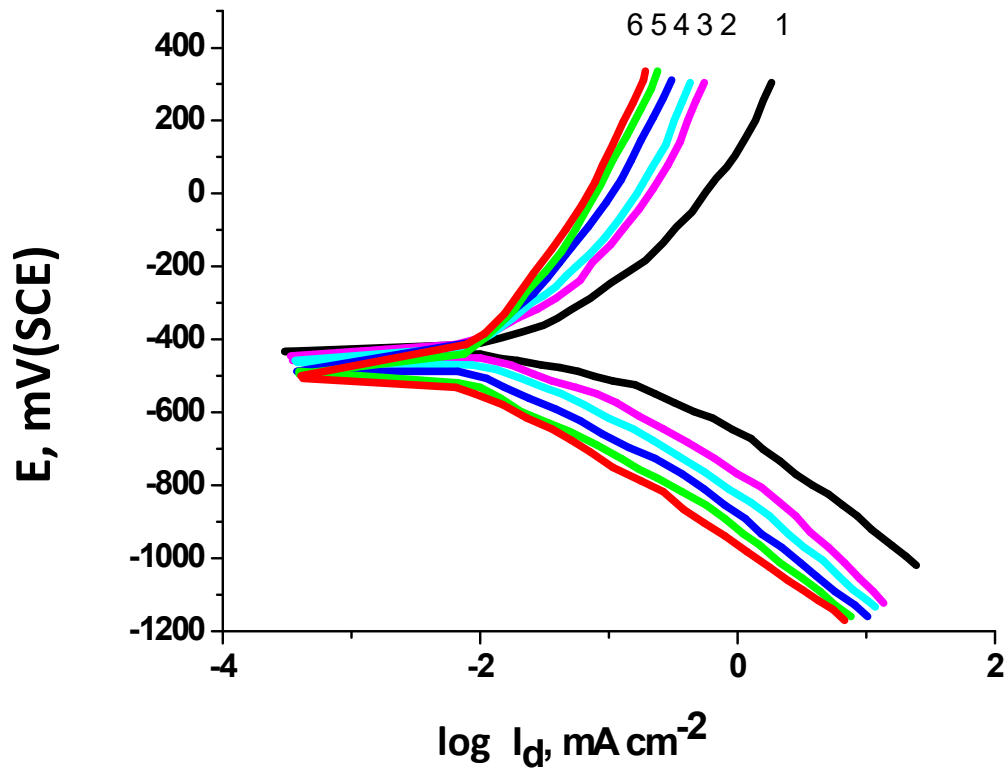


Fig.(3.18): Galvanostatic polarization curves for the dissolution of C-steel in 1.0M HCl solution in presence and absence of various concentrations of compound IV at 30°C.  
(1)0.0 ppm (2)100 ppm (3)200 ppm (4)300 ppm (5)400 ppm  
(6)500 ppm.

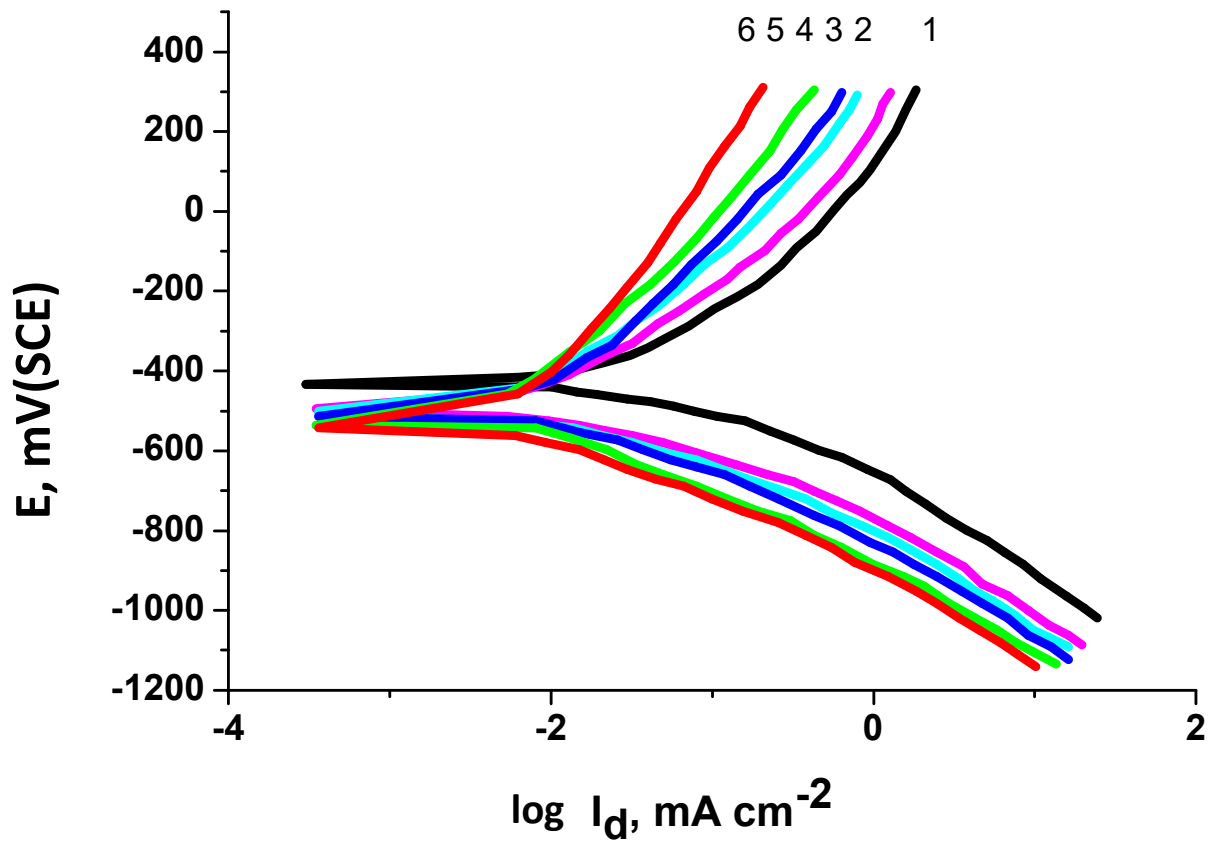


Fig.(3.19): Galvanostatic polarization curves for the dissolution of C-steel in 1.0M HCl solution in presence and absence of various concentrations of compound V at 30°C.

(1)0.0 ppm (2)100 ppm (3)200 ppm (4)300 ppm (5)400 ppm  
(6)500 ppm.

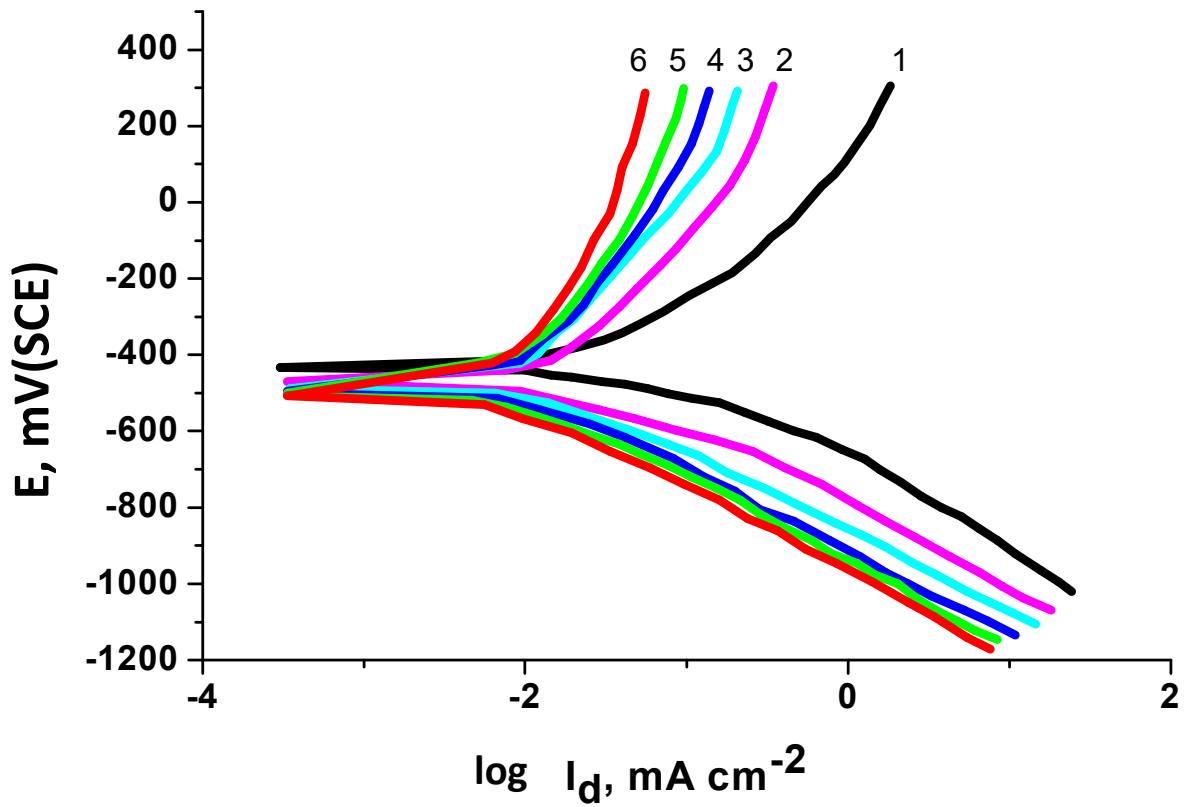


Fig.(3.20): Galvanostatic polarization curves for the dissolution of C-steel in 1.0M HCl solution in presence and absence of various concentrations of compound VI at 30°C.

(1)0.0 ppm (2)100 ppm (3)200 ppm (4)300 ppm (5)400 ppm

(6)500 ppm.



Table(3.15): Effect of increasing the concentration of compound I on the corrosion kinetic parameters obtained from galvanostatic polarization measurements of carbon steel in 1.0M HCl solution.

Inhibitor system	Conc. (ppm)	$\beta_a$ mV dec <sup>-1</sup>	$-\beta_c$ mV dec <sup>-1</sup>	$E_{corr}$ mV (SCE)	$I_{corr}$ (mA cm <sup>-2</sup> )	%I.E
Compound I	0	78	113	-434	1.78	-
	100	140	119	-486	0.423	76.23
	200	150	156	-488	0.370	79.21
	300	188	169	-490	0.343	80.73
	400	198	175	-495	0.293	83.53
	500	200	190	-498	0.288	83.82

Table(3.16): Effect of increasing the concentration of compound II on the corrosion kinetic parameters obtained from galvanostatic polarization measurements of carbon steel in 1.0M HCl solution.

Inhibitor system	Conc. (ppm)	$\beta_a$ mV dec <sup>-1</sup>	$-\beta_c$ mV dec <sup>-1</sup>	$E_{corr}$ mV (SCE)	$I_{corr}$ (mA cm <sup>-2</sup> )	%I.E
Compound II	0	78	113	-434	1.78	-
	100	80	118	-440	0.390	78.08
	200	81	120	-454	0.345	80.61
	300	98	133	-487	0.310	82.58
	400	102	134	-492	0.288	83.82
	500	120	145	-498	0.272	84.71

Table(3.17): Effect of increasing the concentration of compound III on the corrosion kinetic parameters obtained from galvanostatic polarization measurements of carbon steel in 1.0M HCl solution.

Inhibitor system	Conc. (ppm)	$\beta_a$ mV dec <sup>-1</sup>	$-\beta_c$ mV dec <sup>-1</sup>	$E_{corr}$ mV (SCE)	$I_{corr}$ (mA cm <sup>-2</sup> )	%I.E
Compound III	0	78	113	-434	1.78	-
	100	119	108	-471	0.342	80.78
	200	147	122	-488	0.291	83.65
	300	149	175	-491	0.258	85.50
	400	171	194	-494	0.223	87.47
	500	188	203	-499	0.183	89.72

Table(3.18): Effect of increasing the concentration of compound IV on the corrosion kinetic parameters obtained from galvanostatic polarization measurements of carbon steel in 1.0M HCl solution.

Inhibitor system	Conc. (ppm)	$\beta_a$ mV dec <sup>-1</sup>	$-\beta_c$ mV dec <sup>-1</sup>	$E_{corr}$ mV (SCE)	$I_{corr}$ (mA cm <sup>-2</sup> )	%I.E
Compound IV	0	78	113	-434	1.78	-
	100	80	123	-443	0.344	80.67
	200	102	134	-475	0.285	83.98
	300	120	146	-476	0.262	85.28
	400	164	186	-479	0.255	85.67
	500	189	239	-483	0.177	90.05

Table(3.19): Effect of increasing the concentration of compound V on the corrosion kinetic parameters obtained from galvanostatic polarization measurements of carbon steel in 1.0M HCl solution.

Inhibitor system	Conc. (ppm)	$\beta_a$ mV dec <sup>-1</sup>	$-\beta_c$ mV dec <sup>-1</sup>	$E_{corr}$ mV (SCE)	$I_{corr}$ (mA cm <sup>-2</sup> )	%I.E
Compound V	0	78	113	-434	1.78	-
	100	119	108	-471	0.312	82.47
	200	147	122	-488	0.210	88.20
	300	149	175	-491	0.190	89.33
	400	171	194	-494	0.175	90.16
	500	188	203	-499	0.155	91.29

Table(3.20): Effect of increasing the concentration of compound VI on the corrosion kinetic parameters obtained from galvanostatic polarization measurements of carbon steel in 1.0M HC solution

<b>Inhibitor system</b>	<b>Conc. (ppm)</b>	$\beta_a$ mV dec <sup>-1</sup>	$-\beta_c$ mV dec <sup>-1</sup>	$E_{corr}$ mV (SCE)	$I_{corr}$ (mA cm <sup>-2</sup> )	<b>%I.E</b>
<b>Compound VI</b>	0	78	113	-434	1.78	-
	100	79	118	-492	0.284	84.04
	200	80	125	-498	0.218	87.75
	300	87	129	-511	0.180	89.88
	400	113	133	-537	0.162	90.89
	500	120	137	-539	0.132	92.58

## ***PART (C)***

### **Studying the Corrosion Behavior of C-Steel in Aqueous Solutions by potentiodynamic anodic polarization technique**

#### **3.3.1- Effect of NaCl concentration on the pitting curves of carbon steel in 1.0M HCl solution.**

Pitting corrosion is an electrochemical process in which the pit acts as a fixed anode and the remainder of the passive surface acts as cathode [131-135]. The formation of a pit depends on number of factors including, type and concentration of attacking (depassivating) anions , type of material , presence and relative concentration of other anions as well as on temperature [136]

The interesting feature of pitting corrosion of carbon steel by halogen ions in aqueous solution is that, it does not start immediately after the metal is present in the corrosive solutions but at a certain time, so called induction period elapses before the start of dissolution. The time decreases with increasing concentration of the depassivation anion [137-138]. Pitting corrosion does not occur unless the potential of the working electrode surpasses a certain definite value, normally known as the ((break through)) or critical pitting potential [139]. The value of this potential depends on the type materials used, the concentration of the halides and the presence of other anions[140].

The value of the critical pitting potential or induction period can be taken as a measure of the resistance of protective film towards corrosion. The critical pitting potentials are always known as the potential below which the metal surface remains passive and above it the pits nucleate and develop. This potential for most metal and alloys turns into negative active

direction with an increase in the aggressive halogen ion concentration [141,142]. Pitting corrosion of carbon steel like metals and alloys occurs when passivity breakdown takes place at local points on the surface exposed to the corrosive environments at which anodic dissolution proceeds whilst the major part of the surface remain passive.

Fig.(3.21) represents the potentiodynamic anodic polarization curves of C-steel electrode in 1.0M HCl solution containing different concentrations of NaCl solutions as pitting corrosion agent at a scanning rate  $1\text{mVsec}^{-1}$ . The slow scan rate permits that the pitting initiation occurs at less positive potential. It is obvious that from Fig.(3.21) , at higher  $\text{Cl}^-$  ion concentrations result in a sudden and noticeable increase of current density at some specific potentials denoting the destruction of the passive film and initiation of visible pits. The higher concentrations of  $\text{Cl}^-$  ion, the higher the shift of pitting potential toward active(negative) direction. The breakdown of passivity can be attributed to the adsorption of chloride ions on the passive film formed on the steel surface that creates an electrostatic field across the film / solution interface [143,144]. Thus, when the electrostatic field reaches a certain value, the adsorbed anions begin to penetrate the passive film and the pitting corrosion is initiated. Examination of the electrode surface after polarization experiments showed visible pits whose number per unit area increases with the increase  $\text{Cl}^-$  ion content of the solution.

The relationship between the pitting corrosion potential ( $E_{\text{pitt}}$ ) and the logarithm of the molar concentrations of chloride ions shown in Fig(3.22). A straight line relationship was obtained satisfying the following equation:-

$$E_{\text{pitt}} = a_1 - b_1 \log C_{\text{Cl}^-} \quad (3.9)$$



where,  $a_1$  and  $b_1$  are constants which depend on both the nature of the electrode used and type of aggressive anions. As the concentration of chloride ions increases the pitting potential is shifted to more negative direction indicating the destruction of passive film and initiation of pitting corrosion.

The differentiation between pit initiation and pit propagation is well explained by Aziz and Godard [145]. The pit can be started by artificial stimulation at otherwise normal sites on the metal surface and continue to propagate if appropriate environmental conditions are given. This concept has been used widely to explain the phenomenon of pitting corrosion.

Hoars et al. [146] related pit initiation on a supposed oxide film, followed by their penetration through the film (without exchange) to the influence of an electrostatic field across the film /solution interface. When the last field reaches a certain critical value, corresponding to the pitting potential, pitting occurs, and it is assumed that the oxide film is not limited either by vacancy condensation at the metal interface, or it releases cations rapidly at the electrolyte interface so that in either cases pitting proceeds.

The induction period for pitting is related to the time required for supposed penetration of the ions through the oxide film regarding this mechanism. Leckie and Uhlig [147] have argued that, if this is true, then another anion with a greater molecular size than halogen ions for example,  $\text{SO}_4^{2-}$ ,  $\text{ClO}_4^-$ ,  $\text{NO}_3^-$  and  $\text{OH}^-$ , which practically have no pitting tendency, can also, penetrate the passive oxide film causing the formation of pit.

Rosenfeld et.al. [148] proposed another model based on the visible competitive adsorption of the aggressive ions with oxygen for adsorption sites on the metal surface. This model assumes adsorbed oxygen rather than oxide which is the cause of passive formation.

Oxygen usually has a higher affinity than  $\text{Cl}^-$  ions for adsorption sites on the metal surface, but as the potential of the working electrode is shifted into the passive direction, higher  $\text{Cl}^-$  ions move into the double layer when the concentration of the latter reaches a certain definite value, corresponding to the pitting potential, it succeeds at favored sites in destroying passivity by displacing adsorbed  $\text{O}_2$  ions. The introduction time for pitting is attributed here to the slow process of competitive adsorption. . It is interesting to mention that a similar view was also reported by Schwenk et al. [149].

In contrast to the competitive adsorption model, Foroulis and Thubriker [150] based their argument on the findings that, the critical pitting potential of the polarized electrode depends on the thickness of oxide layer at the metal surface. They concluded that, if competitive adsorption over the metal surface is the controlling mechanism, then thickness of any overlying oxide would have no influence on the critical potential at which the  $\text{Cl}^-$  ions displace the adsorbed oxygen on the metal bare. Foroulis [151] proposed a pit initiation model for C-steel which includes field supported adsorption of the chloride ions from the solution to a hydrated C-steel oxide surface, followed by formation for a basic Ferric chloride salt on the surface. This chloride salt is soluble and leads to the immediate separation of one or more adjacent cations from the oxide lattice.

In agreement with Foroulis suggestion [152] it is assumed that the initiation of pitting on Zn-Ti-Cu alloy involves, as a rate controlling step, the adsorption of chloride ions on a layer of mixed oxide/hydroxide of Zn, Ti and or Cu followed by the formation of the corresponding chloride-metal oxide or hydroxide complexes. The deadly soluble of these complexes can go into solution, most probably the Zn complexes as soluble  $\text{Zn}^{2+}$ . These results in pit initiation with the continues anodic dissolution of

$Zn^{+2}$  at the point of attack .This latter model was confirmed by the use of the electron microscope analyzer of performed pits

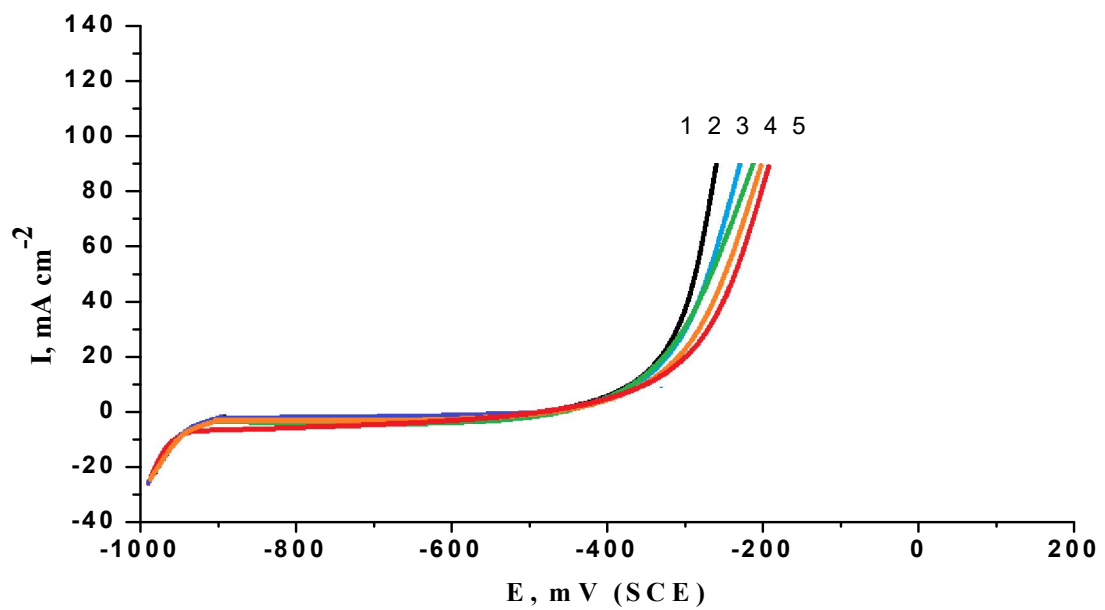


Fig.( 3.21): Potentiodynamic anodic polarization curves of C-steel in different concentrations of NaCl solutions at a scan rate  $1\text{mV sec}^{-1}$ .

(1)0.5 M (2)0.1 M (3)0.05M (4)0.01 M (5)0.001 M.

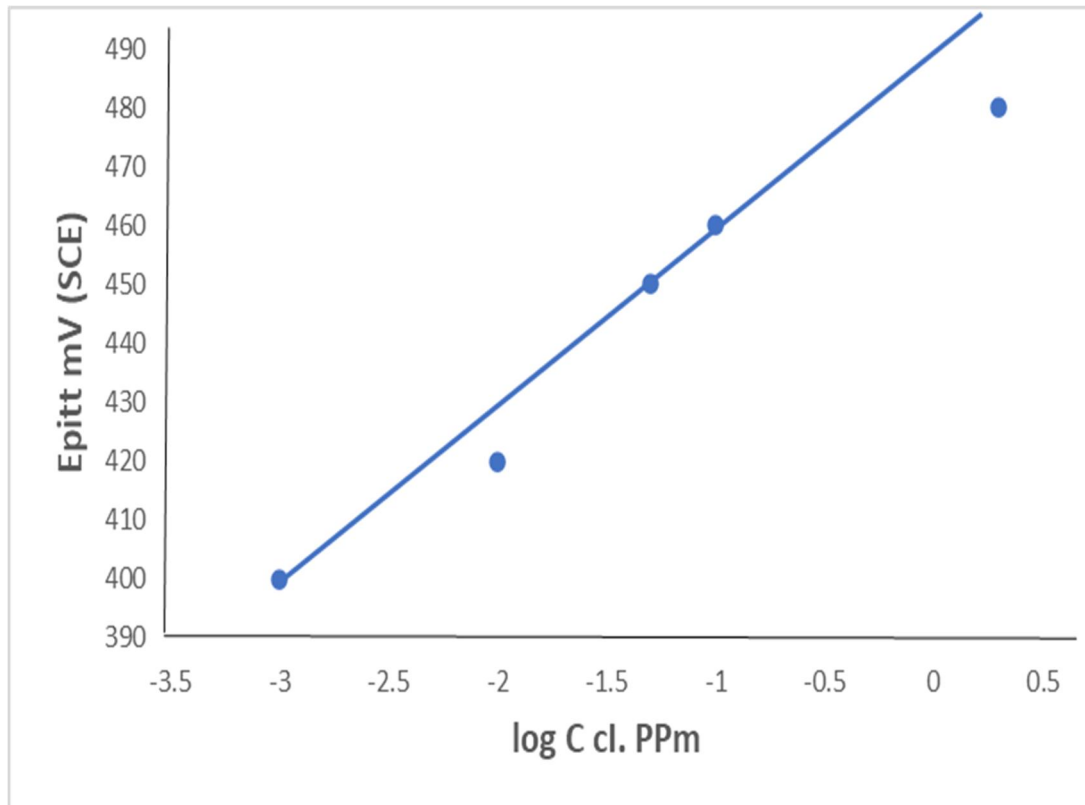


Fig.(3.22): The relation between  $E_{pitt}$  and logarithm of chloride ion concentration.

### 3.3.2. Effect of addition of some polymer compounds on the pitting corrosion of carbon steel.

The primary step in the action of corrosion inhibitor in neutral solution usually is the adsorption of inhibitors on the metal surface [161]. The adsorption process depends upon electronic characteristic of the inhibitor, the nature of surface, temperature, steric effect, multilayer adsorption and the degree of surface activity.

Figures (3.23-3.28) represent the effect of different concentrations of six polymer compounds on the potentiodynamic anodic polarization curves of carbon steel electrode in 1.0 M HCl + 0.1 M NaCl at a scan rate of  $1\text{ mV sec}^{-1}$ . It was found that the pitting potential of C-steel electrode is shifted to more positive (noble) direction with increasing the concentration of polymer compounds. This indicates that increased resistance to pitting attack and the investigated polymer compounds act as pitting corrosion inhibitors.

Fig.(3.29) shows the relationship between pitting potential;  $E_{\text{pit}}$  and logarithm of concentration of the polymer compounds. Straight line relationship was obtained and the following conclusions can be drawn:

- i) The increase of inhibitor concentration causes the shift of pitting potential into more positive values in accordance with the following equation:

$$E_{\text{pit}} = a_2 + b_2 \log C_{\text{inh.}} \quad (3.10)$$

where,  $a_2$  and  $b_2$  are constants which depend on both the composition of additives and the nature of the electrode.

- ii) Inhibition afforded by these compounds using the same different concentrations of the additives decreases in the following order:

Comp.VI > Comp. V > Comp. IV > Comp. III >Comp.II >Comp.I

The shift of pitting potential of Carbon steel electrode into the noble (positive) direction upon addition of increased concentrations of compounds could be explained in view of the oxide film theory of passivity [153] According to this theory inhibitors are adsorbed on the active sites of the oxide through which  $\text{Cl}^-$  ions would otherwise penetrate the oxide film, causing pitting. In this way the inhibitor contaminates the oxide and making it more conductors, thereby favoring oxide growth and pitting inhibition. In another explanation one can also, attribute the inhibiting action of these anions to their low polarizabilities. These anions are expected to concentrate in the diffuse part of the double layer and inhibit pitting corrosion through the reduction of the zeta potential at the oxide film solution interface. This reduces in turn the potential field and retards the electro chemisorption of the  $\text{Cl}^-$  ions from the solution on the oxide film.

Two major effects seem to be possible for the inhibition of pitting corrosion. First is the competitive adsorption between aggressive and inhibitive compounds. The adsorption of the latter ions predominates and the electrode will be protected. In this case, the pitting corrosion potential is shifted into the anodic direction. This mechanism seems to be the most effective way to avoid pitting corrosion. A second way is related to the incorporation of the inhibitive molecules into the passive layer on the metal surface forming an improved stability against the aggressive ions. Once ,

when pitting corrosion has been started, the inhibitor can be adsorbed within the pits preventing active metal dissolution. As shown from the figures, the order of decreasing  $E_{\text{pit.}}$  of C-steel in the presence of the investigated compounds is in agreement with the order of decreasing % IE of these compounds, obtained from weight loss and potentiodynamic polarization and electrochemical impedance spectroscopy measurements.

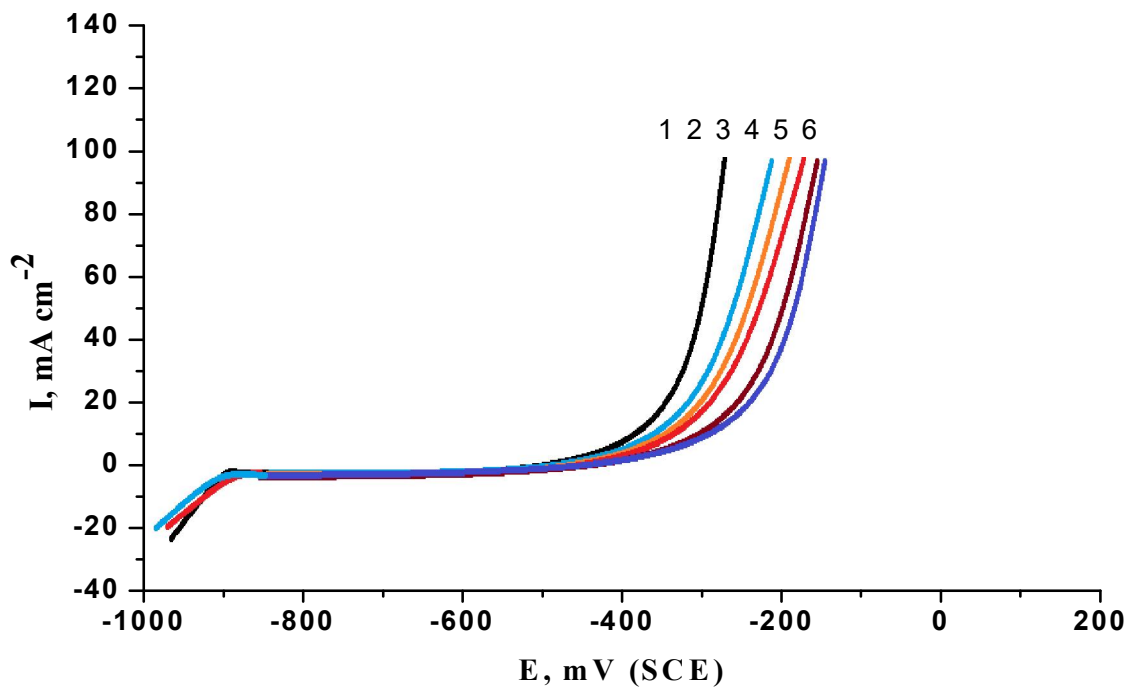


Fig.(3.23): Potentiodynamic anodic polarization curves of C-steel in 1.0 M HCl + 0.1 M NaCl solution containing different concentrations of compound I at a scan rate of  $1\text{mV sec}^{-1}$ . (1)0.0 ppm (2)100 ppm (3)200 ppm (4)300 ppm (5)400 ppm (6)500 ppm.



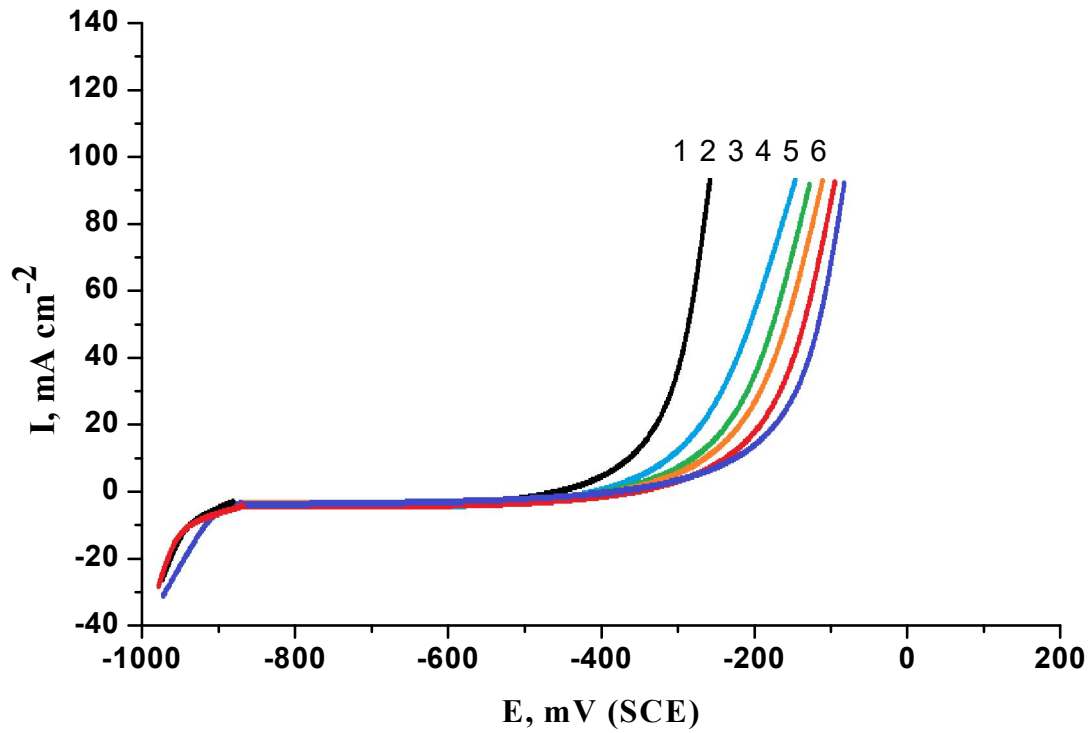


Fig.(3.24): Potentiodynamic anodic polarization curves of C-steel in 1.0 M HCl + 0.1 M NaCl solution containing different concentrations of compound II at a scan rate of  $1\text{mV sec}^{-1}$ . (1) 0.0ppm (2)100ppm (3)200ppm (4)300ppm (5)400ppm (6)500ppm.

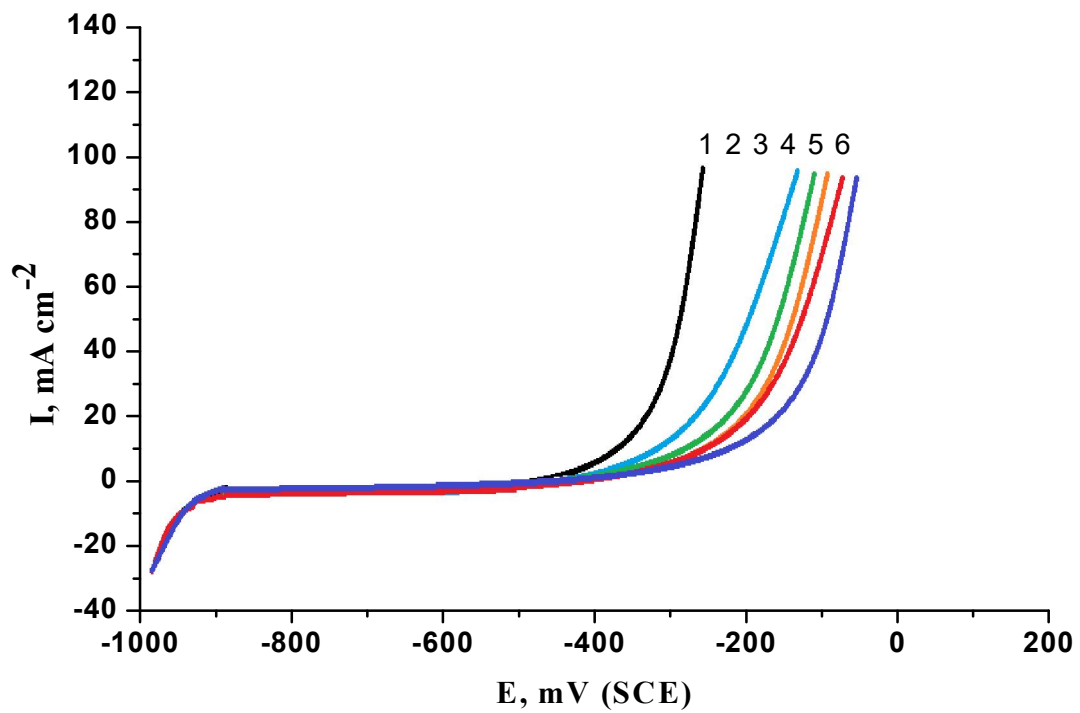


Fig.(3.25): Potentiodynamic anodic polarization curves of C-steel in 1.0 M HCl + 0.1 M NaCl solution containing different concentrations of compound III at a scan rate of  $1\text{ mV sec}^{-1}$ . (1) 0.0 ppm (2)100ppm (3)200ppm (4)300ppm (5)400 ppm (6)500 ppm.

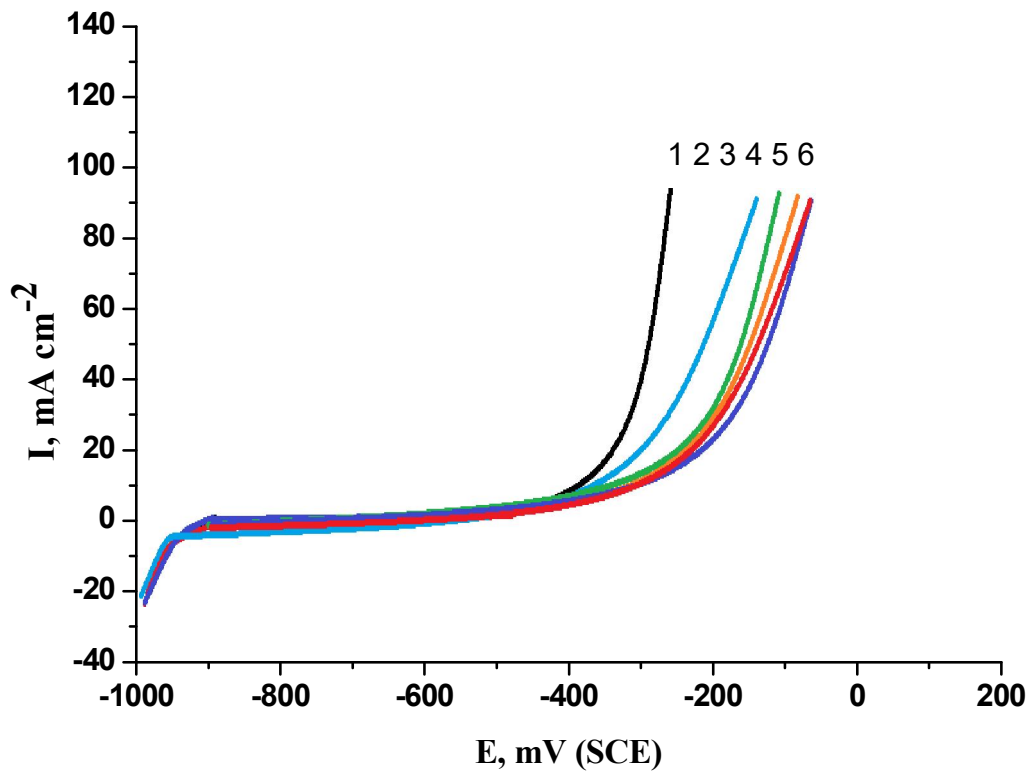


Fig.(3.26): Potentiodynamic anodic polarization curves of C-steel in 1.0 M HCl + 0.1 M NaCl solution containing different concentrations of compound IV at a scan rate of  $1\text{ mV sec}^{-1}$ . (1)0.0 ppm (2)100 ppm (3)200 ppm (4)300 ppm (5)400 ppm (6)500 ppm.

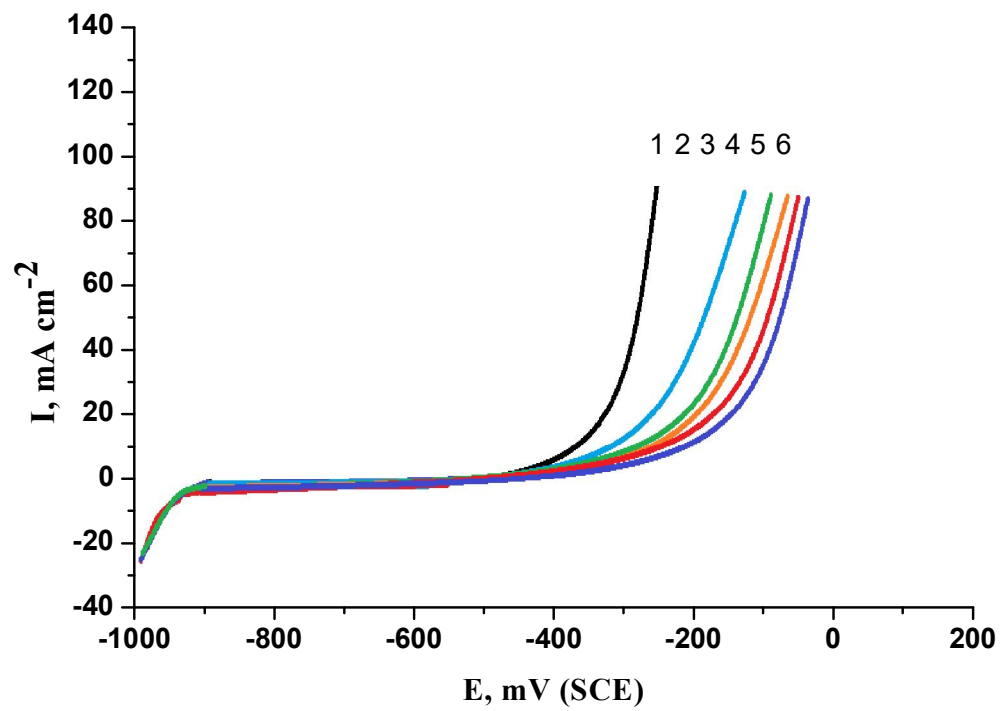


Fig.(3.27): Potentiodynamic anodic polarization curves of C-steel in 1.0 M HCl + 0.1 M NaCl solution containing different concentrations of compound V at a scan rate of  $1\text{ m V sec}^{-1}$ . (1)0.0 ppm (2)100 ppm (3)200 ppm (4)300 ppm (5)400 ppm (6)500 ppm.

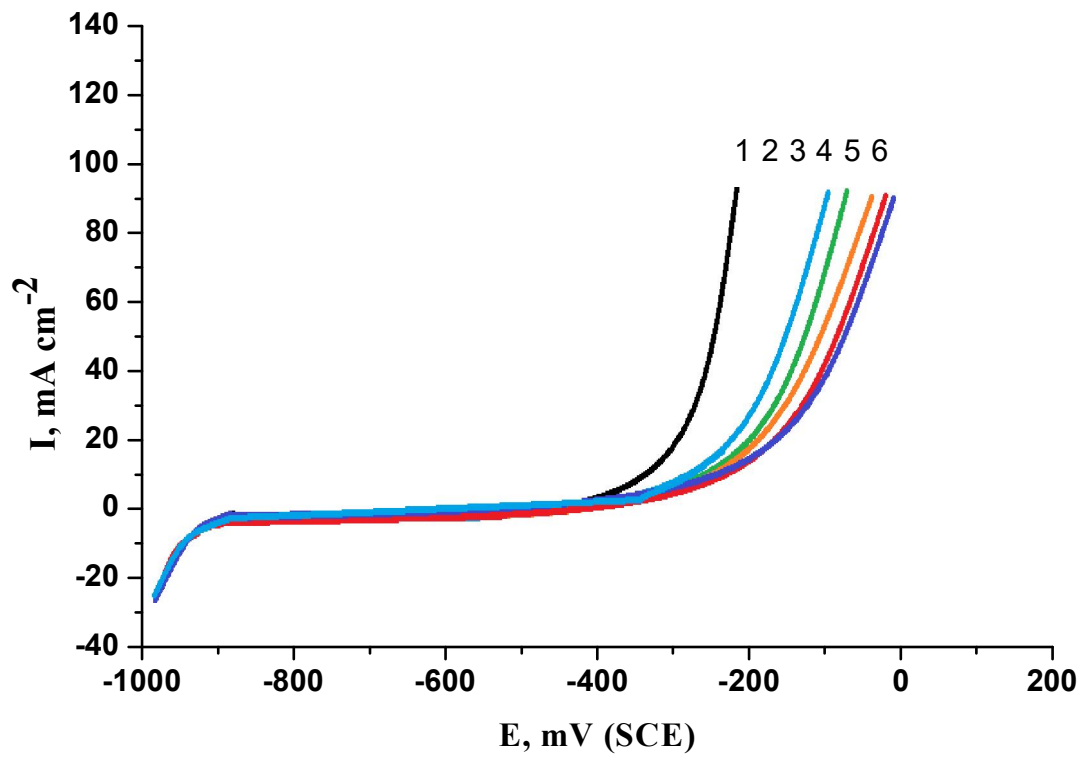


Fig.(3.28): Potentiodynamic anodic polarization curves of C-steel in 1.0 M HCl + 0.1 M NaCl solution containing different concentrations of compound VI at a scan rate of  $1\text{ mV sec}^{-1}$ . (1)0.0 ppm (2)100 ppm (3)200 ppm (4)300 ppm (5)400 ppm (6)500 ppm.

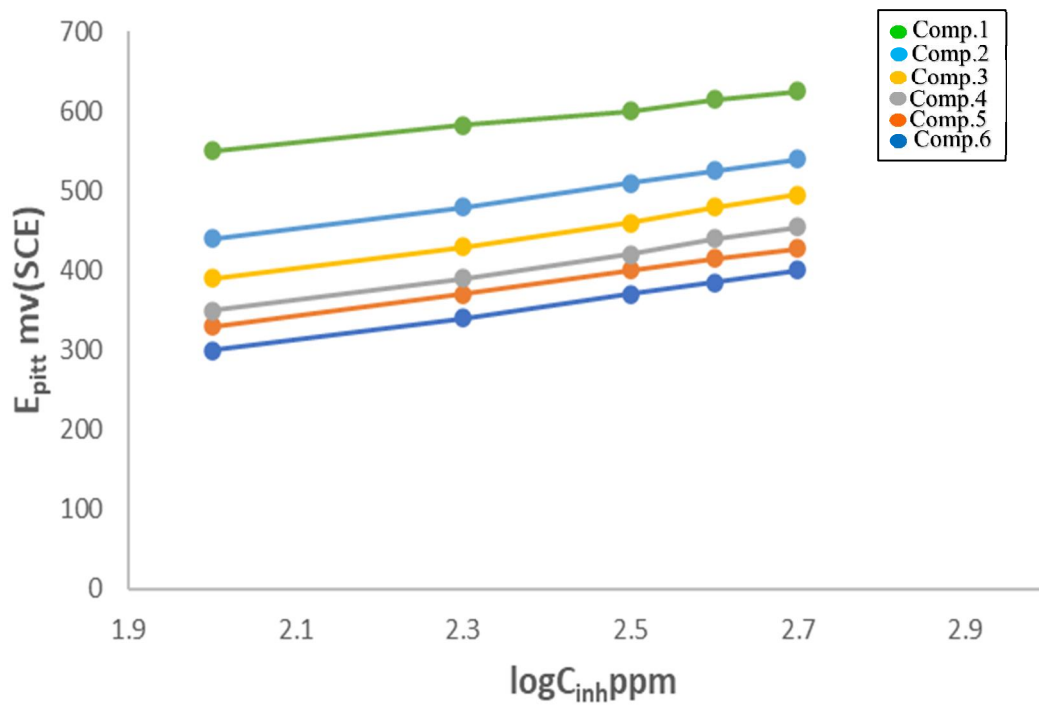


Fig.(3.29) Variation of  $E_{pitt}$  of carbon steel electrode versus  $\log C_{inh}$

## ***PART (D)***

### **Studying the Corrosion Behavior of C-Steel in Aqueous Solutions by Impedance spectroscopy**

#### **3.4. The electrochemical impedance spectroscopy (EIS )**

It is becoming more and more important as an analysis technique in the field of electrochemical measurements. EIS method has been widely used in the recent years to measure the corrosion rate. EIS method provides important information about the kinetics and mechanistic of electrode processes. Moreover, it sheds more light on the surface properties of electrodes. These measurements are performed at different ac frequencies and consequently, the name impedance spectroscopy is adopted later. Analysis of the system response contains information about the interface, its structure and reactions taking place there[154].Therefore, EIS measurements are widely used for investigating corrosion inhibition processes. The effects of inhibitory action of six polymer compounds on the corrosion of C-steel in 1M HCl solution was investigated by EIS method. The measurements at different frequencies were conducted at OCP after 15 minutes immersion in test solution.

Two main plot formats are frequently used in impedance data presentation, the Nyquist and Bode plot formats. In the thesis Nyquist format is applied . In Nyquist format the real component of the impedance is plotted against the imaginary component at different frequencies. The values of  $R_s$  and  $R_{ct}$  can be obtained from the intercepts of the semicircle with the axis of the real component.  $C_{dl}$  can be calculated from the angular frequency ( $\omega = 2\pi f$ ) at the maximum imaginary component and the charge transfer resistance according to the following equation:

$$C_{dl} = [1/\omega_{max} \cdot R_p] = [1/2\pi \cdot f_{max} \cdot R_p] \quad (3.18)$$

Where  $f$  is frequency,  $\omega$  is the angular velocity.

The present work is concerned with the possible adsorption of an polymer compounds at the C-steel / electrolyte interfaces by which the corrosion rate is reduced. Therefore, ac impedance measurements were primarily used to determine the capacity of the double layer  $C_{dl}$ . On addition of the inhibitor, a change in the  $C_{dl}$  value is expected to reflect structural modifications of the metal-electrolyte interface due to the presence of the polymer compound.

In order to appreciate the variations of electrochemical cell impedance with frequency, it is convenient to consider a hypothetical equivalent circuit, i.e. a combination of electrical circuit elements that behaves in a similar manner to the corroding electrode. The equivalent circuit proposed by Randles has been found to have wide application in many electrochemical systems. The results described below can be interpreted in the terms of the Randles circuit, which has been used previously to model the iron/acid interface [155]

The impedance measurements were carried out at the steady-state potential,  $E_{corr}$ , which attained after immersing the C-steel electrode in the corrosive media for a period of 15 min.

Fig.(3.30-3.35) show the Nyquist plots for carbon steel in 1M HCl solution in the absence and presence of different concentrations of inhibitors at 25°C. It is seen from these Figures that the impedance diagram in most of these cases does not show perfect semicircles. This behavior can be attributed to the frequency dispersion[156] as a result of roughness and inhomogeneities of the electrode surface. Increase in the diameters of the



semicircles with the concentration of the additives indicates that an increase in the protective properties of the C-steel surface. Thus, the capacitive semicircle is correlated with the dielectric properties and the thickness of barrier adsorbed film.

Impedance parameters, such as, charge transfer resistance  $R_{ct}$ , which is equivalent to  $R_p$ , and the double layer capacitance  $C_{dl}$ , are derived from the Nyquist plots and are given in Tables (3.21-3.26). for carbon steel in 1.0 M HCl acid solution in the presence and absence of the investigated polymer compounds It is observed that the values of  $R_{ct}$  increase with increasing the concentration of the inhibitors and this in turn leads to the increase of the percentage inhibition efficiency due to the formation of adherent film on the C-steel/solution interface Impedance diagrams for all polymer examined have a semicircular appearance; these diagrams indicate that the corrosion of carbon steel in 1.0 M HCl solution is mainly controlled by a charge transfer process.

The values of double layer capacitance,  $C_{dl}$ , decrease with increasing the concentration of the additives. This is due to the gradual replacement of water molecule by the adsorption of the polymer compounds which form a protective film on the Al surface and led to the decrease in local dielectric constant of the steel solution interface.

The percentage inhibition efficiency is calculated using charge transfer resistance as follow[156-157]:

$$\% IE = [(R_{ct(inh)} - R_{ct}) / R_{ct(inh)}] \times 100 \quad (3.11)$$

where,  $R_{ct}$  and  $R_{ct(inh)}$  are the charge transfer resistance values in the absence and presence of inhibitors for C steel in 1M HCl, respectively.

The computed values of %IE are given in Tables (3.21-3.26). As the concentrations of the polymer compounds increases, the values of %IE increases. The order of percentage inhibition decreases in the following order:

Comp. VI > Comp. V > Comp. IV > Comp. III > Comp. II > Comp. I

The order of inhibition efficiency obtained from the EIS technique were in full accord with those obtained from the weight loss, potentiodynamic anodic polarization and galvanostatic technique. This proves the validity of these tools in the measurements of the investigated inhibitors.

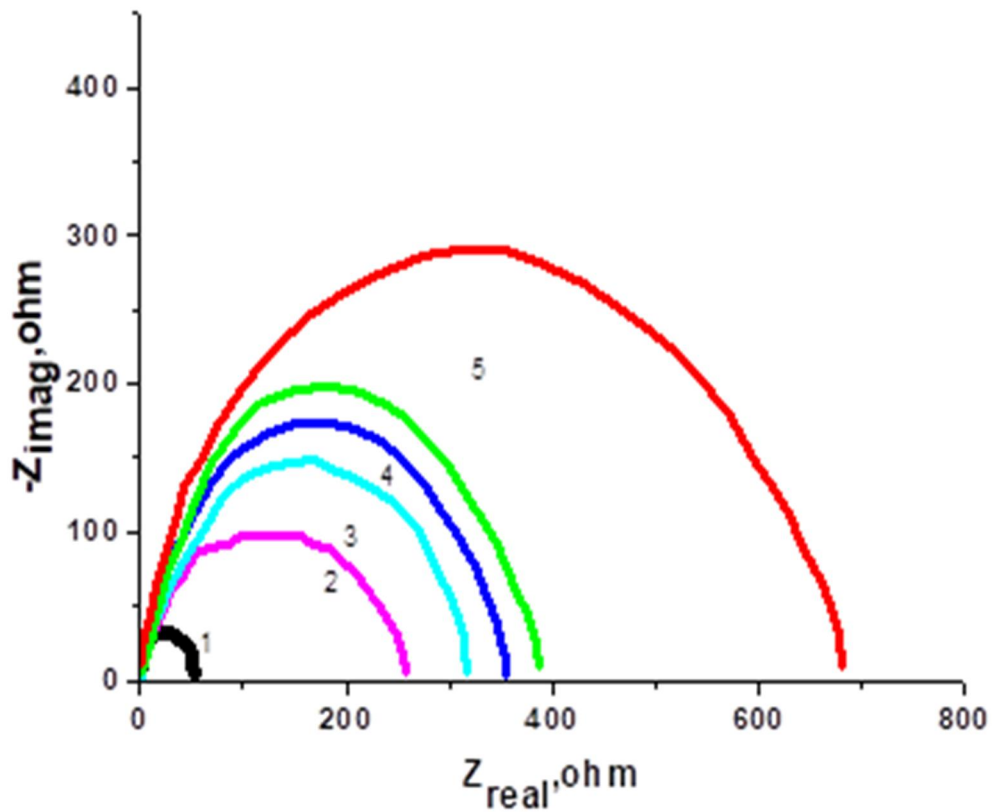


Fig.(3.30): Nyquist plot of C-steel in 1.0M HCl solution in absence and presence of different concentrations of compound I.

(1)0.00 ppm (2)100 ppm (3)200 ppm (4)300 ppm

(5)400 ppm.(6)500 ppm.

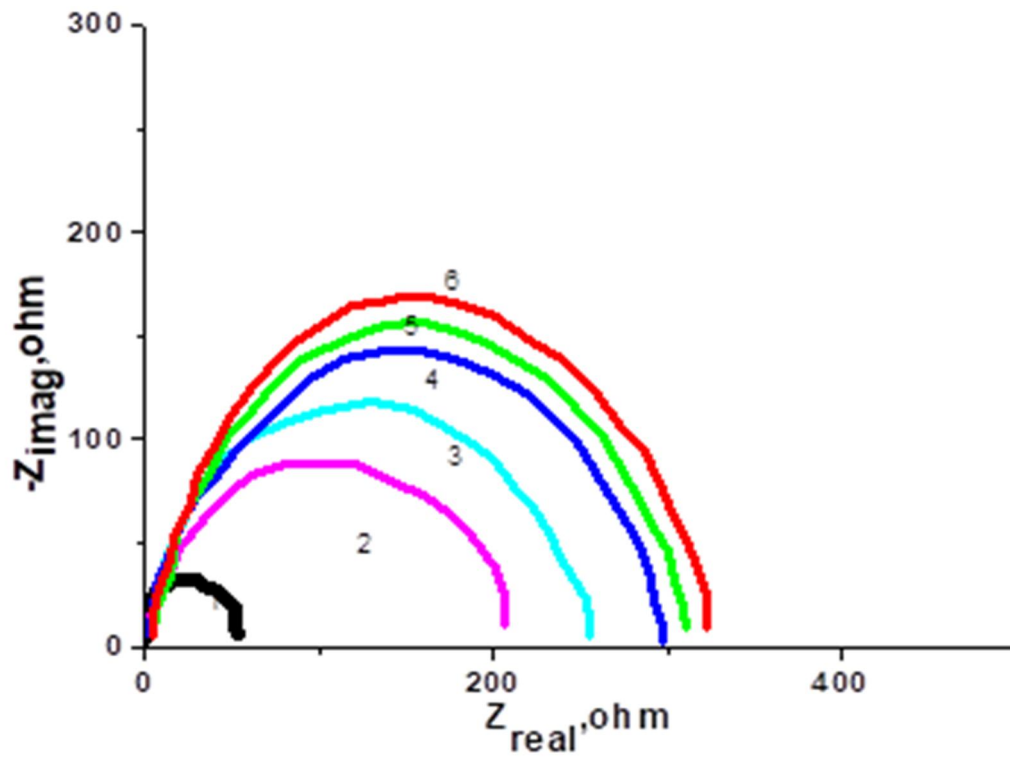


Fig.(3.31): Nyquist plot of C-steel in 1.0M HCl solution in absence and presence of different concentrations of compound II.

(1)0.0 ppm (2)100 ppm (3)200 ppm (4)300 ppm

(5)400 ppm(6)500 ppm.

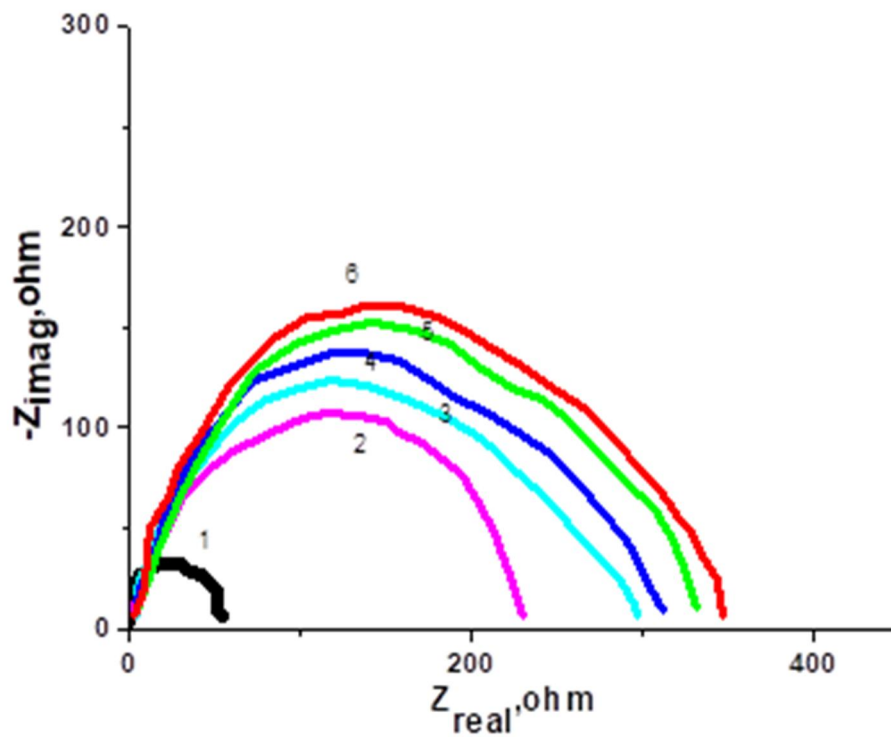


Fig.(3.32): Nyquist plot of C-steel in 1.0M HCl solution in absence and presence of different concentrations of compound III.  
(1)0.0 ppm (2)100 ppm (3)200 ppm (4)300 ppm  
(5)400 ppm (6)500 ppm.

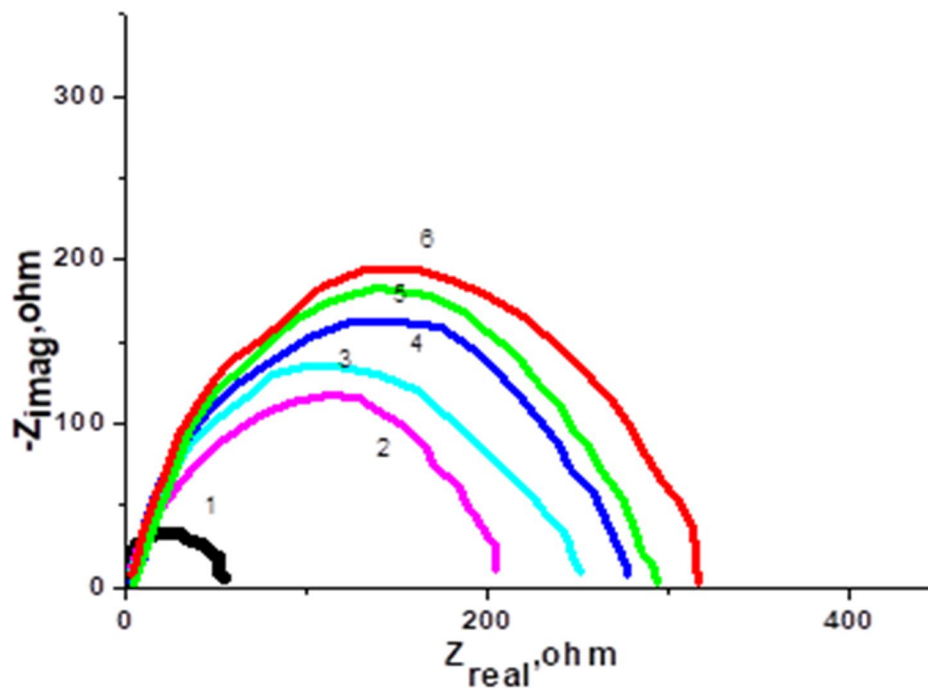


Fig.(3.33): Nyquist plot of C-steel in 1.0M HCl solution in absence and presence of different concentrations of compound IV.  
(1)0.00 ppm (2)100 ppm (3)200 ppm (4)300 ppm  
(5)400 ppm (6)500 ppm.

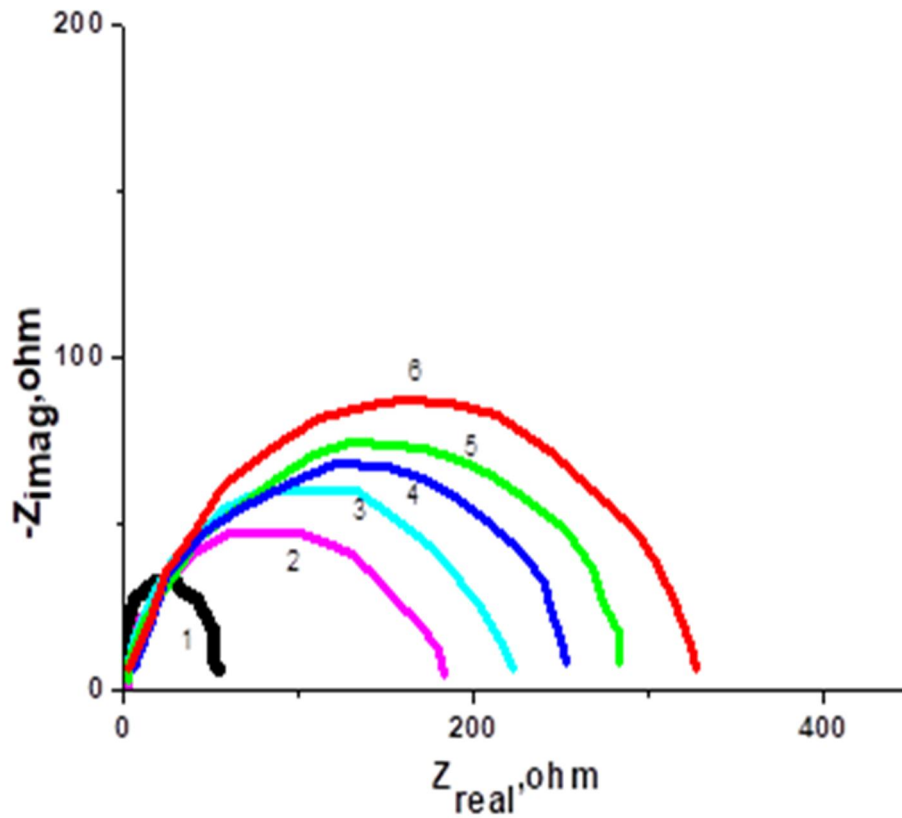


Fig.(3.34): Nyquist plot of C-steel in 1.0M HCl solution in absence and presence of different concentrations of compound V.

(1)0.0 ppm (2)100 ppm (3)200 ppm (4)300 ppm

(5)400 ppm (6)500 ppm.

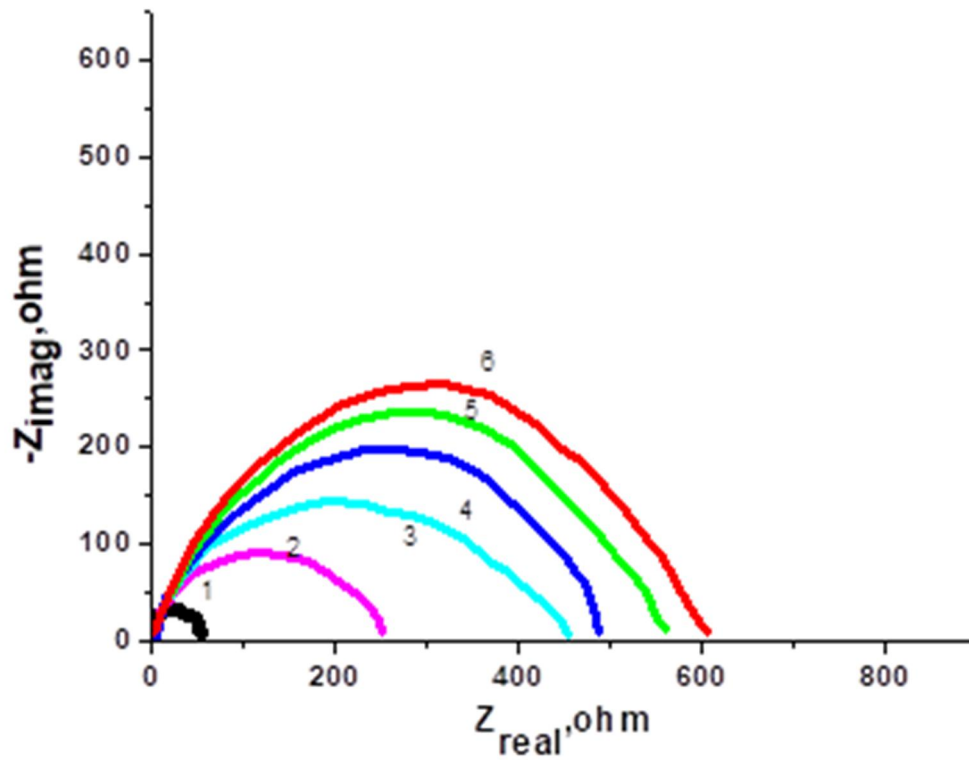


Fig.(3.35): Nyquist plot of C-steel in 1.0M HCl solution in absence and presence of different concentrations of compound VI.

(1)0.00 ppm (2)100 ppm (3)200 ppm (4)300 ppm

(5)400 ppm (6)500 ppm.



Table(3.21): Electrochemical parameters obtained by EIS measurements of carbon steel electrode in 1.0M HCl solution at different concentrations of compound I.

<b>Inhibitor System</b>	<b>Concentration (ppm)</b>	<b><math>R_s</math> (<math>\Omega \text{ cm}^2</math>)</b>	<b><math>R_{ct}</math> (<math>\Omega \text{ cm}^2</math>)</b>	<b><math>C_{dl}</math> (<math>\mu\text{F cm}^{-2}</math>)</b>	<b>%I.E<sub>(b)</sub></b>
<b>Blank</b>	HCl (1M)	2.66	58	187	-----
<b>Compound I</b>	100	2.50	211	159	72.50
	200	2.43	246	152	76.42
	300	2.42	291	141	80.00
	400	2.38	306	138	81.05
	500	2.35	324	133	82.10

Table(3.22): Electrochemical parameters obtained by EIS measurements of carbon steel electrode in 1.0M HCl solution at different concentrations of compound II.

<b>Inhibitor System</b>	<b>Concentration (ppm)</b>	$R_s$ ( $\Omega \text{ cm}^2$ )	$R_{ct}$ ( $\Omega \text{ cm}^2$ )	$C_{dl}$ ( $\mu\text{F cm}^{-2}$ )	$\%I.E_{(b)}$
<b>Blank</b>	HCl (1M)	2.66	58	187	-----
<b>Compound II</b>	100	2.45	206	151	71.84
	200	2.39	249	147	76.70
	300	2.37	271	139	78.60
	400	2.31	286	132	79.72
	500	2.29	327	128	82.26

Table(3.23): Electrochemical parameters obtained by EIS measurements of carbon steel electrode in 1.0M HCl solution at different concentrations of compound III.

<b>Inhibitor System</b>	<b>Concentration (ppm)</b>	$R_s$ ( $\Omega \text{ cm}^2$ )	$R_{ct}$ ( $\Omega \text{ cm}^2$ )	$C_{dl}$ ( $\mu\text{F cm}^{-2}$ )	$\%I.E_{(b)}$
<b>Blank</b>	HCl (1M)	2.66	58	187	-----
<b>Compound III</b>	100	1.98	176	146	67.04
	200	1.87	228	142	74.56
	300	1.81	247	137	76.51
	400	1.77	289	128	79.93
	500	1.69	331	123	82.47

Table(3.24): Electrochemical parameters obtained by EIS measurements of carbon steel electrode in 1.0M HCl solution at different concentrations of compound IV.

<b>Inhibitor System</b>	<b>Concentration (ppm)</b>	<b><math>R_s</math> (<math>\Omega \text{ cm}^2</math>)</b>	<b><math>R_{ct}</math> (<math>\Omega \text{ cm}^2</math>)</b>	<b><math>C_{dl}</math> (<math>\mu\text{F cm}^{-2}</math>)</b>	<b>%I.E<sub>(b)</sub></b>
<b>Blank</b>	<b>HCl (1M)</b>	<b>2.66</b>	<b>58</b>	<b>187</b>	<b>-----</b>
<b>Compound IV</b>	<b>100</b>	<b>2.48</b>	<b>231</b>	<b>154</b>	<b>74.90</b>
	<b>200</b>	<b>2.44</b>	<b>286</b>	<b>149</b>	<b>79.72</b>
	<b>300</b>	<b>2.40</b>	<b>302</b>	<b>140</b>	<b>80.80</b>
	<b>400</b>	<b>2.37</b>	<b>326</b>	<b>136</b>	<b>82.20</b>
	<b>500</b>	<b>2.31</b>	<b>343</b>	<b>131</b>	<b>83.10</b>

Table(3.25): Electrochemical parameters obtained by EIS measurements of carbon steel electrode in 1.0M HCl solution at different concentrations of compound V.

<b>Inhibitor System</b>	<b>Concentration (ppm)</b>	<b><math>R_s</math> (<math>\Omega \text{ cm}^2</math>)</b>	<b><math>R_{ct}</math> (<math>\Omega \text{ cm}^2</math>)</b>	<b><math>C_{dl}</math> (<math>\mu\text{F cm}^{-2}</math>)</b>	<b><math>\%I.E_{(b)}</math></b>
<b>Blank</b>	<b>HCl (1M)</b>	<b>2.66</b>	<b>58</b>	<b>187</b>	<b>-----</b>
<b>Compound V</b>	<b>100</b>	<b>2.43</b>	<b>258</b>	<b>142</b>	<b>77.51</b>
	<b>200</b>	<b>2.38</b>	<b>466</b>	<b>138</b>	<b>87.55</b>
	<b>300</b>	<b>2.33</b>	<b>498</b>	<b>133</b>	<b>88.35</b>
	<b>400</b>	<b>2.28</b>	<b>564</b>	<b>126</b>	<b>89.71</b>
	<b>500</b>	<b>2.26</b>	<b>593</b>	<b>121</b>	<b>90.21</b>

Table(3.26): Electrochemical parameters obtained by EIS measurements of carbon steel electrode in 1.0M HCl solution at different concentrations of compound VI.

<b>Inhibitor System</b>	<b>Concentration (ppm)</b>	<b><math>R_s</math> (<math>\Omega \text{ cm}^2</math>)</b>	<b><math>R_{ct}</math> (<math>\Omega \text{ cm}^2</math>)</b>	<b><math>C_{dl}</math> (<math>\mu\text{F cm}^{-2}</math>)</b>	<b>%I.E<sub>(b)</sub></b>
<b>Blank</b>	HCl (1M)	2.66	58	187	-----
<b>Compound VI</b>	100	2.53	254	166	77.16
	200	2.48	311	158	81.35
	300	2.51	345	151	83.20
	400	2.52	371	148	84.36
	500	2.48	678	142	91.44

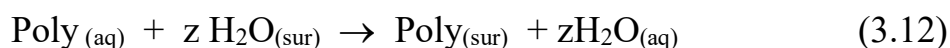
## *PART (E)*

### Adsorption isotherm and inhibition mechanism

#### 3.5.1. Adsorption isotherm:

The adsorption behavior of the polymer compounds on the interface of the carbon steel solution can be conveniently explained by finding an appropriate isotherm that describes the variation of experimentally obtained values of the amount of adsorbed substance per unit area of the metal surface with its concentration in the bulk at constant temperature. Therefore, the adsorption isotherm highlights the relationship between the adsorbed amount on the metal surface and the bulk quantity. It also gives an idea of the interaction parameters, which aids in the adsorption of the inhibitors on the metal surface.

The tested polymer compounds inhibit the corrosion process by adsorption onto the steel surface. Theoretically, the adsorption process can be considered as a substitution process between the polymer compounds in the aqueous phase [ $\text{Poly}_{(\text{aq})}$ ] and water molecules at the carbon steel surface [ $\text{H}_2\text{O}_{(\text{sur})}$ ] to give the polymer compounds adsorbed on the surface of carbon steel [ $\text{Poly}_{(\text{sur})}$ ] and thus increased inhibition efficiency due to subsequent equation:



where,  $z$  is the size ratio and simply equals the number of adsorbed water molecules replaced by a single inhibitor molecule

The adsorption depends on the inhibitor structure, the type of the metal, the nature of its surface, the nature of the corrosive medium and the pH value, the temperature, the electrochemical potential of the metal-solution interface. Also, the adsorption provides information about the interaction

between the adsorbed molecules themselves as well as their interaction with the metal surface. Indeed, the adsorbed molecule may make the surface more difficult or less difficult for another molecule to become attached to a neighboring site and multilayer adsorption may take place. There may be than one inhibitor molecule per surface site. Finally, different surface sites can have varying degrees of activation. For these reasons many mathematical adsorption isotherm expressions have been developed to consider some imperfect effects

Trials were made to fit  $\theta$  values to the several adsorption isothermal relationships, such as Frumkin, Freundlich, Langmuir and Temkin isotherms. It was found that the obtained results obeyed Freundlich isotherm, which governed by the following equation [158]:

$$\log \theta = \log K_{\text{ads}} + n \log C_{\text{inh}} \quad (3.13)$$

where,  $K_{\text{ads}}$  and  $C_{\text{inh}}$  are the equilibrium constant for the adsorption and concentration of the polymer, respectively.

Figure(3.36) represents the relationship  $\log \theta$  and  $\log C_{\text{inh}}$  for C-steel electrode in 1.0 M HCl solution and containing various concentrations of six polymer compounds. A straight lines relationship was obtained with intercept  $\log K_{\text{ads}}$ . This indicates that the adsorption of polymer compounds on the C-steel surface follows Freundlich isotherm

The equilibrium constant of adsorption  $K_{\text{ads}}$  is calculated from the intercept of the straight lines and it is related to the standard free energy of adsorption ( $\Delta G^{\circ}_{\text{ads}}$ ) by the relation [159,160]:

$$K_{\text{ads}} = 1/55.5 \exp [ -\Delta G^{\circ}_{\text{ads}} / RT ] \quad (3.14)$$

where R is the universal gas constant, the value 55.5 is the concentration water in the solution in mole. The values K and  $\Delta G^{\circ}_{\text{ads}}$  were of



computed and recorded in Table (3.27 ).The large values of  $K_{ads}$  imply the efficient adsorption of the polymer compounds on the carbon steel surface and hence higher inhibition efficiency.

An examination of the data of this Table shows that the negative signs of  $\Delta G^{\circ}_{ads}$  indicate that the adsorption of the tested polymer compounds on the C-steel surface is proceeding spontaneously and is accompanied by a highly efficient adsorption[161] It is well known that values of  $\Delta G^{\circ}_{ads}$  of the order of  $-40 \text{ kJmol}^{-1}$  or higher involve charge sharing or transfer from the inhibitor molecules to metal surface to form coordinate type bond(chemisorption). While the values of  $\Delta G^{\circ}_{ads}$  up to  $-20 \text{ kJ mol}^{-1}$  , the types of adsorption were regarded as physisorption ,the inhibition act due to the electrostatic interaction between the charged molecules and the charged metal[162,163]. The standard free energy of adsorption is associated with water adsorption / desorption equilibrium which forms an important part of the overall free energy changes of adsorption.  $\Delta G^{\circ}_{ads}$  increase with the increase of the solvation energy of adsorbed species which in turn increases with increasing molecular size [169] The computed values of  $\Delta G^{\circ}_{ads}$  are in the range  $-36.42$  to  $-40.18 \text{ kJ mol}^{-1}$  indicate that the adsorption of the polymer compounds on the C-steel surface functions by physicochemical adsorption(mixed of physical and chemical adsorption).

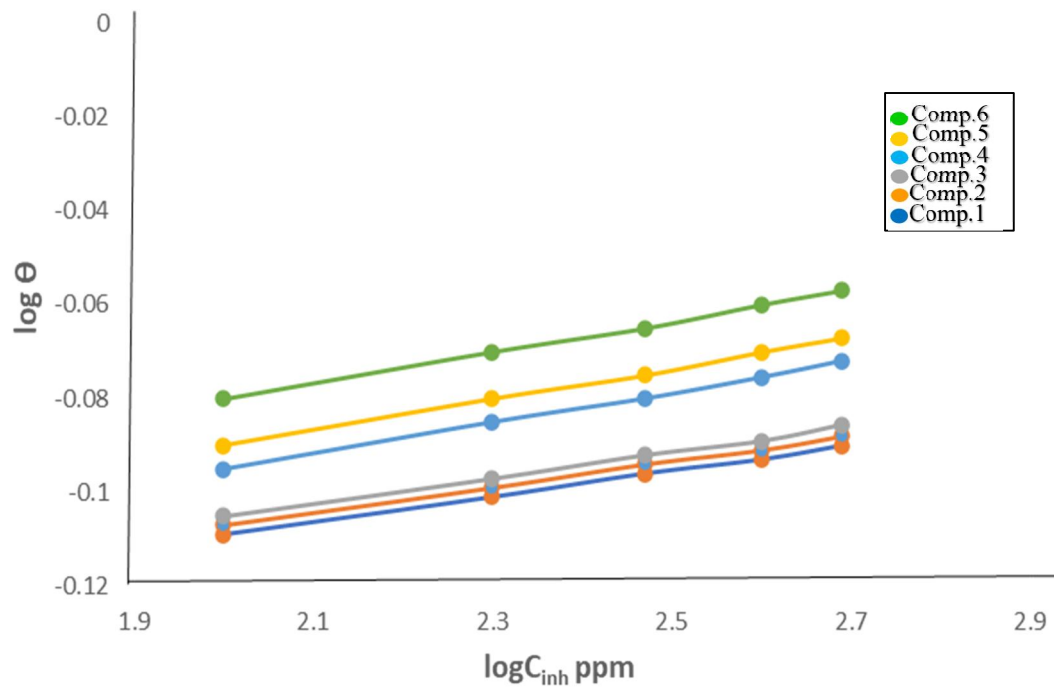


Fig.(3.36): Freundlich isotherms for corrosion of carbon steel in inhibited 1.0 M HCl solution

Table (3.27 ): The values  $K_{ads}$  and  $\Delta G^{\circ}_{ads}$  for C-steel in 1.0 M HCl solution in the absence and presence of 500 ppm of the studied polymer compounds

Polymer Compound	$K_{ads} \times 10^{-1}$	$-\Delta G^{\circ}_{ads}$ (kJ/mol)
Compound I	8.5	36.42
Compound II	9.2	37.12
Compound III	9.7	38.03
Compound IV	10.1	38.92
Compound V	10.7	39.75
Compound VI	11.4	40.18

### 3.5.2. Mechanism of inhibition :

The inhibiting vigor of polymer compounds toward the corrosion of carbon steel in 1.0 M HCl solution was determined by chemical techniques such as weight loss(WL), electrochemical techniques such as galvanostatic polarization(GP), potentiodynamic anodic polarization and electrochemical impedance spectroscopy(EIS). It is evident that the percentage inhibition efficiency of polymer compounds computed from the various techniques depends on the concentration, nature of metal, the mode of adsorption of the inhibitors and surface conditions.

The following corrosion parameters were noticed with increasing the concentration of polymer compounds.

1. Weight loss decreases.
2. Low corrosion rate.
3. Increased surface coverage.
4. The corrosion current density was reduced.
5. The charge transfer resistance increases.
6. The double layer capacity decreases.
7. The pitting corrosion potential is shifted to more noble direction
8. The inhibition efficiency increases.

These results show that the explanation of the inhibitory effect of polymer compounds is due to the adsorption of these compounds on the carbon steel interface. The nature of the inhibitor interaction on the carbon steel surface during corrosion inhibition can be explained in terms of adsorption

properties[164]. Four types of adsorption may occur in inhibitory phenomena, namely,

- (i) The Electrostatic attraction between charged molecules and charged metals.
- (ii) Interaction of electron pairs in the oxygen and/or nitrogen atoms in the organic additive molecules with the metal.
- (iii) Interaction of  $\pi$ -electrons with the metals.
- (iv) A combination of the above.

However, the percentage inhibition efficiency depends on several factor ssuch as molecular structure of the polymer , the number of adsorption active centers in the molecule, the presence of electro donating or repelling groups, which include their charge density,molecular size, mod of adsorption, temperature, and the ability to the formation of metallic complexes. The adsorption of these compounds on the metal surface cans retards the anodic or the cathodic reaction by formation of physical barrier layer between the metal and inhibitor or reducing the metal reaction through alternating the nature of metal surface or by changing the structure of the metal/solution interface[165-170].

The obtained results by different techniques indicate that the order of inhibition efficiency of the polymer compound depending on the chemical structure of the polymer compounds and decreases in the following orde  
Comp.VI > Comp. V > Comp. IV > Comp. III > Comp. II > Comp.I

Obviously from the above arrangement , the percentage inhibition efficiency is related with the molecular weight of the tested polymer

compounds . The compound VI has the highest inhibition efficiency owing to the molecular weight is higher compared to other tested polymer compounds .On the other hand the compound I has the lowest percentage inhibition efficiency because its lower molecular weight.

The high molecular weight of the tested polymer compounds leads to covering a large area of the carbon steel surface due to the strong spontaneous adsorption of it, as evidenced by the values of computed free energy of adsorption  $\Delta G^{\circ}_{ads}$  . This leads to the formation of a protective layer that prevents the hydrochloric acid solution from reaching the carbon steel surface and thus increases the surface coverage, thus increases the inhibition efficiency of polymer compounds .The amount of surface coverage decreases at lower molecular weight .The existence of some hetero oxygen atoms, OH group and  $NH_2$  facilitates the adsorption process by forming a coordination bond between the polymer compound and the carbon steel by transferring lone pairs of electrons from hetero oxygen atoms to the steel surface. The formed complex is blocked adsorbed onto the steel surface due the formation of more than one active centre. Among all four techniques used the %IE of compound VI is a more efficient inhibitor than other tested polymer compounds. This is due to the possibility of a more complex formation in the compound VI due to the presence of more than an oxygen hetero atoms and the presence of many OH and  $NH_2$  accelerates the adsorption process. The % IE varies from compound to compound depending on the presence of some active centers in the compound . So, we find that with the decrease of the active centers in the compound accompanied by the least effective inhibition, and therefore, we find compound I which is the lowest values of % IE for all the tested polymer compounds.

The inhibition of pitting corrosion of carbon steel in 1.0 M HCl solution by the investigated polymer compounds (as indicated from potentiodynamic anodic polarization) may be assumed to occur as a result of the competitive adsorption of between the polymer compounds and the chloride ions until the polymer compounds are the predominant than chloride ions. Therefore, the polymer compounds is faster adsorbed than chloride ions onto the surface of the carbon steel, and thus the pitting corrosion is inhibited by shifting the pitting corrosion potential into positive (noble) direction.

# **SUMMARY**



## ***ENGLISH SUMMARY***

The corrosion is a great problem, which faced the world, we can not hide this problem from our life but we can reduce it by several methods as the environment need. The aim of the present work is to study the reactivity of six polymer compounds as corrosion inhibitors for carbon steel in hydrochloric acid solutions.

This work contains three main chapters:

### **Chapter (1)**

This chapter discusses definition of corrosion, Types corrosion inhibitors, Electrochemical theory of corrosion, corrosion monitoring techniques, Types of inhibitors and literature survey for corrosion of carbon steel in aqueous solution and its inhibition.

### **Chapter(2)**

This chapter deals with the experimental part. It includes the chemical composition, chemical additives and solution, chemical structure of polymer, classified as chemical techniques such as weight loss and electrochemical techniques such as potentiodynamic polarization and impedance spectroscopy.

### **Chapter(3)**

It deals with the results obtained and their discussion and is divided into five sections.

**part (A):** contains the results of weight loss measurements for carbon steel in 1.0 M hydrochloric acid solutions containing different concentrations of polymer compounds. The results revealed that these compounds behave similarly and the weight loss is generally decreases with increasing the

concentration of these compounds. It also depend upon the nature of the polymer compound used. The inhibition efficiency of these compounds is in the following order:

Comp.VI > Comp. V > Comp. IV > Comp. III > Comp. II > Comp.

The effect of temperature on corrosion inhibition of carbon steel in 1.0 M HCl solution was determined over a temperature range 25-55<sup>0</sup> C using weight loss measurements. The rate of corrosion increases with increasing the temperature and hence the inhibition efficiency decreases . This indicates that the adsorption of the polymer compounds onto the carbon steel surface is physical. Some activation thermodynamic in presence of 500ppm of the investigated compounds were calculated and interpreted.

**part (B)** :contain the results of Galvanostatic polarization the data reveals that, all polymer compound slightly shifted  $E_{\text{corr}}$  to more negative potential and also the values of  $I_{\text{corr}}$  decrease .both anodic and cathodic tafel slopes  $\beta_a, \beta_c$  in the presence of polymer compound increasing .The inhibition efficiency increased with concentration of inhibitor increase.

**part(C)** :involves the results of potentiodynamic anodic polarization measurements for carbon steel in 1.0 M HCl in absence and presence of different concentrations of NaCl as pitting corrosion agents. As the concentration of Chloride ions increases the pitting potential is shifted to more negative direction indicating the destruction of passive film and initiation of pitting corrosion.

The addition of different concentration of polymer compounds to 0.1M NaCl solution shifted the pitting potential towards more positive values, This indicates that increased resistance to pitting attack.

**part (D)** : contains the results of electrochemical impedance spectroscopy .Nyquist plots of carbon steel in 1.0 M HCl solution containing different concentrations of polymer compounds are plotted. Impedance parameters ,such as,charge transfer resistance  $R_{ct}$  ,and the double layer capacitance  $C_{dl}$  are derived from the Nyquist plots are determined for carbon steel in 1.0M HCl solution.The values of  $R_{ct}$  increase with increasing the concentration of the inhibitors and this in turn leads to a decrease in corrosion rate of carbon steel.

**Part (E)** : The inhibition mechanism of the general and pitting corrosion of carbon steel 1.0 M HCl solution by six polymer compounds is demonstrated by its adsorption on the surface of carbon steel. The adsorption is spontaneous and obeys Freundlich adsorption isotherm. The presence of many active centers of the polymer compounds facilitates the adsorption process, , and therefore increases the values of inhibition efficiency. It has also been shown that polymer compounds of large molecular weight give a high inhibition effect.

In conclusion, chemical and electrochemical measurements support the assumption that corrosion inhibition is primarily caused by adsorption of polymer compounds onto the carbon steel surface. The agreement between these different independent techniques indicates the validity of the obtained results.

## **REFERNCES**

## ***REFERENCES***

- 1.Updating Corrosion Map of India- A Report National Corrosion Council of India, CECRI, *Karaikudi*, (1996), 1.
- 2.H.H. Uhlig, J. Wiley ,S. Inc Corrosion and corrosion Control, *New York*(1996).
- 3.K.G. Compton, NACE Basic Corrosion Course, *Houston* (1971).
- 4.W.A. Wesley. , *Proc. ASTM*, 40 (1940) 690.
- 5.M.J. Prjor. , and D.S. keir , *J. Electrochem. Soc.*,104 (1957) 269.
- 6.Y.J.Tan. , *Corrosion*, 50 (1994) 226.
- 7.J.W. Oldfield , *Bull. Electrochem.* ,3 (1987) 597.
- 8.P.K. De Vivekanand Kani. , and S. Banerjee, *Proc. International Conference on Corrosion*, (1997) 1258.
- 9.R.L. Cowen , and C.S. Tedmon. , Jr., *Advances in Corrosion Science and Technolgy*, Vol. (3), Ed. M. G. Fontana and R. W. Starchle, *Plenum Press*, *New York*, (1973) 293.
- 10.M .Henthorne, *ASTM-STP*, 516 (1972)66.
- 11.D. Sazou, and M.J .Pagitsas, *Electroanal Chem.*, 304 (1991),171.
- 12.W.J. Lorenz, and K. E. Heusler, *Corrosion Mechanism*, 1 (1987).
- 13.J.L. Hudson, J.C. Bell , and Jaiger N. I., *Phys. Chem.*, 92 (1988) 1383.
- 14.D. Sazou. , and M.J.Pagitsas, *Electroanal Chem.*, 312 (1991) 185.
- 15.G. Wranglen, *An Introduction to Corrosion and Protection of Metals*; *London, New York* (1985).
- 16.R.C. Newman, and R. P. Procter., *Br. Corros. J.*, 25 (1990) 259.

- 17.P. Hurst , A .S. Rafel , and D. R. Tice , *Am. Nu. Soc.*, (1997) 430 .
- 18.Y. Wany. R. Akid, *Corrosion*, 52 (1996) 92.
- 19.D.S. Ramachandra Murthy, G. Raghava, and Gandhi. *NCCI*, (1992) 22.
- 20.R. Narayan; An Introduction to Metallic Corrosion and its Prevention; Oxford and IBH publishing *Co. Pvt. Ltd.*, (1998).
- 21.R. B. Waterhouse, Fretting Corrosion, *Pregamon Press* (1972).
- 22.W.R. Whitney, *J. Am. Chem. Soc.*, 25 (1903) 395.
- 23.W.H. Walkar, ,M. Cadehralm, and L. N. Bent, , *J. Am. Chem. Soc.*, 29, (1907) 1251.
- 24.J.N. Friend, *Trans. Am. Electrochem. Soc.*, 40 (1921) 63.
- 25.J.N. Friend, *J. West Society., Iron- Institute.*, 31 (1923) 74.
- 26.H.G. Reddic, and S. E. J. Winderman, *J. New English Water Works Association*, 46 (1932) 146.
- 27.U.R. Evans , *Corrosion of Metal*, *Arnold publishers*, (1924).
- 28.F. Z. Mylius; *Metallk.*, 233, (1922).
- 29.Industrial corrosion monitoring committee on corrosion; “Department of chemistry”, HMS, (1978) .
- 30.*Corrosion testing and monitoring-The institution of corrosion science and technology*; Chameleon press Ltd., *London* .
- 31.L. L. Shrier Mewness, *Butterworth Corrosion, Vol. 2, Ed, London*, (1978).
- 32.S.N. Banerjee, *An Introduction to Science of Corrosion and its Inhibition*; Ox-anion Press, *Pvt Ltd., New Delhi*, (1985).

- 33.W. H. Ailor ; Handbook of corrosion testing and evaluation, *John and Wiley (London)*. (1971).
- 34.F. A. Champion; “Corrosion testing procedures”; *Second Edition, Chapman and Hill, London*, (1964) .
- 35.W. A. Badawy, F. M. El-Kharafi and A. S. El-Azab; *Current Topics in Electrochem.* 6, (1998) 149,
- 36.M. I. Slim, A. A. Yassin and B. G. Ateya ; *Corros. Sci.*, 17 (1977). 923,
- 37.W. Faiza El-Nezomy; M. Sc Thesis; *Cairo university*, (1979).
- 38.M. Stern and R. M. Roth; *J. Electrochem. Soc.*, 104, (1957) 390.
- 39.R.V. Skold and T. E. Larson, *Corrosion* , 13 (1957) 139.
- 40.A. C. Markvides, *J. Electrochem. Soc.*,167 (1960)869.
- 41.E. Mcafferty and A. C. Zettlemoyer, *J. Phy. Chem.*; 71 (1967) 2444.
- 42.D. D. Mac Donald, *Corrosion*, 46 (1990) 229.
- 43.C. Gabrielli and M. Keddam, *Corrosion*, 48 (1992) 794.
- 44.J. M. Walls, *Methods of Surface Analysis*, (1998).
- 45.G. Sozhan , *Central Electrochemical Research Institute; India*, (2001)
- 46.P.R. Roberge, Handbook of Corrosion Engineering,  
*McGraw-Hill*,(1999).839.
- 47.R. Wiston, Uhlig’s Corrosion Handbook, 2nd Edition, p.1093, *John Wiley and Sons Inc.*,(2000).
- 48.P.R. Roberge, Handbook of Corrosion Engineering,  
*McGraw-Hill*,(1999)836.

- 49.P.R. Roberge, Handbook of Corrosion Engineering, *McGraw-Hill*,(1999) 837.
- 50.R., Wiston Uhlig's Corrosion Handbook, 2nd Edition, John Wiley and *Sons Inc.*,(2000)1901.
- 51.S. A. Abd El-Maksoud and A.S. Fouda, *Mater. Chem. & Phys.*, 93 (2005) 84.
- 52.H.Ashassi-Sorkhabi, M. R .Majidi and K. Seyyedi, *Appl. Surf. Sci.*, 225 (2004) 176.
- 53.A.S .Fouda, A.A .Al-Sarawy, E .E. El-Katori, *Desalination* 201 (2006)1.
- 54.M. Abdallah, E. A . Helal and A .S. Fouda, *Corros. Sci.*, 48 (2006) 1639.
- 55.G.K. Gomma and M.H. Wahdan, *Indian J. Chem. Techn.*, 2 (1995) 157.
- 56.S. Ramesh, S. Rajeswari, *Electrochim. Acta*, 49 (2004) 811.
- 57.S. A. Abd El-Maksoud and A.S. Fouda, *Mater. Chem. & Phys.*, 93 (2005) 84.
- 58.A. Popova, *Corros. Sci.*, 49 (2006) 2144.
- 59.Mohamed A. Amin, Sayed S. Abd El-Rehim, E. E. F. El Sherbini and Rady S. Bayoumi, *Electrochim. Acta.*, 52 (2007) 3588.
- 60.S. A. Abd El-Maksoud, S. A. Rashwan, M. A. Ibrahim and S. A. Abd El-Wahaab, *Electrochimica Acta.*, 50 (2004) 1985.
- 61.Guo Gao, Cheng Hao Liang and Hua Wang, *Corros. Sci.*, 49 (2007) 1833.
62. S.A. Abd El-Maksoud, *Mater. and Corros.*, 54 (2003) 106.



- 63.Z. Ait Chikh, D. Chebabe, A. Dermaj, N. Hajjaji, A. Srhiri, M. F. Montemor, M. G. S. Ferreira, A. C. Bastos, *Corros. Sci.*, 47 (2005) 447.
64. M. I. Awad, *J. Appl. Electrochem.*, 36 (2006) 1163.
65. H. Wang, R. Lui and J. Xin, *Corros. Sci.*, 64 (2004) 2455.
- 66.S.AbdelHameed,M.Abdallah,Prot.Met.Phys.Chem.Surf.,54(2018)113.
67. A. J. Szyprowski, *Corros. Sci.*, 37 (2002) 141.
68. F. Bentiss, M. Traisnel and M. Lagrenee, *J. Appl. Electrochim.*, 31 (2001) 41.
- 69.B. G. Ershov, A. I. Milaev, V. G. Petrosyan, P. Ya. Glasunov and S. A. Tevlin, *Rad. Phys. and Chem.*, 26 (2002) 587.
70. A. C. Audelo, J. R. Gancedo, J. F. Marco, F. Creus, E. Gallego Lienesma, J. Desimoni and R. C. Mercader, *Appl. Surf. Sci.*, 148 (1999) 171.
- 71.R. Hasanov, M. Sadikoglu and S. Bilgic: *Appl. Surf. Sci.*, 253 (2007) 3913.
- 72.M. Quraishi, M. A. Wahdkhan and A. Aimal, *Bull. Electrochem.*, 11 (1995) 274.
- 73.K. C. Emregul, A. A. Akayb and O. Atakol, *Electrochim. Acta*, 50 (2005) 2515.
74. H.H. Uhlig. *The Corrosion Handbook*, John Wiley & Sons N.Y.P.65(1948).
- 75.A.S.Fouda,A.A.Al-Sarawy,E.E.El-katori, *Desalination* 201 (2006)1.
- 76.E. A. Noor and H. Aisha . Al- Moubaraki: *Mater. Chem. & Phys.*, 110 (2008) 145.

- 77.H.Amar, T. Braisaz, D. Villemin and B. Moreau, *Mater. Chem. & Phys.*, 110 (2008) 1.
- 78.O.Olivares-Xometl,N.V.Likhanova,M.A.Dominguez-Aguilar,E.Arce, H. Dorantes and P. Arellanes-Lozada, *Mater. Chem. & Phys.*, 110 (2008) 344.
- 79.M.Abdallah,S.T.Atwa,N.M.Abdallahand,A.S.Fouda,*Anti-Corros. Methods and Materials*, 58 (1) (2011)31.
- 80.A. M. El-Shamy, T. Y. Soror, H. A. El-Dahan, E. A. Ghazy, A. F. Eweas, *Mater. Chem.& Phys.*, 114(2009)156.
- 81.A. S. Fouda, S. A. El. Sayyed and M. Abdallah, *Anti. Corros. Methods and Materials*, 58(2) (2011)63
- 82.V. Saliyan, Ramesh, Airody Vasudeva Adhikari, *Mater. Chem.& Phys.*, 114(2009)211.
- 83.Qing Qu, Zhengzheng Hao, Lei Li, Wei Bai, Yongjun Liu, *Corros. Sci.*,51(2009)569.
- 84.M. Ehteshamzadeh, A. H. Jafari, Esmaeel Naderi, M. G. Hosseini, *Mater. Chem.& Phys.*, 113(2009)986.
85. N. S. Patel, S. Jauhari, G. N. Mehta, *Chemical Papers*, 64(1) (2010) 51.
- 86.M. Abdallah, A. Y. El-Etre, M. G. Soliman and E. M. Mabrouk, *Anti-Corros. Methods and Materials.*, 53 (2006) 118.
- 87.S. Takasaki and, y. Yamada, Kurita Water Industries Ltd., *Corros. Sci.*, 49 (2007) 240.
88. E. Patrick . Hazelwood, P. M. Singh, J. S. Hsieh, *Ind. Eng. Chem. Res.*, 23 (2006) 7789.

- 89.S. M . Abd El Haleem, S. Abd El Wanees, E. E. Abd El Aal, A. Diab, *Corros. Sci.*, 52 (2010) 292.
90. M. Abdallah, M. M. El-Naggar, *Mater. Chem. & Phys.*, 291(2001) 298.
- 91.M. Abdallah, H. E. Megahed and M. Sobhi, *Monatsh Chem.*141 (2010)1287.
- 92.A. C. Audelo, J. R. Gancedo, J. F. Marco, M. F. Creus, E. Gallego Lienesma, J. Desimoni and R. C. Mercader, *Appl. Surf. Sci.*, 148 (1999) 171.
- 93.M. M. El-Naggar, *Corros. Sci.*, 49 (2007) 2226.
- 94.S. K. Shukla, M. A. Quraishi, *Corros. Sci.*, 50(2009)413.
95. M. Alfakeer , M. Abdallah, A. Fawzy, *Int. J. Electrochem. Sci.*, 15 (2020) 3283 .
- 96.Z. Y. Chen, X. P. Guo, *Qzhang, Surf. Review & Letters*, 13 (2006)
97. I. Zaafarany, M. Abdallah, *Int. J. Electrochem. Sci.*, 5 (2010) 18.
- 98.M. A. Hegazy, M. Abdallah and H. Ahmed, *Corros. Sci.*, 52(2010)2897.
99. A. Fawzy , M. Abdallah, I. A. Zaafarany , S. A. Ahmed, I. I. Althagafi , *J. Mol.Liq.*,265 (2018) 276.
- 100.F.M.AL.Nowaiser,M.Abdallah and E. H. El. Mossalamy, *Chem.and. Tech. of Fuels and Oils*, 47(1) (2011)66.
101. A. Y. El-El-Etre and M.Abdallah, *Corros.Sci.*,42 (2000) 731.
- 102.A. Y. El-El-Etre, *Mater. Chem.& Phys.*, 108 (2008) 278.
103. R. M. Saleh, A .A. Ismail and A.H. El-Hosary, *Br. Corros. J.*, 17, 131 (1982).

- 104.M. Abdel-Gaber, B. A. Abd-El-Nabey, I. M. Sidahmed, A. M. El-Zayaday and M. Saadawy, *Corros. Sci.*,48, (2006) 2765.
- 105.E. A. Chaieb, A. Bouyanzer, B. Hammouti and M. Benkaddor, *Appl. Surf. Sci.*, 246, (2005) 199.
- 106.A. Bouyanzer, B. Hammouti and L. Majidi, *Mater. Lett.* 60, 2840 (2006).
- 107.A. Y. El-Etre, *Appl. Surf. Sci.*, 252, 8521 (2005).
- 108.A.Y .El-Etre, M. Abdallah, and Z.E. El-Tantawy, *Corros. Sci.*, 47 (2005) 385.
- 109.A. Y. El-Etre, *Corros. Sci.* 43, 1031(2001).
- 110.Y. Li, P. Zhao, Q. Liang and B. Hou, *Appl. Surf. Sci.* 252, 1245 (2005).
- 111.A. Y. El-Etre and Z. E. El-Tantawy, *Port Electrochim. Acta* 24, 347(2006).
- 112.A. Ostovari, S. M .Hoseinieh, M. Peikari, S.R. Shadizadeh and S. J. Hashemi, *Corros. Sci.*,51 (2009) 1935.
- 113.F. S. de Souza, A. Spinelli, *Corros. Sci.*, 51(2009) 642
- 114.N. O. Eddy, *Port. Electrochim Acta*, 27(5), (2009) 579.
115. A. M. Abdel-Gaber, P. A .Abd-El-Nabey and M. Saadawy, *Corros. Sci.*, 51 (2009) 1038.
116. M. Abdallah, M .A. Radwan, Shahera M. Shohayed and S. Abdelhamed, *Chem. and Tech. of Fuels and Oils*, 46 (2010)354.
- 117.M. Abdallah, *Port. Electrochim. Acta.*, 22, (2004)161.

- 118.R.G.Medeinos,J.Tonholo,R.Babban:The electrochemical *Society*,205(2019)317.
119. M. Abdallah, I. Zaafarany, J.H. Al-Fahemi, Y. Abdallah and A. S. Fouda, *Int. J. Electrochem Sci.*,7(8), ( 2012)6622.
- 120.A.Singh,N.Soni,Y.Deyuan,A.kumar,*Results in Physics*,13(2019)102-116.
- 121.S.Muralidharan, K. L. N. Phani, S. Pitchuman, S. Ravichandran, S. V.K .Lger, *The Electrochemical Society*,95(1995)12.
- 122.S.A.Umoren, O. Ogbobe, I. Olgwe, E. E. Ebens: *Corros.Sci.*, 50(2008)1998.
- 123.M. Alfakeer , M. Abdallah, A. Fawzy, *Int. J. Electrochem. Sci.*, 15 (2020) 3283.
- 124.D.Gopi, N. Bhuvaneshwaran, S. Rajeswarai, K.Ramadas, *Anti-Corros. Meth. Mater.*,(47)6(2000)332.
- 125.S.Tamilselvi, S. Rajeswari, *Anti-Corros. Meth. Mater.*,50(3)(2003)223.
126. P.W.AtKins ,Quot, *Physical Chemistry* ,(1994) 877.
127. G.Trabanelli, in Corrosion Mechanisms(Edited by F. Mansfeld, Marcel Dekker, *New York*,119(1987).
128. K.M.Ralls, T. H. Courtney, J. Wulf , *Wiley and sons, New York*.,214(1976).
129. M.I.Slim, A. A. Yassin and B.G.Ateya,*Corros.Sci.*17(1977)923.
- 130.I.Epelboin, P.Morel and J. Tackenoutij. *Electrochem. Soc.*,118(1971)1282.

131. Mc Cafferty and A.Z.Zettelemoyer, *J.phys.Chem.*, 71(1967)2452.
132. H.H. Uhlig. *The Corrosion Handbook, John Wiely& Sons N.Y.P.* (1948) 65.
- 133.A.I.Hofman ,V.J. Van Buul and F.J.P.Brouns: *Nutration health*, 56(12),(2016)2091.
- 134.I.Maribel Baker. P. Walsh Steven, D. Barbara, *Ullmanns Encyclo.*5(2012)1451.
- 135.L. Rui-Hong ,C .Junliu.,W. Chang, M. Yu , Y. Zhou, X. Aine, *Carbohydrate Poly.*, 87(1), (2012)76-83.
136. S. M. Abd. El-Haleem, *Br. Corros. J*, 14(3) (1979)171.
137. M. Abdallah, *Bull Electrochem.*, 134(4) (1997)149.
138. K. Videm and A. M. Koren, *Corrosion*, 49, (1993)746.
139. M. Edward, J. Rehring and T. Meyer, *Corrosion*, 50, (1994)336.
140. S. M. Abd. El-Haleem, *Werkstoffe U Korros.*, 30, (1979) 63.
141. M. Abdallah and A. Mead, *Annali Di Chimica (Rome)*, 83, (1993) 423.
142. A.K. Mohamed, H. A. Moustafa, G. Y. El-Awady and A. S. Fouda , *Port. Electrochim Acta*, 18, (2000)99.
143. E. M. Abd EL-Wahab and A. M. Shams El Din, *Br. Corros. J.*, 13, (1978)39.
144. M. Abdallah, A. Y. El-Etre, E. Abdallah and S. Eid,*J of the Korean Chemical Soc*, 53 (2009) 485.
145. P. M. Aziz and H. P. Godard: *Corrosion Ind , Eng. Chem.*, 44, (1952)179.

- 146.T. P. Hoars, D. Mears and G. Rothwell, *Corro Sci.*, 5, (1969)279.
- 147.H. P. Leckie and H. H. Uhlig, *J. Electrochem. Soc.*, 62, (1958)626.
- 148.I. Rosenfeld and W. Maximateochuk, *Z. Physik. Chem.*,215, (1960) 25.
- 149.W. Schwenk and E. Brauns, *Archive Eisenhuttnw.*,32, (1975) 387.
- 150.A. Z. Foroulis and M. J . Thubriker, *Werks. U. Korros.*, 26, (1975) 350.
- 151.A. Z. Foroulis:5 th International Congress on Metallic Corrosion,32, (1959)457.
- 152.M. G. Akedr, F. M. Abd El-Wahab and S.M. Abd EL-Haleem : *Bull Delosoc Chem. DeFrance*, (11-12), (1983)273.
153. K.F.Khaled, *Int.J.Electrochem. Sci*, 3(2008)462.
- 154.B. E. Conway, J. Bockris, and R.E. White, Edts, Kluwer Academic ., *New York*,32(1999)143.
- 155.S Haruyama, T.Tsuru, B Gijutsu, *J. Jpn. Soc. Corros. Engg.*, 27(1978)573.
- 156.L.Elkadi, B. Mernari, M. Traisnal, F. Bentiss, M. Lagrenee, *Corros. Sci.*,42 (2000)703.
157. I.L .Rosenfeld, *Corrosion Inhibitors*, McGraw-Hill, *New York*,1981.
158. F. M. Al- Nowaiser, M. Abdallah and E. H. El-Mossalamy, *Chem. Tech. Fuels .Oils*, 47 (2012) 453.
- 159.M.Alfakeer, M.Abdallah and R.S.Abdel Hameed, *Prot.Met. Phys.Chem.Surf.*,54(2020)225
- 160.M. Abdallah and B.A. Al Jahdaly, *Int. J. Electrochem. Sci.*, 10 (2015) 9808.

161. M. Abdallah, *Corros. Sci.*, 46(2004)1981.
162. T.P.Hoar, R.B. Mears and G.P.Rothwell, *Corros.Sci.*, 5 (1965) 297.
163. F. Mansfeld, *Corrosion*, 36, (1981) 301
164. K. Juttner, *Electrochim. Acta*, 35(10), (1990) 1501.
165. F. M. Al- Nowaiser, M. Abdallah and E. H. El-Mossalamy, *Chem. Tech. Fuels .Oils*, 47 (2012) 453.
166. M.Boukalah, B.Hamm, M.Lagrene, *Corros.Sci.*, 48(2006) 2831.
167. A .S .Fouda, A. M. Attia and A. M. Rashed, *Prot. Metals and Phys. Chem. Surf.*, 53(4)(2017)743.
168. M.Lagrene, B.Mernari, M.Bouanis, *Corros.Sci.*, 44(2002)573.
169. S.A.Umoren, M.JBanera, T.AlonsoGarcia, C.A.Gervasi and M.V.Mirifico, *Cellulose*, 20(2013)
170. M. Abdallah A.S. Fouda, D.A.M. El-Nagar, M. M. Alfakeere M. M. Ghoneim, *Surf. Eng. Appl.Electrochem.* 55(2019)172-182.



# **ARABIC SUMMARY**

## الملخص العربي

إن مشكلة التآكل من أكبر المشاكل التي تواجه العالم وحتى الان لا يمكن منع التآكل نهائيا ولكن يمكن تقليله باستخدام عدة طرق. وهذه الرسالة تتناول دراسة تآكل الصلب الكربوني في حامض الهيدروكلوريك ومحاولة تثبيطه باستخدام بعض المركبات ذات النشاط السطحي.

وقد اشتملت الرسالة على ثلاث أبواب رئيسية:

### الباب الأول

يشتمل على المقدمة التي تحتوي على تعريف التآكل وأنواعه ومقدمة عن مثبطات التآكل (تعريفها وأنواعها) ونظريات التآكل ومثبطات التآكل (تعريفها وأنواعها) وتم إستعراض الأبحاث المنشورة عن مختلف الدراسات السابقة ذات الصلة بموضوع البحث 'كما اشتمل هذا الباب على الهدف من الرسالة.

### الباب الثاني

يتضمن تركيب الصلب الكربوني المستخدم في الدراسة وأيضاً طرق تحضير حمض الهيدروكلوريك وتركيب البوليمرات المستخدمة في الدراسة ووصف طرق القياس المستخدمة مثل طريقة فقد في الوزن والقياسات الكهروكيميائية مثل الإستقطاب البوتنشوديناميكي وكذلك تحضير الأقطاب والخلية الكهروكيميائية.

### الباب الثالث

يشتمل على جميع النتائج التي تم الحصول عليها في هذه الدراسة وتم تمثيل هذه النتائج في منحنيات وجداول وقدتم تقسيم الباب إلى خمسة أقسام :

### القسم الأول

فيه تم دراسة سلوك تآكل الصلب الكربوني في محلول 1 مولار من حمض الهيدروكلوريك وتثبيطه باستخدام بعض المركبات العضوية بوليمرات. وقد أظهرت النتائج أن الفقد في وزن الصلب الكربوني يقل بزيادة تركيزات هذه البوليمرات ، وقد بينت النتائج أن ترتيب فعالية المركبات التي تم استخدامها على النحو التالي

مركب VI < مركب V < مركب IV < مركب III < مركب II < مركب I

و قد استخدمت هذه الطريقة لمعرفة تأثير درجة الحرارة على تثبيط تآكل الصلب الكربوني في محلول حامض الهيدروكلوريك في مدى 25 – 55 درجة مئوية , و وجد أن معدل التآكل يزداد بزيادة درجة الحرارة مع نقص كفاءة التثبيط مما يبين أن التثبيط يحدث عن طريق إدمصاص فيزيائي للمثبطات.

و قد تم حساب وتفسير طاقات التنشيط و بعض الدوال الترموديناميكية الخاصة بعملية التنشيط.

### القسم الثاني

فيه تم دراسة تآكل الصلب الكربوني باستخدام طريقة الاستقطاب الجلفانوستاتيكي في محلول 1 مولار من حمض الهيدروكلوريك في وجود وعدم وجود تركيزات معينة من المثبطات البوليمرية ووجد ان هناك إزاحة لمنحنيات الاستقطاب المهبطي والمصعدي على السواء مما يدل على ان هذه المركبات تعمل كمثبطات مختلطة وبتطبيق معادلة تافل وجد ان معدل التآكل يقل مع زيادة التركيز وبالتالي زيادة التثبيط ووجد ان كفاءة المثبطات تكون على النحو التالي:

مركب VI < مركب V < مركب IV < مركب III < مركب II < مركب I

### القسم الثالث

فيه تم دراسة التآكل الثاقب للصلب الكربوني في تركيبات مختلفة من كلوريد الصوديوم ووجد أن جهد التآكل الثاقب يتجه الى الاتجاه السالب بزيادة تركيز كلوريد الصوديوم مما يدل على حدوث التآكل الثاقب بإضافة المثبطات ووجد ان جهد التآكل الثاقب يتجه الى الإتجاه الموجب مما يدل على مقاومة الصلب الكربوني للتآكل الثاقب.

### القسم الرابع

يتضمن دراسة تآكل الصلب الكربوني بطريقة المعاوقة الكهروكيميائية الطيفية بالتيار المتردد في وجود تركيبات مختلفة من المثبطات وذلك في 1مولار حمض الهيدروكلوريك في غياب وفي وجود إضافات مختلفة للمثبطات عند جهد الإتزان لمعدن الصلب الكربوني وقد دلت النتائج التي تم الحصول عليها من تسجيل منحنيات المعاوقة أن هذه المنحنيات تأخذ الشكل المميز لشبه الدائرة والذي يتم ظهوره على أن عملية التآكل محكومة بعملية إنتقال الشحنة ،كما دلت النتائج أيضا على أن قيمة كلا من سعة الطبقة الكهربائية المزدوجة ومقلوب مقاومة إنتقال الشحنة ينخفض بزيادة تركيز المثبطات في المحلول . وتم تفسير هذه النتائج على أساس ان زيادة تركيز المثبطات يؤدي إلى زيادة إدمصاصها على سطح الصلب الكربوني مما يؤدي الى خفض كمية السعة الكهربائية المزدوجة وكذلك تثبيط التآكل ونقص معدله.

### القسم الخامس

تم إثبات آلية تثبيط التآكل العام والثاقب للصلب الكربوني 1 مولار حمض الهيدروكلوريك بواسطة المركبات البوليمرية من خلال امتزازه على سطح الصلب الكربوني. وهذا الامتزاز فيزيائي ويتبع امتزاز فروليندلش. كما إن وجود العديد من المراكز النشطة لمركبات البوليمر يسهل عملية الامتزاز ،

وبالتالي يزيد من قيم كفاءة التثبيت. وقد ثبت أيضاً أن مركبات البوليمر ذات الوزن الجزيئي الكبير تعطي تأثير تثبيت مرتفع.

خلاصة القول أن القياسات الكيميائية والكهروكيميائية تؤيد افتراض أن تثبيت التآكل يتم عن طريق إمتزاز المركبات البوليمرية على سطح الصلب الكربوني و الإتفاق بين وسائل القياسات المختلفة يدل على صحة النتائج التي تم الحصول عليها.

وصلى الله على سيدنا محمد وعلى آله وصحبه وسلم..



المملكة العربية السعودية

جامعة أم القرى

كلية العلوم التطبيقية

قسم الكيمياء

## إستخدام بعض البوليمرات القابلة للذوبان في الماء كمثبطات لتآكل الصلب الكربوني في المحاليل المائية.

الاسم: هناء هوساوي

المشرفين

الاسم	الوظيفة	التوقيع
أ.د/متولي عبد الله محمد	أستاذ الكيمياء الفيزيائية جامعة ام القرى	
أ.د/أحمد فوزي	أستاذ الكيمياء الفيزيائية جامعة ام القرى	

المحكمين

الاسم	الوظيفة	التوقيع
أ.د/متولي عبد الله محمد	أستاذ الكيمياء الفيزيائية جامعة ام القرى	
أ.د/رضا عبد الحميد عبد الغني سعيد	أستاذ الكيمياء الفيزيائية جامعة حائل	
د/أمينة محسن ناصر البنيان	أستاذ الكيمياء الفيزيائية المشارك جامعة ام القرى	

عميد كلية العلوم التطبيقية

د./ حاتم محمد الطيس

وكيل كلية العلوم التطبيقية للدراسات العليا

أ.د/ باسم حسين أصغر

رئيس قسم الكيمياء

د./ معتر مراد



المملكة العربية السعودية

جامعة أم القرى

كلية العلوم التطبيقية

قسم الكيمياء

# إستخدام بعض البوليمرات القابلة للذوبان في الماء كمثبطات لتآكل الصلب الكربوني في المحاليل المائية.

رسالة مقدمة الى

قسم الكيمياء-كلية العلوم التطبيقية- جامعة أم القرى

كمطلب للحصول على درجة دكتوراة الفلسفة في العلوم

(كيمياء - كيمياء فيزيائية)

مقدمة من

هناء محمد إبراهيم هوساوي

(ماجستير في الكيمياء)

تحت إشراف

الأستاذ الدكتور

أحمد فوزي

أستاذ الكيمياء الفيزيائية

الأستاذ الدكتور

متولي عبد الله محمد

أستاذ الكيمياء الفيزيائية

2020-هـ1441



المملكة العربية السعودية

جامعة أم القرى

كلية العلوم التطبيقية

قسم الكيمياء

# إستخدام بعض البوليمرات القابلة للذوبان في الماء كمثبطات لتآكل الصلب الكربوني في المحاليل المائية.

رسالة مقدمة الى

قسم الكيمياء-كلية العلوم التطبيقية- جامعة أم القرى

كمطلب للحصول على درجة دكتوراة الفلسفة في العلوم

(كيمياء - كيمياء فيزيائية)

مقدمة من

هناة محمد إبراهيم هوساوي

(ماجستير الكيمياء)

تحت إشراف

الأستاذ الدكتور

أحمد فوزي

أستاذ الكيمياء الفيزيائية

الأستاذ الدكتور

متولي عبد الله محمد

أستاذ الكيمياء الفيزيائية

1441هـ-2020